

# UNCLASSIFIED

AD NUMBER
AD837500
NEW LIMITATION CHANGE
TO Approved for public release, distribution unlimited
FROM Distribution authorized to U.S. Gov't. agencies and their contractors; Administrative/Operational use; Jun 1968. Other requests shall be referred to Air Force Material Laboratory, Attn: MAMP Wright-Patterson Air Force Base, Ohio 45433.
AUTHORITY
AFML, USAF ltr, 12 Jan 1972

THIS PAGE IS UNCLASSIFIED

AD837500

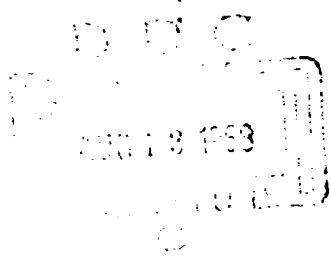
AFML-TR-68-148

DEVELOPMENT OF HIGH-STRENGTH  
ALUMINUM ALLOYS WITH IMPROVED  
STRESS-CORROSION RESISTANCE

J. Corey McMillan and Michael V. Hyatt  
The Boeing Company

TECHNICAL REPORT AFML-TR-68-148

June 1968



This document is subject to special export controls and each transmittal to foreign governments or foreign nationals may be made only with prior approval of the Air Force Materials Laboratory, MAMP, Wright-Patterson Air Force Base, Ohio 45433.

AIR FORCE MATERIALS LABORATORY  
AIR FORCE SYSTEMS COMMAND  
WRIGHT-PATTERSON AIR FORCE BASE, OHIO

**DEVELOPMENT OF HIGH-STRENGTH  
ALUMINUM ALLOYS WITH IMPROVED  
STRESS-CORROSION RESISTANCE**

**J. Corey McMillan and Michael V. Hyatt**

This document is subject to special export controls and each transmittal to foreign governments or foreign nationals may be made only with prior approval of the Air Force Materials Laboratory, MAMP, Wright-Patterson Air Force Base, Ohio 45433.

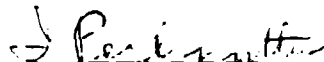
## FOREWORD

This report was prepared by the Metals Research Group, Commercial Airplane Division, The Boeing Company, Renton, Washington, under USAF Contract AF33(615)-3697. The contract was initiated under Project No. 7351, "Metallic Materials," Task No. 735105, "High Strength Metallic Materials." The program was administered by the Air Force Materials Laboratory, Air Force Systems Command, United States Air Force, with Dr. T. M. F. Ronald, MAMP, as Project Engineer. This report covers the period May 1, 1967, through March 30, 1968. The manuscript was released by the authors in April 1968 for publication as a technical report.

The authors acknowledge the assistance of the Materials Technology Laboratories in conducting this program. G. R. Harmon and D. D. Nakkula provided general laboratory support during the testing stages. Mrs. W. Diane Smith was responsible for the optical metallography, and D. D. Early conducted the transmission electron microscopy study.

This report has been assigned document number D6-60091 by The Boeing Company.

This technical report has been reviewed and is approved.



I. Perlmutter  
Chief, Metals Branch  
Metals and Ceramics Division  
Air Force Materials Laboratory

## ABSTRACT

The objective of this program was to develop a stress-corrosion-resistant, high-strength aluminum alloy through addition of minor elements and variations in heat treatment. On the basis of Phase I results, five step-aged special-chemistry alloys were selected for study in Phase II, along with commercial 7075-T651 plate material. The Phase II alloys consisted of a base alloy (6.4% Zn, 2.55% Mg, 1.0% Cu) with the following additions: silver; silver + zirconium (no chromium); silver + higher copper content; and silver + higher zinc and magnesium content. The materials evaluation consisted of metallographic, aging, and quench-sensitivity studies; stress-corrosion testing; and determination of mechanical, fracture, and fatigue properties. The resulting data were compared with data from evaluation of 11 other commercial and experimental aluminum alloys including 7079-T611, 7075-T73, AZ74.61, 7178-T7651, and X7080-T7. All of the five step-aged special-chemistry alloys met the goals of the program in that they had longitudinal 0.2-percent yield strengths above 70 ksi and stress-corrosion resistance superior to that of alloys 7079-T6 and 7075-T6. The use of silver in a production alloy does not appear warranted. Silver did not increase stress-corrosion resistance in the overaged condition. Strength properties were slightly increased by silver (0.25 inch thick), but quench sensitivity also increased, which would negate this slight strength advantage for thicker sections. The allowable chemistry range for the alloy that best meets the goals of this program should be: 5.9-6.9% Zn, 2.2-2.9% Mg, 0.7-1.5% Cu, 0.10-0.25% Zr, 0.05-0.15% Mn, 0.05% max Cr, 0.10% max Ti, 0.20% max Fe, 0.20% max Si. The ease with which the Phase II alloys were cast and fabricated indicates that the recommended alloy is commercially feasible. Additional testing is recommended to complete the development of this alloy.

This abstract is subject to special export controls and each transmittal to foreign governments or foreign nationals may be made only with prior approval of the Air Force Materials Laboratory, MAMP, Wright-Patterson Air Force Base, Ohio 45433.

## TABLE OF CONTENTS

<u>Section No.</u>	<u>Title</u>	<u>Page</u>
I	INTRODUCTION . . . . .	1
II	ALLOY PROPERTIES . . . . .	3
	1. CHEMICAL COMPOSITIONS . . . . .	3
	2. MICROSTRUCTURES . . . . .	3
	3. AGING . . . . .	10
	4. QUENCH SENSITIVITIES . . . . .	18
	5. MECHANICAL PROPERTIES . . . . .	18
	6. FRACTURE TOUGHNESS . . . . .	21
	7. FATIGUE LIFE . . . . .	24
III	STRESS-CORROSION TESTING . . . . .	31
	1. CONDITIONS AND PROCEDURES . . . . .	31
	2. RESULTS . . . . .	33
	a. Alternate-Immersion Testing . . . . .	33
	b. Testing of Double-Cantilever Beam (DCB) Specimens . . . . .	72
	c. Industrial-Environment Testing . . . . .	74
	d. Exfoliation Testing . . . . .	74
IV	DISCUSSION . . . . .	77
	1. EFFECT OF SILVER ADDITIONS . . . . .	78
	a. Stress-Corrosion Resistance . . . . .	78
	b. Mechanical Properties . . . . .	79
	c. Quench Sensitivities . . . . .	80
	d. Fracture Toughness . . . . .	81
	e. Fatigue Properties . . . . .	81
	f. Economic Considerations . . . . .	83
	g. Summary . . . . .	83
	2. MEETING THE STRESS-CORROSION GOAL . . . . .	84
	a. Composition Effects . . . . .	85
	b. Other Metallurgical Effects . . . . .	86

## TABLE OF CONTENTS (CONTINUED)

<u>Section No.</u>	<u>Title</u>	<u>Page</u>
	3. MEETING THE MECHANICAL PROPERTY GOAL . . . . .	87
	4. CONTROLLING QUENCH SENSITIVITY . . . . .	88
	5. MAINTAINING FRACTURE TOUGHNESS . . . . .	88
	6. MAINTAINING FATIGUE PROPERTIES . . . . .	92
	7. THE RECOMMENDED ALLOY . . . . .	92
V	CONCLUSIONS . . . . .	95
VI	RECOMMENDATIONS FOR FURTHER WORK . . . . .	97
	REFERENCES . . . . .	99
	APPENDIX I: PREPARATION OF EXPERIMENTAL ALLOYS .	102
	APPENDIX II: ACTUAL MECHANICAL AND FRACTURE PROPERTIES OF PHASE II ALLOYS . . . . .	103
	APPENDIX III: STRESS-CORROSION TEST DATA . . . . .	104
	APPENDIX IV: END-OF-TEST PHOTOGRAPHS . . . . .	116

## LIST OF ILLUSTRATIONS

<u>No.</u>	<u>Title</u>	<u>Page</u>
1	Chemical Compositions of Phase II and Comparison Alloys (Zn, Mg, and Cu) . . . . .	6
2	Microstructure of Alloy 16 . . . . .	7
3	Microstructure of Alloy 17 . . . . .	7
4	Microstructure of Alloy 18 . . . . .	8
5	Microstructure of Alloy 19 . . . . .	8
6	Microstructure of Alloy 20 . . . . .	9
7	Microstructure of 7075-T651-1 . . . . .	9
8	Typical Microstructures (Transmission Electron Micrographs) . . . . .	11
9	Aging Behavior at 250° F after 2 Hours at Room Temperature . . . . .	14
10	Aging Behavior at 320° F after 2 Hours at Room Temperature + 24 Hours at 250° F . . . . .	15
11	Quench Sensitivities of Phase II Alloys and X7080 . . . . .	16
12	Longitudinal Mechanical Properties . . . . .	20
13	Typical Fracture Surfaces of Precracked Charpy Specimens of Phase II Alloys . . . . .	22
14	Fracture Profiles from Phase II Alloy Center-Notched Panels . . . . .	23
15	Typical Electron Fractographs of Fractured Charpy Specimens of 7075-T651-1 and Alloy 18 . . . . .	25
16	Fatigue-Crack Propagation Curves for Phase II Alloys . . . . .	26
17	Fatigue Crack Growth Rate Versus Stress Intensity for Phase II Alloys . . . . .	27
18	Typical Electron Fractographs of Fatigued Center-Notched Panels of Alloys 7075-T651-1, 16, and 17 Tested in Two Environments . . . . .	29
19	Stress-Corrosion Test Specimen and Leg Deflections . . . . .	32
20	Extent of Cracking and Pitting on Phase II and Comparison Alloys Tested by Alternate Immersion in 3.5-Percent Sodium Chloride Solution . . . . .	35
21	Time-Sequence and Cross-Section Photographs of 16-23 at 26 KSI . . . . .	37
22	Time-Sequence and Cross-Section Photographs of 17-16 at 26 KSI . . . . .	38
23	Time-Sequence and Cross-Section Photographs of 18-8 at 26 KSI . . . . .	39
24	Time-Sequence and Cross-Section Photographs of 19-5 at 26 KSI . . . . .	40
25	Time-Sequence and Cross-Section Photographs of 20-11 at 26 KSI . . . . .	41



# LIST OF ILLUSTRATIONS (CONTINUED)

<u>No.</u>	<u>Title</u>	<u>Page</u>
26	Time-Sequence and Cross-Section Photographs of 7075-T651-1-23 at 26 KSI . . . . .	42
27	Time-Sequence and Cross-Section Photographs of 7075-T651-2-11 at 26 KSI . . . . .	43
28	Time-Sequence and Cross-Section Photographs of AZ74.61 (2-2) at 26 KSI . . . . .	44
29	Time-Sequence and Cross-Section Photographs of AZ74.61 (A-7) at 26 KSI . . . . .	45
30	Time-Sequence and Cross-Section Photographs of 7075-T73 (B-7) at 26 KSI . . . . .	46
31	Time-Sequence and Cross-Section Photographs of X7080-T7 (D-8) at 26 KSI . . . . .	47
32	Time-Sequence and Cross-Section Photographs of 7079-T611-A (C-7) at 26 KSI . . . . .	48
33	Time-Sequence Photographs of 7079-T611-G (F-9) at 26 KSI . . . . .	49
34	Time-Sequence and Cross-Section Photographs of 7079-T6-G (E-9) at 26 KSI . . . . .	50
35	Time-Sequence and Cross-Section Photographs of 7575-8 at 26 KSI . . . . .	51
36	Time-Sequence and Cross-Section Photographs of 7578-8 at 26 KSI . . . . .	52
37	Time-Sequence and Cross-Section Photographs of 7178-T7651-1 at 26 KSI . . . . .	53
38	Time Sequence and Cross-Section Photographs of 16-19 at 32 KSI . . . . .	56
39	Time-Sequence and Cross-Section Photographs of 17-21 at 32 KSI . . . . .	57
40	Time-Sequence and Cross-Section Photographs of 18-3 at 32 KSI . . . . .	58
41	Time-Sequence and Cross-Section Photographs of 19-3 at 32 KSI . . . . .	59
42	Time-Sequence and Cross-Section Photographs of 20-21 at 32 KSI . . . . .	60
43	Time-Sequence and Cross-Section Photographs of 7075-T651- 1-19 at 32 KSI . . . . .	61
44	Time-Sequence and Cross-Section Photographs of 7075-T651- 2-9 at 32 KSI . . . . .	62
45	Time-Sequence and Cross-Section Photographs of 16-6 at 44 KSI . . . . .	64
46	Time-Sequence and Cross-Section Photographs of 17-13 at 44 KSI . . . . .	65
47	Time-Sequence and Cross-Section Photographs of 18-6 at 44 KSI . . . . .	66
48	Time-Sequence and Cross-Section Photographs of 19-10 at 44 KSI . . . . .	67

# LIST OF ILLUSTRATIONS (CONTINUED)

<u>No.</u>	<u>Title</u>	<u>Page</u>
49	Time-Sequence and Cross-Section Photographs of 20-13 at 44 KSI . . . .	68
50	Time-Sequence and Cross-Section Photographs of 7075-T651- 1-13 at 44 KSI . . . . .	69
51	Time-Sequence and Cross-Section Photographs of 7075-T651- 2-8 at 44 KSI . . . . .	70
52	Photographs of Unstressed Phase II Alloy Coupons after 90 Days . . . .	71
53	Double-Cantilever Beam (DCB) Specimen for Stress-Corrosion Testing . . . . .	73
54	Stress-Corrosion Crack Propagation Curves for DCB Specimens . . . . .	75
55	Fracture Toughness Parameter $K_{IC}$ Versus Tensile Yield Strength for Several 7000-Series Aluminum Alloys . . . . .	82
56	Correlation Between Precracked Charpy V-Notch Impact Data and $G_C$ for Several 7000-Series Aluminum Alloys . . . . .	91
	End-of-Test Photographs . . . . .	116

# LIST OF TABLES

<u>No.</u>	<u>Title</u>	<u>Page</u>
I	Summary of Heat-Treatment Information . . . . .	4
II	Wet Chemical Analysis . . . . .	5
III	Average Mechanical and Fracture Properties . . . . .	17
IV	Summary of Stress-Corrosion Test Data (Alternate Immersion) . . . . .	34
V	Comparative Growth Rates of Stress-Corrosion Cracks or Linear Pits . . . . .	73
VI	Actual Mechanical and Fracture Properties of Phase II Alloys . . . . .	103
VII	Stress-Corrosion Test Data (3.5 Percent Sodium Chloride, Alternate Immersion) . . . . .	104
VIII	Stress-Corrosion Test Data (Industrial Environment) . . . . .	113

## NOMENCLATURE

a	1/2 crack length (in.)
DC	direct chill
E	Young's modulus (psi)
$F_{tu}$	tensile ultimate strength (psi, ksi)
$F_{ty}$	tensile yield strength (psi, ksi)
f	frequency of fatigue cycling (cpm)
$G_C$	$K_C^2/E$
IACS	International Annealed Copper Standard
K	stress intensity factor ( $\text{ksi}\sqrt{\text{in.}}$ )
$K_C$	plane-stress fracture toughness parameter ( $\text{ksi}\sqrt{\text{in.}}$ )
$K_t$	elastic stress concentration factor
L	longitudinal grain direction
$M'$	a hardening precipitate in 7000 series aluminum alloys
R	ratio of minimum cyclic stress to maximum cyclic stress
RA	reduction in area (percent)
$R_B$	Rockwell B hardness
RH	relative humidity (percent)
r	radius
T	transverse grain direction
W/A	fracture toughness parameter for Charpy specimens ( $\text{in.-lb/in.}^2$ )
w	panel width (in.)
$\Delta a/\Delta n$	fatigue-crack growth rate ( $\mu\text{-in./cycle}$ )
$\mu$	micron, $10^{-6}$ meter
$\sigma_g$	gross area stress at fracture (psi)
$\sigma_{net}$	net stress at fracture (psi)
$\sigma_{ty}$	tensile yield strength (psi)
$\Theta$	finite-width correction factor

## SECTION I

### INTRODUCTION

The objective of this program was to develop a commercially feasible high-strength aluminum alloy with a minimum yield strength of 70,000 pounds per square inch (psi) and a stress corrosion resistance substantially greater than those of 7075-T6 or 7079-T6 aluminum alloys. This alloy was to have a short-transverse stress-corrosion threshold stress of at least 25,000 psi, and fatigue and fracture toughness properties comparable to those of current high-strength commercial alloys.

The program was conducted from an engineering approach by defining material property goals. The 24-month period of work was divided into Phase I, which was the subject of a previous technical report (1), and Phase II, the results of which are summarized in this report.

Phase I was a study of the effects of several minor alloying additions on the mechanical properties and stress-corrosion resistance of a 7075 base alloy. The minor additions evaluated were silver, boron, cerium, yttrium, and zirconium (1). Results of these tests showed that only silver improved the stress-corrosion resistance of alloys in the T6 temper, but in this heat-treat condition the resistance was inadequate to meet the goals of the contract. Overaging treatments increased the stress-corrosion resistance to adequate levels for all alloys tested and the silver-bearing alloys maintained higher strengths.

Results with the more highly alloyed silver-bearing alloys in Phase I showed that, to meet the strength goals, the overaging must be limited to approximately 10 hr at 320°F after a T6 type treatment; this was especially true for the low-copper-content alloys because of their lower inherent strengths. The low-copper-content alloys resisted cracking and pitting better than the other Phase I alloys.

On the basis of the Phase I results, five experimental alloys--a base alloy and four variations--were selected for study in Phase II. Commercial 7075-T651 plate material was also tested. The alloy designations and major chemistry variations are listed below:

- Alloy 16--Base alloy
- Alloy 17--Base alloy + silver
- Alloy 18--Base alloy + silver + zirconium; no chromium
- Alloy 19--Base alloy + silver + higher copper content
- Alloy 20--Base alloy + silver + higher zinc and magnesium contents
- 7075-T651-1--Commercial 7075-T651 plate

Chromium was omitted in alloy 18 to reduce the alloy's quench sensitivity (2). Higher zinc and magnesium contents were specified in alloy 20 to simulate a high-strength version of the base alloy. This was required to establish lower bounds for stress-corrosion resistance and fracture toughness.

Concurrent with Phase II testing, several other high-strength commercial and experimental aluminum alloys were evaluated by the Materials Technology Laboratories. Since these alloys provided significant comparisons, the results of the test program are included in this report. (These alloys are referred to as "comparison alloys.") Eleven lots of material, designated as follows, were evaluated:

7075-T6S1-2	7079-T611-G
7075-T73	7079-T6-G
AZ74.61	7575
AZ74.61-A	7578
X7080-T7	7178-T7651
7079-T611-A	

These alloys include nearly all the high-strength 7000-series alloys that are commercially available in the United States, including the new chromium-free X7080-T7 alloy. Also included are a commercial silver-bearing alloy (AZ74.61), experimental silver-bearing alloys (7575 and 7578), and experimental heat treatments for 7079 (7079-T611-G and 7079-T6-G).

## SECTION II

### ALLOY PROPERTIES

The five experimental Phase II alloys were cast and fabricated into 0.250-in.-thick plate by Kaiser Aluminum and Chemical Corporation. Details of the casting and fabrication procedures are given in Appendix I. The casting and fabrication of these alloys presented no problems, and edge cracking of the ingots and plates during fabrication was insignificant. The comparison alloys were not all available in the form of plate. When plate was not available, forged or extruded material was used. The fabrication and heat-treatment procedures varied considerably among the comparison alloys and were generally different from those used to produce the Phase II alloys. The forms and procedures, as far as they are known, are given in Table I.

Processing history can have a significant bearing on properties and stress-corrosion performance, and must be considered when comparing the various alloys.

#### 1. CHEMICAL COMPOSITIONS

Wet chemical analyses of the alloys are shown in Table II. The relative contents of the primary alloying elements (zinc, magnesium, and copper) for each alloy are shown in Fig. 1 along with composition limits for several commercial alloys.

The comparison alloy 7575 is an experimental silver-bearing, low-copper version of 7075; it contains more silver than any of the Phase II alloys. The comparison alloy 7578 is an experimental silver-bearing, low-copper version of 7178, similar to Phase II alloy 20 except for a higher silver content. All other comparison alloys are commercially available.

#### 2. MICROSTRUCTURES

##### a. Optical Microscopy of Phase II Alloys

Three-dimensional composite photomicrographs (Figs. 2 through 7) were prepared for each Phase II alloy. All the alloys contain a subgrain structure, not clearly visible in the photographs. The only obvious differences between alloys are:

- (1) A larger grain size in 7075-T651-I.
- (2) A noticeably cleaner matrix in the chromium-free, zirconium-bearing alloy 18. This is due to the absence of the small chromium-rich intermetallics that are responsible for the hazy background precipitate in the unetched composites of the other alloys.
- (3) A higher density of small intermetallic particles in alloy 19. This may be due to the higher copper content of this alloy.
- (4) A contrast in etching response between alloys 16 through 20 and 7075-T651-I, owing to the fact that the latter was not overaged. A heavy etching response is characteristic of the overaged alloys.

Table I. Summary of Heat-Treatment Information

Alloy product form thickness (in.)*	Heat treatment	Hardness (R <sub>B</sub> )	Conductivity (% of IACS)
Alloy 16 Laboratory-produced plate 0.25	35 min at 860°F, 60°F WQ, 48 hr at RT + 24 hr at 250°F + 10 hr at 320°F	87.5	36.5
Alloy 17 Laboratory-produced plate 0.25	35 min at 860°F, 60°F WQ, 48 hr at RT + 24 hr at 250°F + 10 hr at 320°F	87.8	36.2
Alloy 18 Laboratory-produced plate 0.25	35 min at 860°F, 60°F WQ, 48 hr at RT + 24 hr at 250°F + 10 hr at 320°F	89.5	34.8
Alloy 19 Laboratory-produced plate 0.25	35 min at 860°F, 60°F WQ, 48 hr at RT + 24 hr at 250°F + 10 hr at 320°F	89.8	35.0
Alloy 20 Laboratory-produced plate 0.25	35 min at 860°F, 60°F WQ, 48 hr at RT + 24 hr at 250°F + 10 hr at 320°F	89.0	35.0
7075-T651-1 Commercial plate 0.25	Commercial T6--870°F, WQ, 24-28 hr at 250°F	94.1	31.5
7075-T651-2 Commercial plate 0.25	Commercial T6--870°F, WQ, 24-28 hr at 250°F	94.0	31.6
AZ74.61 Die forging 0.5-1.0	30 min at 870°F, 85°F WQ, 18 hr at 250°F + 7 hr at 320°F	88.5	38.7
AZ74.61-A Die forging 0.5-1.0	30 min at 870°F, 95°F WQ, 11 hr at 320°F	88.5	36.8
7075-T73 Die forging ≈0.5	T6 + 24-30 hr at 325°F for plate T6 + 8-10 hr at 350°F for forgings	86.6	38.8
X7080-T7 Die forging 8.0 Dia	Unknown, but boiling-water quenched	84.1	37.4
7079-T611-A Forging Unknown	Commercial T611--830°F, WQ, 5 days at RT + 48 hr at 230-250°F	88.5	31.1
7079-T611-G Forging Unknown	Unknown	81.2	35.4
7079-T6-G Forging Unknown	Unknown	90.2	31.8
7575** Extruded panel 0.5	Commercial 7075-T6 treatment + 8 hr at 320°F	88.6	37.6
7578** Extruded bar 0.5	Commercial 7178-T6 treatment + 8 hr at 340°F	86.5	39.1
7178-T7651 Commercial plate 0.5	Commercial T6 + 12-15 hr at 320°F	89.0	38.7

\*Thicknesses shown are those at time of heat treatment

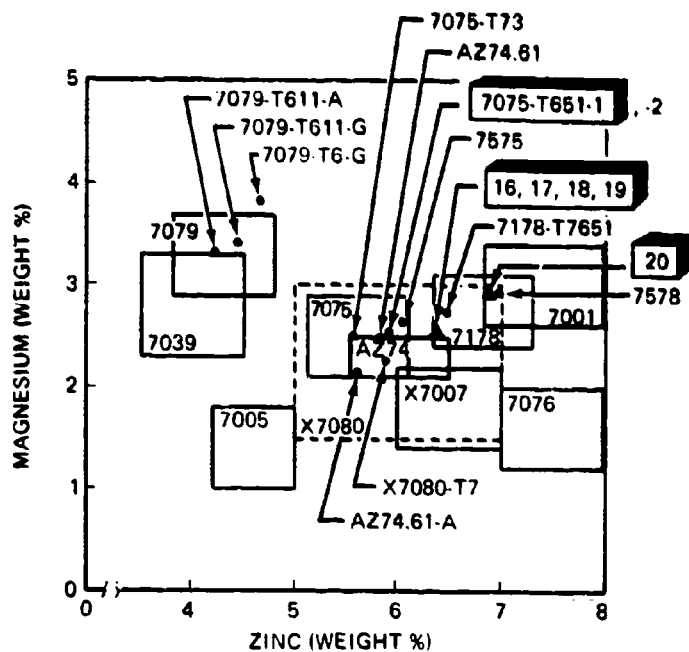
\*\*Not commercial designations.



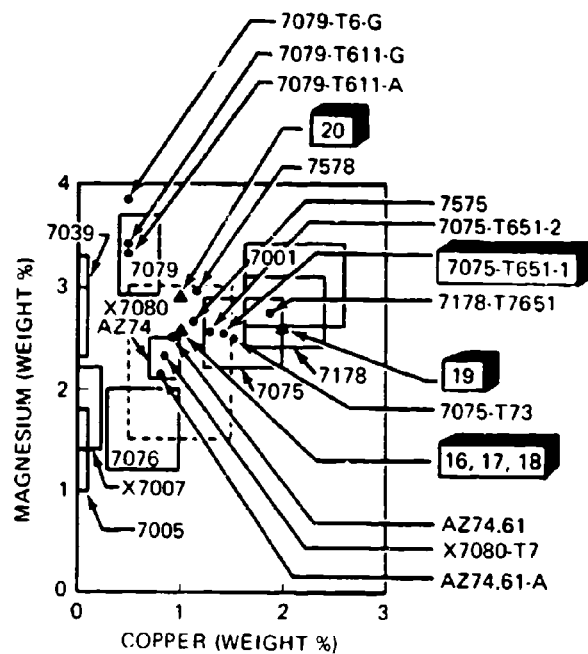
Table II. Wet Chemical Analysis<sup>a</sup>

Alloy	Cast number	Zn	Mg	Cu	Fe	Si	Mn	Cr	Ti	Ag	Zr
16	D2733	6.39	2.59	1.00	0.11	0.09	0.09	0.20	0.04	0.00	0.00
17	D2734	6.34	2.55	0.99	0.10	0.09	0.11	0.20	0.04	0.28	0.00
18	D2735	6.35	2.53	0.99	0.11	0.09	0.11	0.01	0.04	0.28	0.16
19	D2736	6.37	2.56	2.00	0.10	0.09	0.10	0.19	0.04	0.28	0.00
20	D2737	6.83	2.91	0.99	0.10	0.10	0.11	0.20	0.04	0.29	0.00
7075-T651-1		5.94	2.55	1.42	0.16	0.09	0.04	0.21	0.02	0.00	0.00
7075-T651-2		5.90	2.57	1.25	0.20	0.09	<0.05	0.18	0.04	0.00	0.00
AZ74.61		5.85	2.50	0.92	0.15	0.09	<0.10	0.17	0.03	0.39	0.00
AZ74.61-A		5.60	2.14	0.81	0.16	0.09	0.07	0.20	0.07	0.37	0.00
7075-T73		5.56	2.52	1.50	0.17	0.14	0.05	0.20	0.10	0.00	0.00
X7080-T7		5.88	2.30	0.86	0.13	0.08	0.38	<0.05	<0.02	0.00	0.00
7079-T611-A		4.20	3.34	0.53	0.12	0.09	0.17	0.14	0.05	0.00	0.00
7079-T611-G		4.43	3.42	0.53	0.15	0.11	0.13	0.22	0.05	0.00	0.00
7079-T6-G		4.64	3.84	0.50	0.11	0.10	0.15	0.20	0.05	0.00	0.00
7575		6.05	2.67	1.11	0.11	0.05	<0.05	0.20	0.05	0.35	0.00
7578		6.95	2.95	1.14	0.13	0.08	<0.05	0.21	<0.05	0.43	0.00
7178-T7651		6.48	2.75	1.87	0.18	0.13	0.06	0.21	0.04	0.00	0.00

<sup>a</sup>Weight per cent.



A. Magnesium-Zinc



B. Magnesium-Copper

Figure 1. Chemical Compositions of Phase II and Comparison Alloys (Zn, Mg, and Cu)

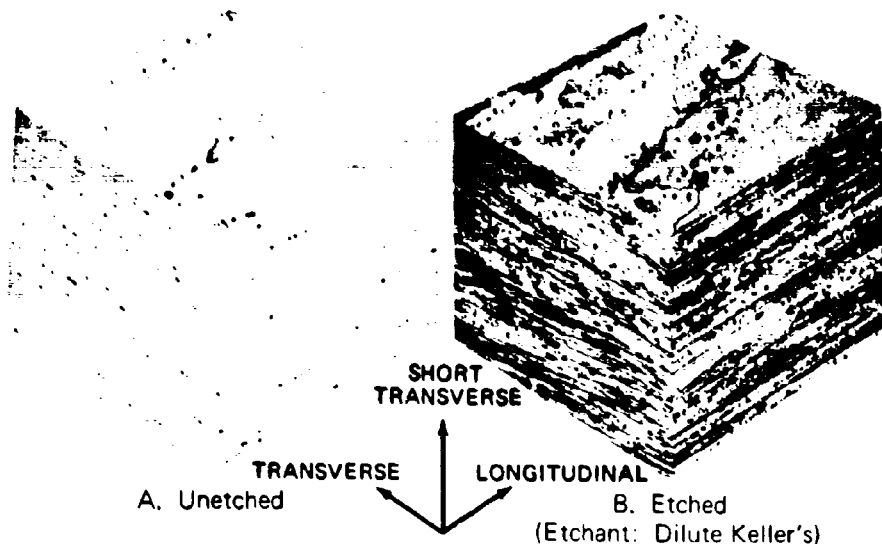


Figure 2. Microstructure of Alloy 16 (100x)

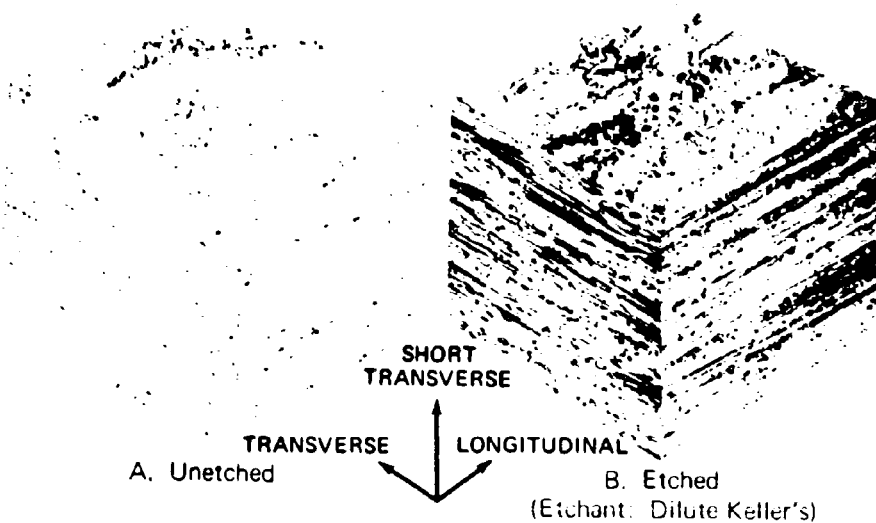
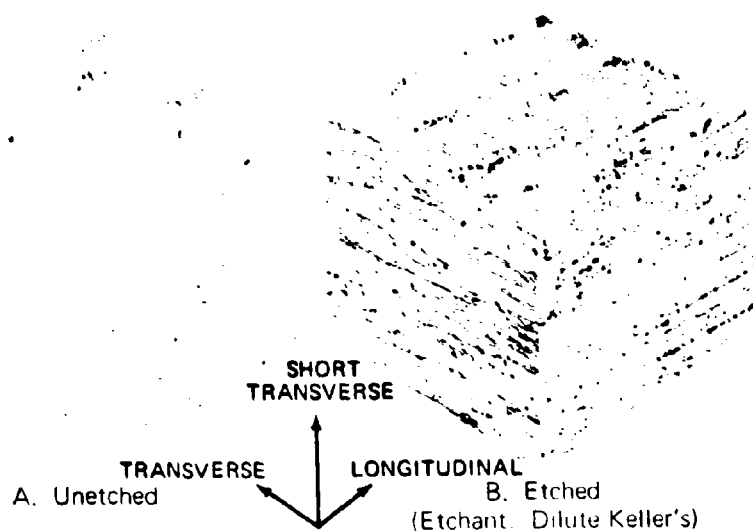
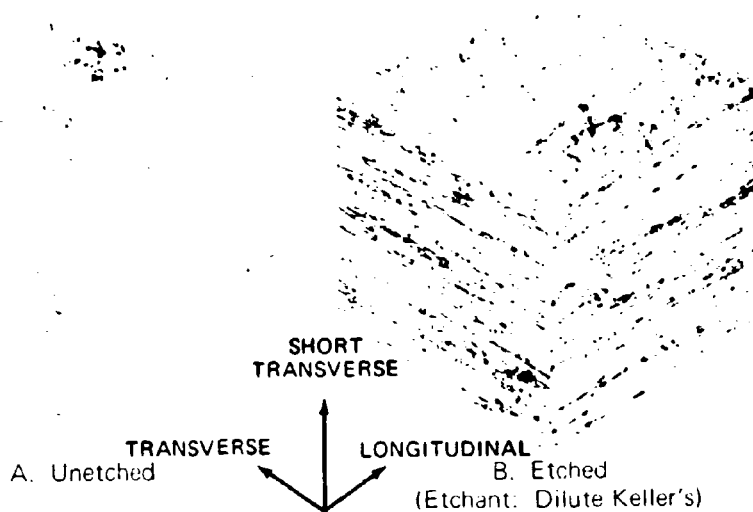


Figure 3. Microstructure of Alloy 17 (100x)



*Figure 4. Microstructure of Alloy 18 (100x)*



*Figure 5. Microstructure of Alloy 19 (100x)*

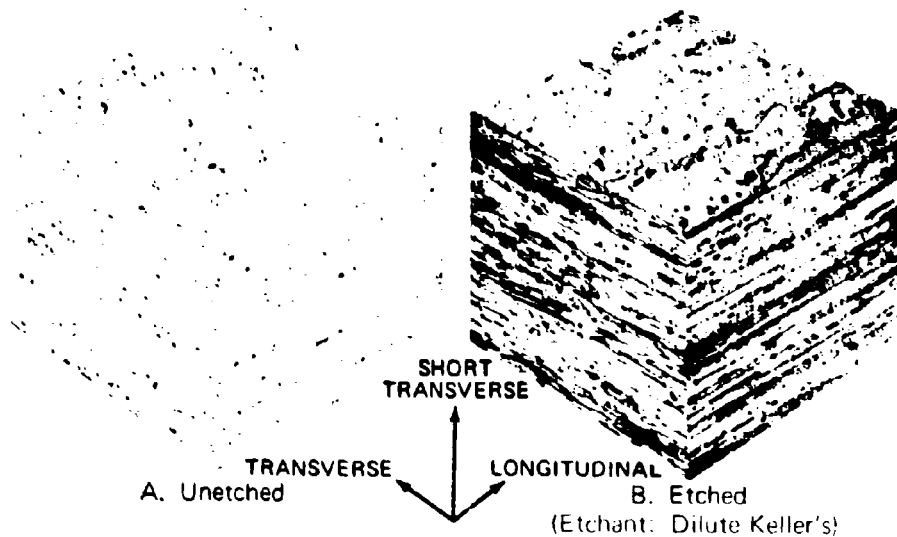


*Figure 6. Microstructure of Alloy 20 (100x)*

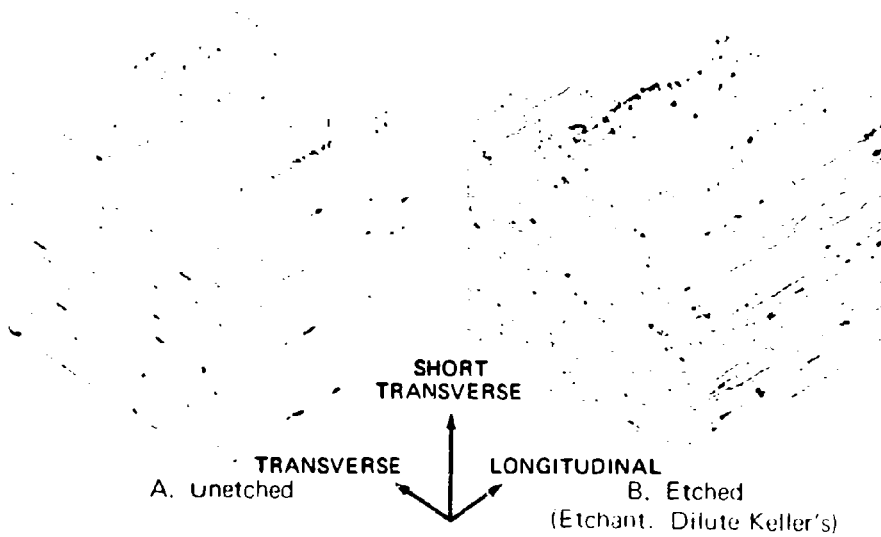


*Figure 7. Microstructure of 7075-T651-1 (100x)*

### b. Transmission Electron Microscopy

Transmission electron micrographs of the Phase II alloys and of comparison alloys 7079-T6-G, 7575, AZ74.61, 7075-T73, X7080-T7, and 7178-T76 are shown in Fig. 8. The 7075-T651-1 and 7079-T6-G contain the small, spherical zone-type precipitates primarily, whereas the other alloys exhibit larger and (in some cases) more plate-shaped precipitates of the M' phase, reflecting their more overaged condition. In the silver-bearing alloy 17, coherency strain fields are visible around some of the M' plates. Alloy 18 appears less overaged than alloys 16, 17, 19, and 20 but is further along in the aging sequence than 7075-T651-1 or 7079-T6-G. Like the photomicrograph in Fig. 4, the transmission electron micrograph of alloy 18 (Fig. 8C) shows no chromium-rich intermetallic particles. The other low-chromium alloy X7080-T7, also contains a low density of the small intermetallic phases. The exact heat treatment given the X7080-T7 is unknown, but from the appearance of the precipitates this alloy appears to be more overaged than alloy 18. Conductivity readings for these two alloys also indicate that this is the case. Alloy 7075-T73 is more overaged than the Phase II base alloy 16, but this is not apparent from the transmission electron micrographs. The presence of silver in the Phase II and comparison alloys has only a small effect on the microstructure, evidenced as a more plate-shaped M' precipitate. Precipitate-free zones are present in both silver-free and silver-bearing alloys.

## 3. AGING

### a. 250°F

Aging studies were conducted on the Phase II alloys, using hardness and conductivity measurements. Figure 9 shows curves for aging at 250°F. The silver addition increases hardness values in the T6 condition (24 hr at 250°F). (Compare alloys 16 and 17.) The higher copper content in alloy 19 and the higher zinc and magnesium contents in alloy 20 also result in higher hardness in the T6 condition. (Compare alloys 19 and 20 with 17.) All Phase II alloys show higher hardness than 7075 up to an aging time of approximately 100 hr at 250°F. Replacement of chromium with zirconium reduces conductivity, as do the higher zinc and magnesium contents and the higher copper content. (Compare alloys 18, 19, and 20 with alloy 17.)

### b. 320°F

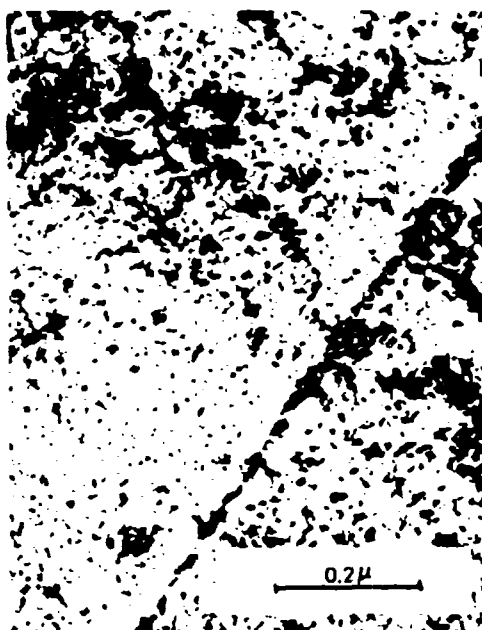
Figure 10 shows aging curves at 320°F after a T6-type treatment. After a few hours initial aging at 320°F the silver-bearing alloy has a higher hardness than the silver-free alloy for any given aging time. After 10 hr at 320°F the difference between alloy 16 (silver-free) and alloy 17 (silver-bearing) is one  $R_p$  point; after 100 hr at 320°F the difference is three  $R_p$  points. This difference, though small, increases steadily as the aging time increases, indicating that the effect of silver on strength is more pronounced at the longer aging times. Alloys 16 and 17 have lower hardness values than any other Phase II alloys for any given aging time. The hardness data show that the higher-copper alloys (19 and 7075-T651-1) have the highest hardness beyond 24 hr at 320°F.



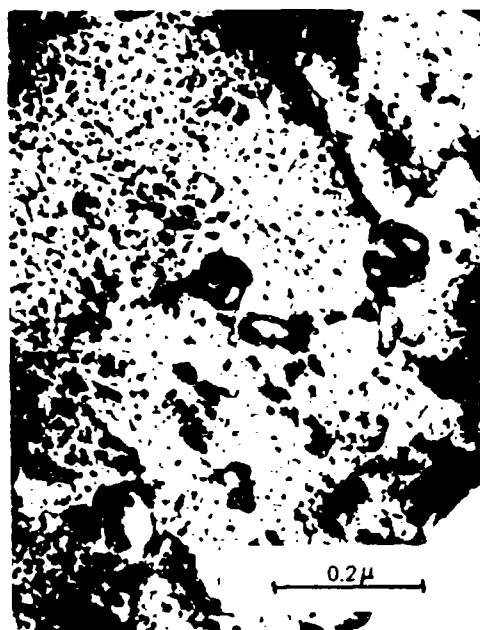
(A) Alloy 16



(B) Alloy 17



(C) Alloy 18

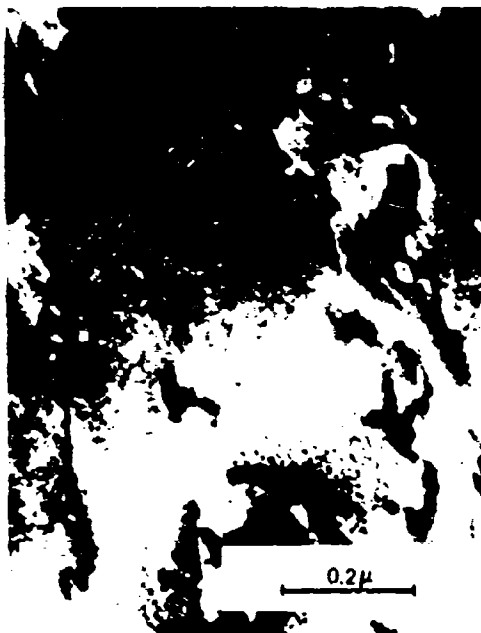


(D) Alloy 19

Figure 8. Typical Microstructures (Transmission Electron Micrographs)



(E) Alloy 20



(F) 7075-T651-1



(G) 7079-T6-G



(H) 7575

*Figure 8. Continued*

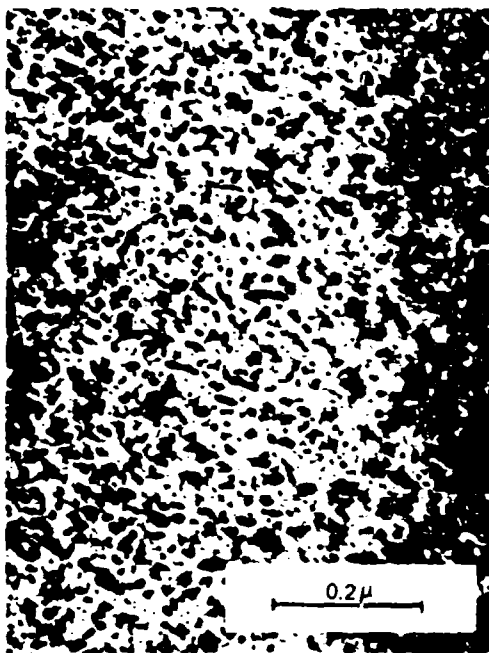




(I) AZ74.61



(J) 7075-T73



(K) X7080-T7



(L) 7178-T7651

*Figure 8. Concluded*

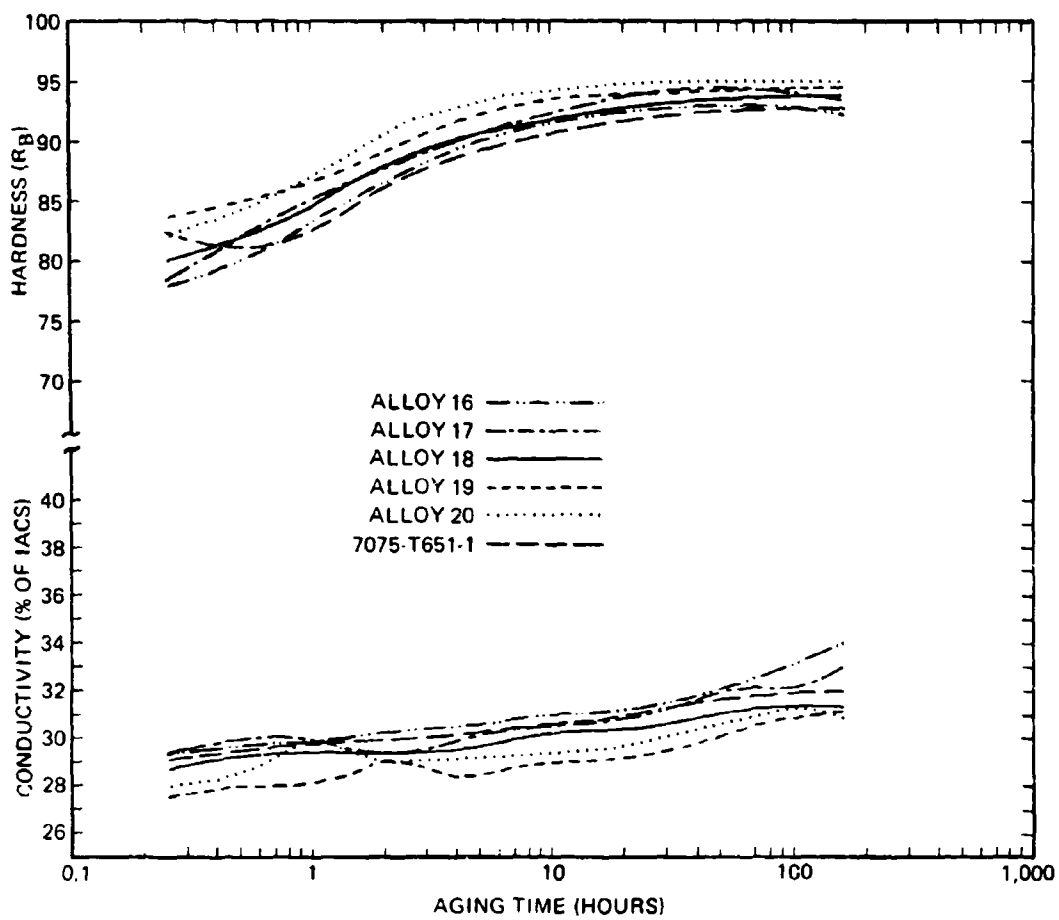


Figure 9. Aging Behavior at 250° F after 2 Hours at Room Temperature

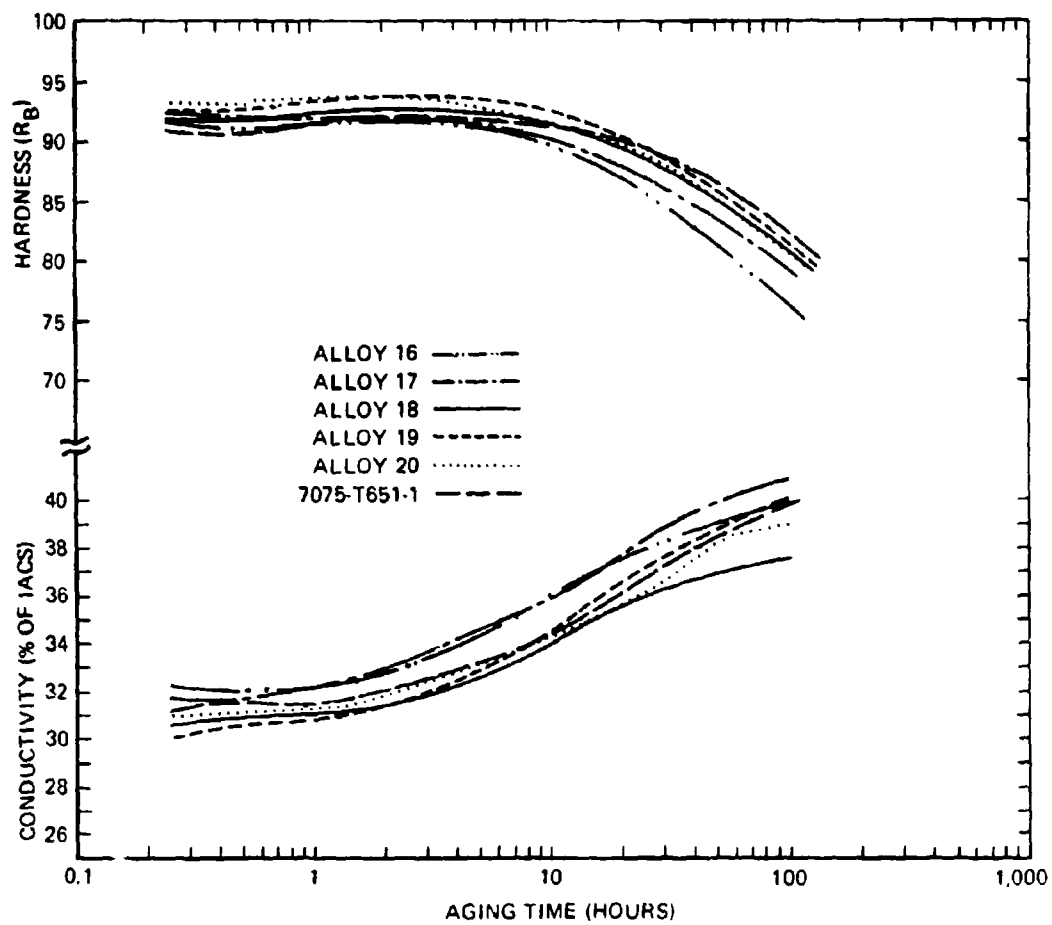


Figure 10. Aging Behavior at 320°F after 2 Hours at Room Temperature + 24 Hours at 250°F

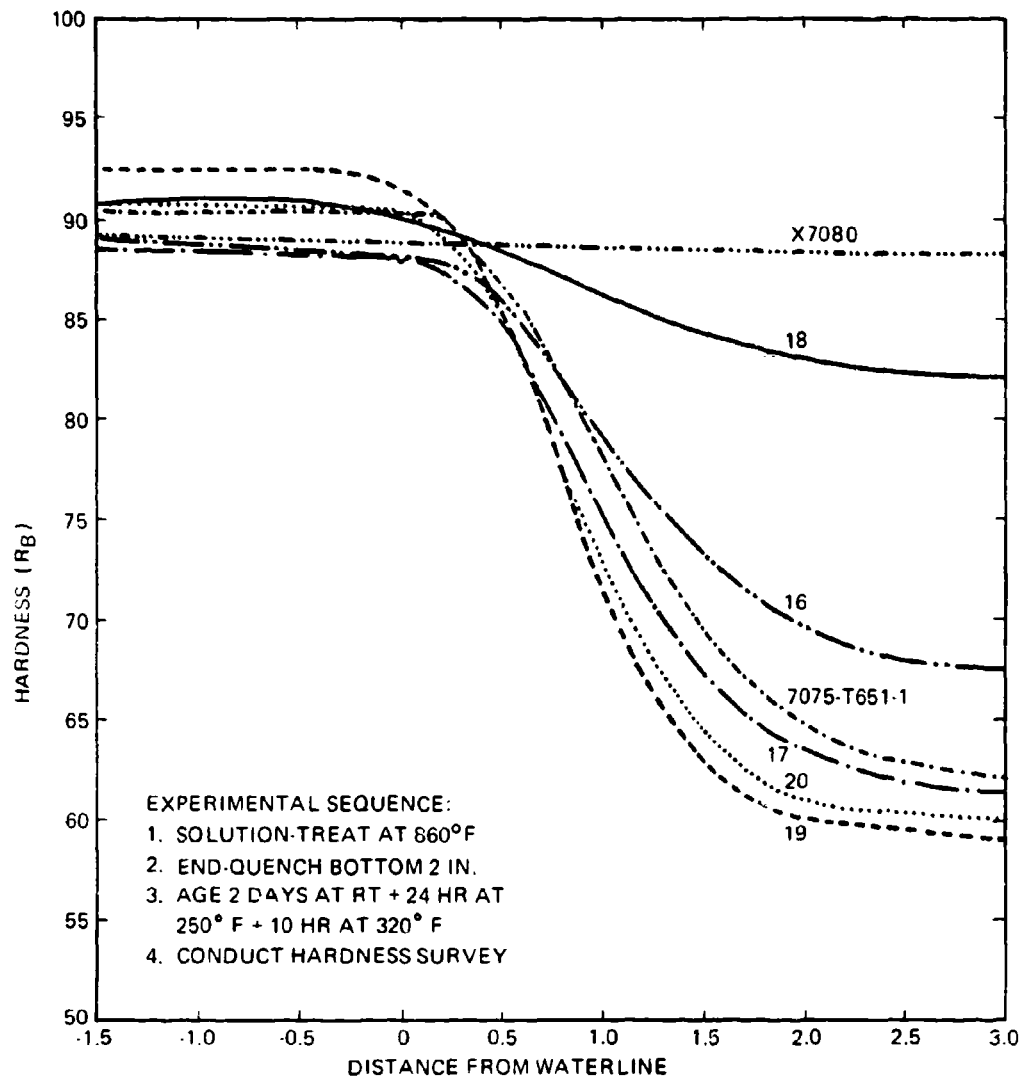


Figure 11. Quench Sensitivities of Phase II Alloys and X7080

Table III. Average Mechanical and Fracture Properties <sup>a</sup>

PHASE II ALLOYS

Alloy	Grain direction	F <sub>tu</sub> (ksi)	F <sub>ty</sub> (ksi)	Elongation (% in 2 in.)	RA (%)	W/A (in.-lb/in. <sup>2</sup> ) <sup>b</sup>	K <sub>C</sub> (ksi √in.) <sup>c</sup>	G <sub>C</sub> (in.-lb/in. <sup>2</sup> ) <sup>d</sup>
16	L	81.0	72.8	11.0	23.5	283	81.3	<sup>e</sup> 90.0
16	T	81.5	73.2	11.0	27.5	---	---	---
17	L	82.1	74.3	10.5	21.5	279	84.6	<sup>e</sup> 98.3
17	T	81.6	73.1	10.5	26.5	---	---	---
18	L	84.5	78.9	10.5	24.0	207	76.4	<sup>e</sup> 80.3
18	T	83.5	77.6	11.0	26.5	---	---	---
19	L	87.6	79.5	10.0	18.0	173	57.5	<sup>e</sup> 60.5
19	T	85.8	76.8	10.5	23.5	---	---	---
20	L	85.3	77.3	10.5	20.5	153	53.9	<sup>e</sup> 57.1
20	T	84.0	75.4	11.0	21.5	---	---	---
7075-T6S1-1	L	84.8	79.9	13.0	27.0	214	62.7	<sup>e</sup> 66.5
7075-T6S1-1	T	86.4	75.7	12.0	21.5	---	---	---

COMPARISON ALLOYS

Alloy	Grain direction	F <sub>tu</sub> (ksi)	F <sub>ty</sub> (ksi)	Elongation (% in 1 in.)	RA (%)	W/A (in.-lb/in. <sup>2</sup> ) <sup>b</sup>
AZ74.61	L	<sup>f</sup> 73.9	<sup>f</sup> 63.8	<sup>f</sup> 10.0	<sup>f</sup> 18.0	<sup>g</sup> 288
AZ74.61-A	L	72.2	65.1	9.7	21.8	---
7075-T73	L	71.2	63.5	10.0	14.5	---
X7080-T7	L	<sup>h</sup> 69.6	<sup>h</sup> 61.4	<sup>h</sup> 11.0	<sup>h</sup> 25.0	<sup>i</sup> 429
7079-T611-A	L	75.3	64.0	13.5	31.0	---
7079-T611-G	L	69.7	55.6	14.5	37.5	---
7079-T6-G	L	77.2	66.0	8.0	11.0	---
7575	L	80.6	71.1	11.0	29.5	<sup>g</sup> 137
7578	L	76.3	65.1	12.0	32.0	<sup>g</sup> 139
7178-T76S1	L	80.9	71.5	10.5	28.0	<sup>g</sup> 117

<sup>a</sup>Average of two specimens unless otherwise indicated.

<sup>b</sup>Precracked Charpy specimens. Phase II Alloys: 0.250 in. thick; comparison alloys: 0.394 in. thick.

<sup>c</sup> $K_C = \sigma_g \sqrt{\pi a} \Theta$ ; thickness = 0.250 in.,  $\Theta = (w/\pi a \tan \pi a/w)^{1/2}$ .

<sup>d</sup> $G_C = K_C^2/E$ .

<sup>e</sup>Using crack length (2a) corrected for "slow" growth.

<sup>f</sup>Average of 40 specimens.

<sup>g</sup>Average of five specimens.

<sup>h</sup>Average of six specimens.

<sup>i</sup>Average of 10 specimens.

The most important observation from the conductivity study at 320° F is that alloy 18 (zirconium, no chromium) has much lower conductivity than alloy 17. A lower conductivity for alloys 19 (higher copper) and 20 (higher zinc and magnesium) compared to alloy 17 might be expected because of their higher alloy content, but the large difference between alloys 17 and 18 with the small addition of zirconium and the removal of chromium was not expected. This is probably due to the fact that the chromium is present primarily in intermetallic form, whereas zirconium is primarily in solid solution. The difference in conductivities between alloys 17 and 18 increases at aging times beyond 20 hr.

#### 4. QUENCH SENSITIVITIES

Quench sensitivities of the Phase II alloys were studied in a modified Jominy test. Bars measuring 0.25 by 0.40 by 6.0 in. were solution-treated at 860° F and end-quenched by immersing the bottom 2 in. in 64° F water. The bars remained partly immersed until they cooled to room temperature. Relating the hardness data from the quench-sensitivity bar for 7075-T6S1-1 to cooling-rate-versus-strength data for 7075 (3), the cooling rate 1 in. above the waterline on the bar was estimated at 11° F per second.

The bars were then aged 2 days at room temperature, followed by 24 hr at 250° F and 10 hr at 320° F. A hardness survey was then conducted along the length of the bar, giving the results shown in Fig. 11.

The silver addition increases quench sensitivity (compare 16 and 17), as do higher copper content (compare 17 and 19) and higher zinc and magnesium contents (compare 17 and 20). Although the 7075 alloys have lower zinc and magnesium contents than alloy 16, 7075-T6S1-1 is more quench-sensitive than alloy 16 because it has a higher copper content.

The most important observation from this study is that the chromium-free alloy 18 (silver and zirconium) is quite insensitive to quenching rate. However, the quench sensitivity of the other chromium-free alloy X7080 is even lower, again indicating that the presence of silver increases quench sensitivity.

#### 5. MECHANICAL PROPERTIES

Mechanical properties of the Phase II alloys were measured on 8-in. flat tensile specimens with a reduced section of 2.25 by 0.5 by 0.25 in. For the comparison alloys, 3-in. round tensile specimens with a reduced section of 1.25 in. by 0.25 in. diameter were used. The gage length for the flat and round specimens was 2.0 in. and 1.0 in. respectively. Duplicate specimens of the Phase II alloys were taken in both the longitudinal and longitudinal-transverse grain directions. Only the data for the longitudinal grain direction are included for the comparison alloys; the number of specimens tested ranged from two to 40.

Table III lists the average mechanical properties of all the alloys. Figure 12 shows these properties in order of decreasing longitudinal yield strength to illustrate the strength relationships between the alloys. Appendix II contains complete tabulations of the tensile data.

With few exceptions (7178-T7651, 7575, 7079-T6-G, and 7578), the longitudinal yield strengths decrease in the same relative order as the as-received hardness values noted in Table I. The transverse mechanical properties are slightly lower than the longitudinal properties for all Phase II alloys except 16. It is not clear why alloy 16 behaves differently.

The silver addition in alloy 17 produces a small increase in yield strength (1.5 ksi) over that of alloy 16, in the longitudinal direction. Transverse mechanical properties of alloys 16 and 17 are nearly identical. Increased zinc and magnesium contents in alloy 20, replacement of chromium with zirconium in alloy 18, and increased copper content in alloy 19 all increase the strength above that of alloy 17. All Phase II alloys have yield strengths above the 70,000-psi goal and show higher strengths than any of the comparison alloys.

The comparison alloys with yield strengths above 70,000 psi are 7178-T7651 and 7575. This would be expected since both alloys are quite similar to some of the Phase II alloys in heat treatment and composition. The 7178-T7651 and alloy 19 have similar compositions (Fig. 1) except for silver content, and both were overaged to a similar degree (Table I). The 7575 and alloy 17 have similar compositions (Fig. 1) and had nearly the same overaging treatment (Table I).

Alloys 7578 and 20 also have nearly identical compositions (Fig. 1) except for silver content. However, 7578 was overaged to a greater degree (T6 + 8 hr at 340°F) so that its strength was lowered below that of alloy 20 (T6 + 10 hr at 320°F). Another consideration is the fact that the 7578 specimens (as well as 7575 and 7178-T7651) were from 0.5-in.-thick material, compared to 0.25 in. for the Phase II alloys. A slower cooling rate would be expected for the 0.5-in. material, and could cause a drop of 1 to 4 ksi in mechanical properties (3).

The alloys 7079-T6-G, AZ74.61-A, 7079-T611-A, AZ74.61, and 7075-T73 all possess similar yield strength ranging from 66 ksi for 7079-T6-G to 63.5 ksi for 7075-T73 (Fig. 12). The 7075-T73 and the two lots of AZ74.61 (AZ74.61 and AZ74.61-A) (Fig. 12) have almost identical strengths. (The data for the AZ74.61 lot represent the average of 40 specimens.)

The yield strength of X7080-T7 is similar to that of 7075-T73; the average of seven specimens was 61.4 ksi. Tensile specimens of X7080-T7 were taken at several depths through an 8-in.-thick die forging which had been quenched in boiling water. The mechanical properties of this forging varied only slightly across its thickness. This would be expected on the basis of this alloy's composition (low chromium, low copper) and quench-sensitivity curve (Fig. 11).

The lowest-strength comparison alloy was 7079-T611-G with a yield strength of 55.6 ksi. Although the heat treatment used on this forging is not known, its high electrical conductivity and low mechanical properties indicate a high degree of overaging. However, the ultimate strength of 7079-T611-G is comparable to those of AZ74.61, AZ74.61-A, 7075-T73, and X7080-T7.

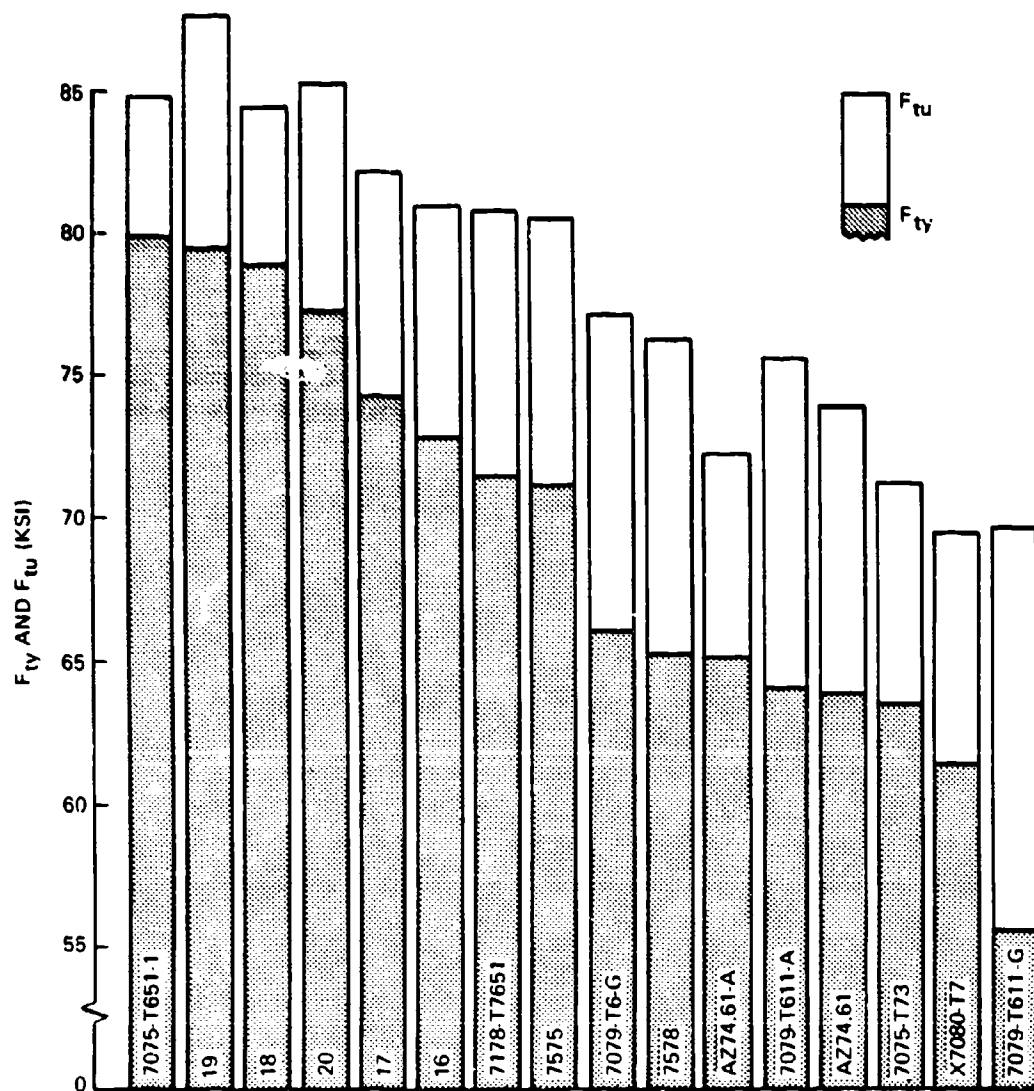


Figure 12. Longitudinal Mechanical Properties (Plotted in order of decreasing yield strength)



## 6. FRACTURE TOUGHNESS

The fracture toughness of Phase II alloys was measured on both center-notched panels (10 by 24 by 0.25 in.) and precracked Charpy specimens (2.16 by 0.39 by 0.25 in.) with the long dimension parallel to the longitudinal grain direction. Only limited precracked Charpy data are available for the comparison alloys. The center-notched panels were fatigue-cycled from an initial 0.5-in. sawcut to a crack length  $2a = 3.5$  in. prior to fracture testing. They were then loaded to fracture in laboratory air at a programmed stress rate of 1,000 psi/sec. The fracture toughness parameter  $K_{IC}$  was calculated from the relationship

$$K_{IC} = \sigma_g \sqrt{\pi a} \Theta$$

where  $\sigma_g$  = gross area stress at fracture (psi)

$a$  = 1/2 crack length before fracture (in.)

$\Theta$  = finite-width correction factor  $(w/\pi a \tan \pi a/w)^{1/2}$

All fracture toughness tests were valid with a  $\sigma_{net}/\sigma_{ty}$  ratio of less than 0.8 at fracture.

During testing of the center-notched fracture toughness panels, high-speed movies (1,000 frames per second) were taken to determine whether "slow" crack growth occurred before final rapid fracture. Some slow growth had occurred on all panels in the final few seconds of loading. The crack lengths ( $2a$ ) increased from 3.5 in. ( $2a$  at start of loading) to approximately 3.8 in. except in alloy 17, where cracks grew as far as 4.6 in. before catastrophic fracture.

Average fracture toughness data obtained from these tests (including those corrected for slow growth) are given in Table III. Complete data for each specimen are tabulated in Appendix II. The only trend observed in the toughness data is that, generally, both  $K_{IC}$  and the fracture toughness parameter  $W/A$  (energy to propagate per unit of crack area for precracked Charpy specimens) decrease as strength increases. The  $K_{IC}$  data indicate that alloys 16, 17, and 18 are tougher than 7075-T651-1, whereas alloys 19 and 20 are not. The  $W/A$  data indicate that all Phase II alloys have higher toughness than 7575, 7578, and 7178-T7651. The lower-strength comparison alloys X7080-T7 and AZ74.61 are tougher than the other comparison alloys and the Phase II alloys.

Examination of the precracked Charpy specimens and center-notched panels from the Phase II alloys revealed several items:

- a. The 7075-T651-1 showed much more intergranular short-transverse delamination or "splitting" on the fracture faces than did any of the overaged Phase II alloys. This difference is illustrated in Fig. 13, which shows the fracture surfaces of typical precracked Charpy specimens, and Fig. 14, which shows fracture profiles of typical center-notched panels taken 0.25 in. from the panel ends.
- b. Macroscopically, all Phase II alloys except 7075-T651-1 showed a nearly 100-percent shear-mode fracture in the center-notched panels (Fig. 14). 7075-T651-1 showed primarily a flat fracture mode.

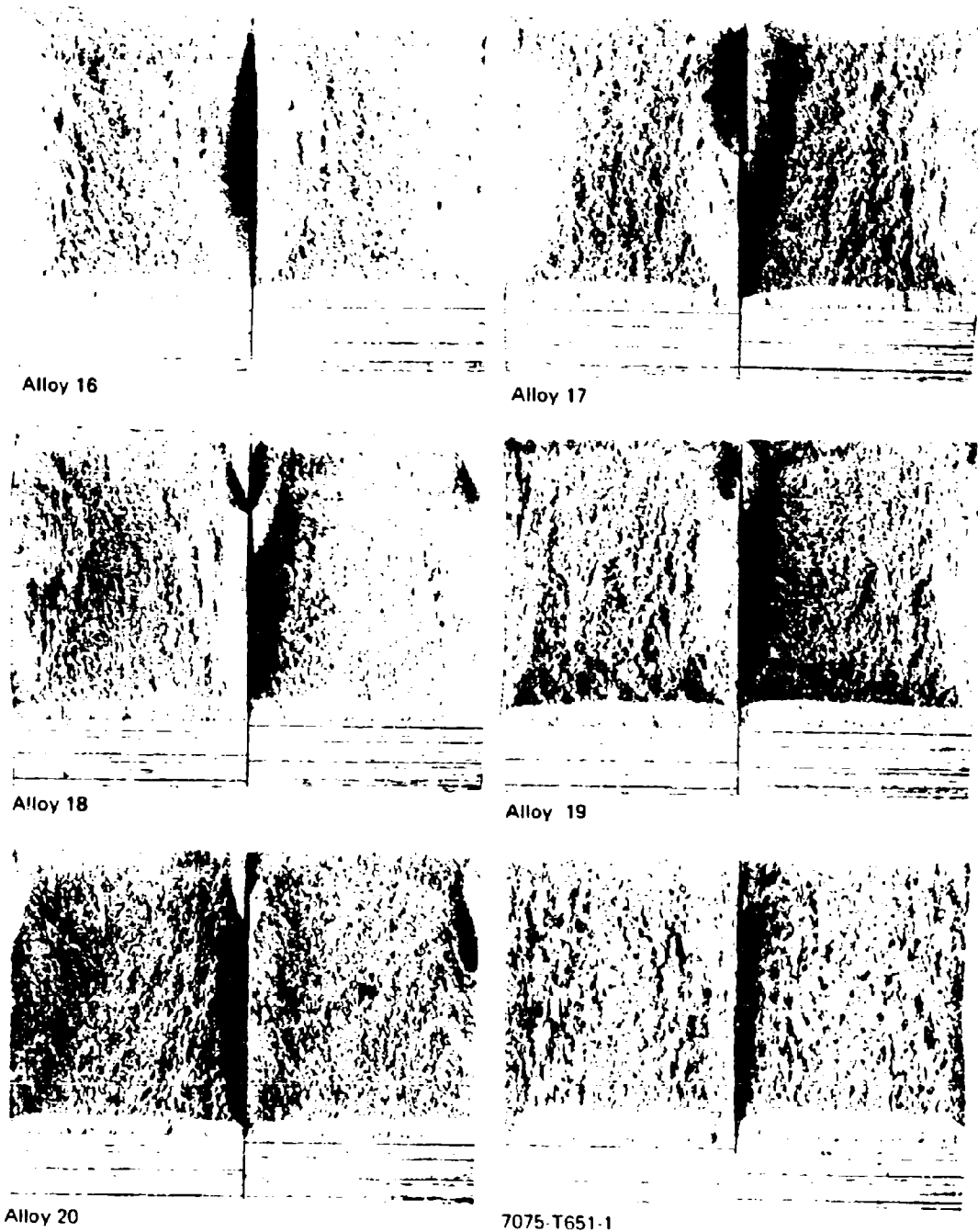


*Figure 15. Typical Fracture Surfaces of Precracked Charpy Specimens of Phase II Alloys (Note extensive short-transverse delamination on the 7075-T651-1 specimen.) (6x)*

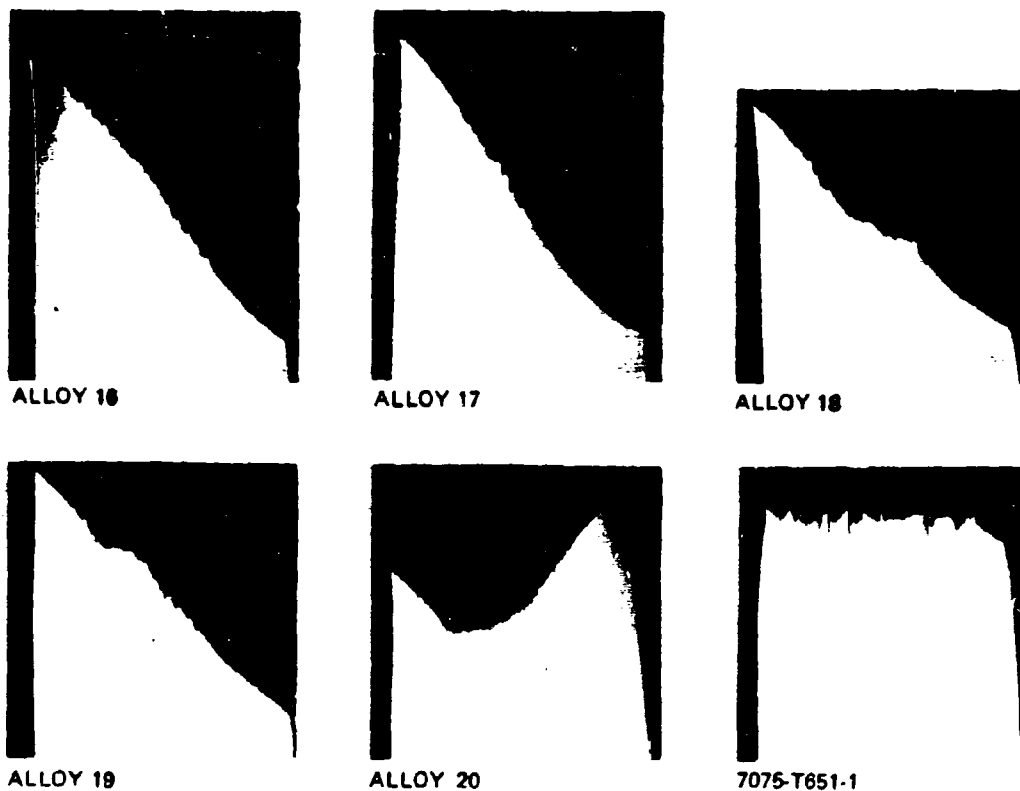


*Figure 14. Fracture Profiles from Phase II Alloy Center-Notched Panels  
(Sectioned 0.25 in. from panel edge) (6x)*

- c. Alloy 18 (zirconium, no chromium) had a fracture surface noticeably different from those of the other alloys in both color and texture. This difference is not readily apparent in Fig. 13.

To determine whether toughness and fracture topography could be correlated for the Phase II alloys, two-stage plastic-carbon replicas were made from precracked Charpy specimens of each alloy. Figure 15 shows the topographies for 7075-T651-1 and alloy 18. The topography shown for 7075-T651-1 was typical for all Phase II alloys except 18. The dimple size for alloy 18 is noticeably larger than for 7075-T651-1 and the other Phase II alloys.

## 7. FATIGUE LIFE

The center-notched panels were used to determine fatigue-crack growth characteristics of the Phase II alloys. The nature and extent of environmental effects on fatigue-crack growth were studied by cycling one panel of each alloy in dry air (< 10 percent relative humidity) and another panel in distilled water. Cyclic loading was applied at 120 cycles per minute (cpm) at a maximum gross area stress of 12,000 psi. The ratio of minimum cyclic stress to maximum cyclic stress was  $R = 0.5$ . Crack growth was monitored from  $2a = 0.5$  in. to  $2a = 3.5$  in.

Figure 16 presents data on crack length versus cycles for each alloy and environment. Figure 17 is a plot of stress intensity factor  $K$  versus crack growth rate  $\Delta 2a/\Delta n$  for each alloy and environment. The slopes of the lines in Fig. 17 range from 2.4 (alloy 19 in distilled water) to 4.4 (alloy 19 in dry air).

All alloys perform similarly in the dry environment; the curves for alloys 19 (high copper) and 20 (higher zinc and magnesium) are steeper at crack lengths longer than 2.0 in. (Fig. 16). The silver addition in alloy 17 has little effect. (Compare alloys 16 and 17.) The replacement of chromium with zirconium in alloy 18 and the higher zinc and magnesium in alloy 20 result in about 17 percent fewer cycles being required for crack growth from 0.5 to 3.5 in. than are required in alloy 17. All overaged alloys except alloy 20 require more cycles than does the peak-aged 7075-T651-1 to propagate the crack to 3.5 in.

The difference between the overaged Phase II alloys and the peak-aged 7075-T651-1 is more pronounced in distilled water. In this environment all overaged Phase II alloys require two to three times as many cycles as the peak-aged 7075-T651-1 to propagate cracks from 0.5 to 3.5 in. Other comparisons noted in the number of cycles required for propagation from 0.5 to 3.5 in. are the following:

- a. The silver addition in alloy 17 increases the number of cycles about 16 percent in comparison with alloy 16;
- b. Replacement of chromium with zirconium in alloy 18 reduces the number of cycles about 32 percent in comparison with alloy 17;
- c. Increasing the copper content in alloy 19 reduces the number of cycles about 38 percent in comparison with alloy 17;



(A) 7075-T651-1



(B) Alloy 18

*Figure 15. Typical Electron Fractographs of Fractured Charpy Specimens of 7075-T651-1 and Alloy 18. (The larger dimple size in alloy 18 is due to the absence of chromium-rich intermetallics.) (3450x)*

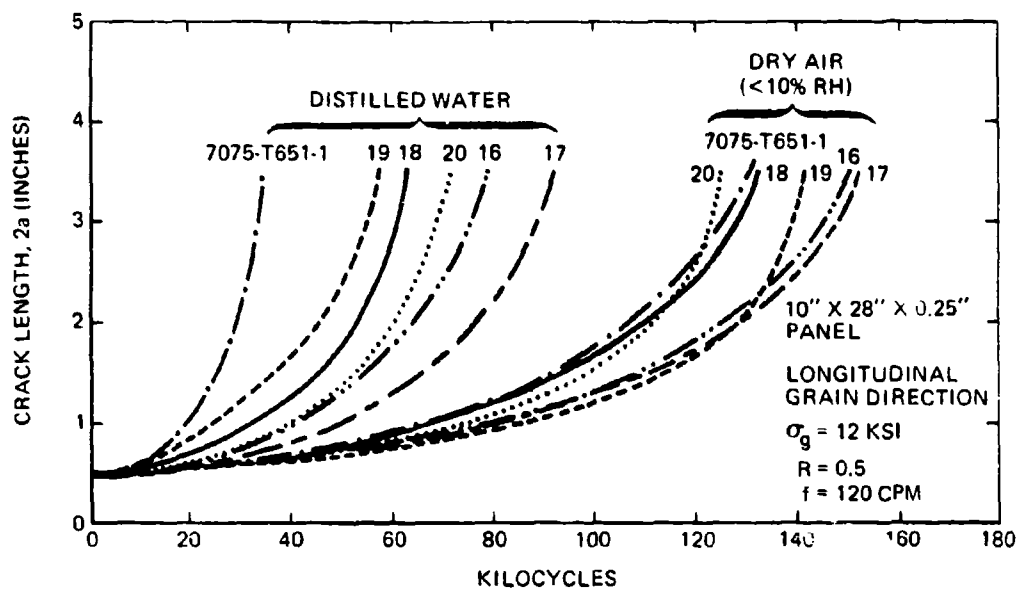


Figure 16. Fatigue-Crack Propagation Curves for Phase II Alloys

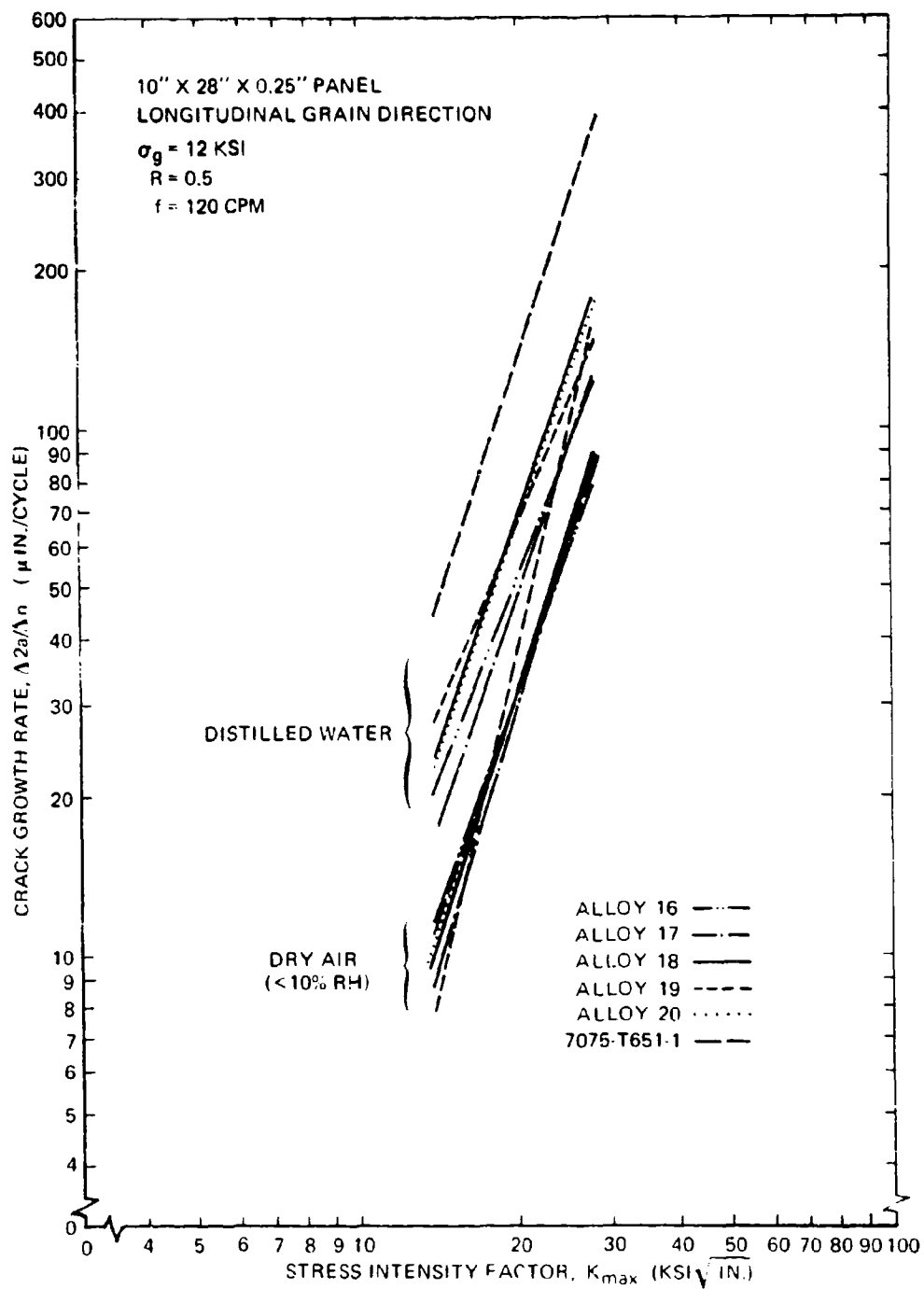


Figure 17. Fatigue Crack Growth Rate Versus Stress Intensity for Phase II Alloys

- d. Increasing the zinc and magnesium contents in alloy 20 reduces the number of cycles about 24 percent in comparison with alloy 17.

Although distilled water accelerates crack growth in all alloys, the effect is less pronounced for the overaged Phase II alloys than for peak-aged 7075-T651-1.

The fracture topographies of these specimens were examined by electron fractography to determine whether the different growth rates could be correlated with fracture features. Figure 18 shows typical fractographs from alloys 16, 17, and 7075-T651-1 in both environments. In these photographs the crack length  $2a$  is 2 in., which corresponds to

$$K = 21 \text{ ksi} \sqrt{\text{in.}}$$

For easy comparison, all the fractographs are at the same magnification. The observations from the fractographs may be summarized as follows:

- a. The fatigue-crack propagation mechanism in dry air produces the characteristic ductile fatigue striations.
- b. The fracture appearance in distilled water is markedly different for peak-aged 7075-T651-1. Ductile striations are only rarely observed, and the predominant propagation mechanism results in brittle striations. Alloys 16 and 17 show brittle striations, but many ductile striations are also observed.

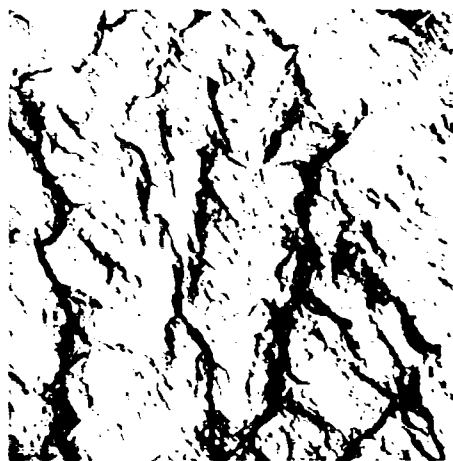




7075-  
T651-1



Alloy  
16



Alloy  
17



Dry Air (<10% R.H.)

Distilled Water

Figure 18. Typical Electron Fractographs of Fatigued Center-Notched Panels of Alloys 7075-T651-1, 16, and 17 Tested in Two Environments (4550x)

## SECTION III

### STRESS-CORROSION TESTING

#### 1. CONDITIONS AND PROCEDURES

The six Phase II alloys and eleven comparison alloy lots were tested as shown in Appendix III. Test conditions and procedures in Phase II were the same as those established in Phase I (1). The test specimen, shown in Fig. 19, was stressed by leg deflection. Values of leg deflection used to impose the various stress levels are shown in the same figure.

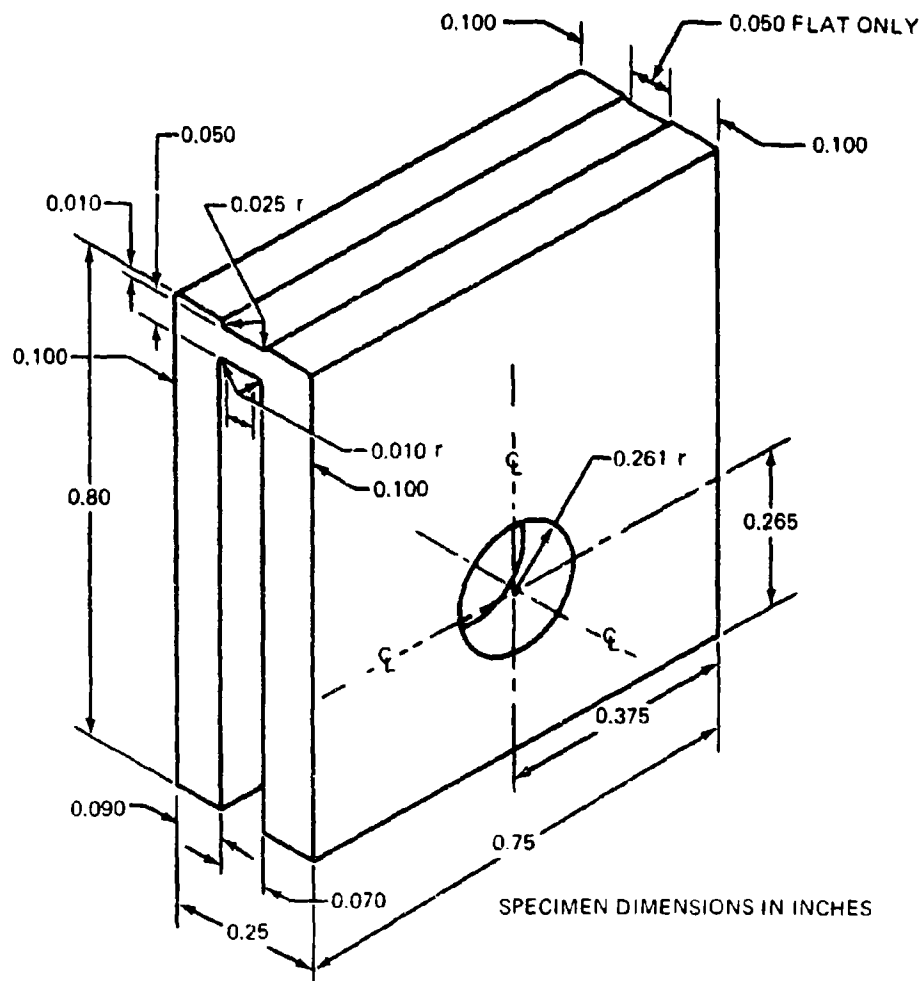
Two test environments were used on the specimen configuration shown in Fig. 19: (1) alternate immersion in an aqueous 3.5-percent sodium chloride solution, and (2) outside exposure in an industrial area. The alternate-immersion test specimens were anodized (chromic acid) to reduce general corrosion and to aid in detecting cracks and linear pits. The outside-exposure specimens were not anodized.

In additional tests, double-cantilever beam (DCB) specimens were exposed to 3.5-percent sodium chloride solution three times a day, and exfoliation coupons were exposed in a salt-fog cabinet to a 5-percent sodium chloride solution buffered with acetic acid to pH = 3.0.

The ambient conditions for Phase II were slightly different from those for Phase I. The air temperature during alternate-immersion testing ranged from 78° F to 81° F for Phase II, compared with 75° F to 82° F for Phase I. The range of relative humidity (RH) was 55 to 62 percent for Phase II and 45 to 55 percent for Phase I. The outside-exposure specimens were in test over different parts of the year (October-February for Phase II compared with January-March and May-August for Phase I) and thus experienced different temperature, humidity, and smog conditions.

All the alternate-immersion specimens were tested in the same 60-gal fill-and-drain system over the same time period, with the exception of the second lot of 7075 material (7075-T651-2), which was placed in test 44 days after the other alloys. Each specimen was photographed every 2 weeks during exposure to record the progressive changes and to aid in determining growth rates of cracks or pits. In addition, each specimen was examined regularly under a 10X wide-field binocular microscope to determine the time to first crack or linear pit and the time to failure (arbitrarily defined as cracks, pits, or linear pits along the entire length of the test section).

At the end of testing, specimens of the various alloy and stress-level combinations were sectioned to determine the nature of the attack that occurred. One specimen of each Phase II alloy at each stress level and one specimen of each comparison alloy stressed at 26 and 56 ksi were examined. The basis for selecting specimens for sectioning was the extent of pitting or cracking; in all cases the most severely attacked specimen of the stress-level group was sectioned. The sectioned specimens are listed in Appendix III.



SHORT-TRANSVERSE STRESS, $\sigma$ (KSI)	LEG DEFLECTION, $\delta^*$ (IN.)
14	0.0065
20	0.0092
26	0.0120
32	0.0147
44	0.0203
56	0.0257

\* MEASURED AT BOTTOM OF LEG

Figure 19 Stress-Corrosion Test Specimen and Leg Deflections

## 2. RESULTS

### a. Alternate-Immersion Testing

Results of the tests are summarized in Table IV. At 32, 44, and 56 ksi, alloys 18 and 19 are less resistant to stress-corrosion cracking than the other Phase II alloys, but both alloys are more resistant than the second heat of 7075 (7075-T651-2). All the comparison alloys showed relatively high resistance with the exceptions of 7079-T6-G and 7575. The higher susceptibility of extruded 7575 as compared with alloy 17 was unexpected, since both alloys have similar compositions and were heat-treated similarly.

The resistance of 7079-T611-A was better than expected. This is related to the fact that several of the six specimens tested contained equiaxed grain structures or grain flow parallel to the stress direction. These specimens were taken from a forging, and not all of them contained the parting plane.

The alloys were compared as to extent of cracking or linear pitting by determining what part of the total length of each specimen contained cracks or linear pits at the end of testing. The summary data are given in Appendix III. The average data as functions of alloy and stress level are plotted in Fig. 20.

The results of this analysis correlate well with the failure-time data, Table IV, except for comparison alloys AZ74.61, 7075-T73, 7178-T7651, and 7578. These alloys are subject to extensive damage at the higher stress levels, but this damage consists predominantly of pitting and linear pitting rather than the pronounced intergranular cracking prevalent in several other alloys.

To rate the alloys accurately, the data of Table IV and Fig. 20 must be used in conjunction with information obtained from cross sections. Cross-section and time-sequence photographs are displayed in Figs. 21 through 51 for stress levels of 26 ksi (Phase II and comparison alloys) and 32 and 44 ksi (Phase II alloys only). The end-of-test photographs of all other specimens are shown in Appendix IV.

#### (1) 14-KSI Specimens

None of the 20 specimens stressed to 14 ksi failed in alternate-immersion testing. End-of-test photographs of the 14-ksi specimens are shown in Appendix IV. Alloy 16 showed some surface pitting after exposure, and alloys 17 and 20 had essentially the same appearance as alloy 16. Additional copper (compare alloy 17 with 19) caused an increase in surface pitting. Alloys 18, 7075-T651-1, and 7075-T651-2 showed little or no corrosion attack.

Cross sections through the pitted areas of these specimens showed that the damage was restricted to shallow pits except in 7075-T651-2. Short, blunt intergranular protrusions extended from the bottoms of the pits. The total depth of attack was less than 0.009 in. One of the two 7075-T651-2 specimens showed sharp intergranular cracking.

Table IV. Summary of Stress-Corrosion Test Data (Alternate Immersion <sup>a</sup>)

Alloy	No. of specimens failed/No. in test - (days to failure)					
	14 ksi	20 ksi	26 ksi	32 ksi	44 ksi	56 ksi
16	0/3	0/5	0/6	1/5 (44) <sup>b</sup>	0/3	0/2
17	0/3	0/5	0/6	0/5	0/3	0/2
18	0/3	0/5	0/6	1/5 (89)	3/3 $\left(\begin{smallmatrix} 61, \\ 89, \\ 83 \end{smallmatrix}\right)$	2/2 $\left(\begin{smallmatrix} 61, \\ 62 \end{smallmatrix}\right)$
19	0/3	0/5	0/6	0/5	1/3 (83)	2/2 $\left(\begin{smallmatrix} 58, \\ 29 \end{smallmatrix}\right)$
20	0/3	0/5	0/6	1/5 (44) <sup>b</sup>	0/3	1/2 (83)
7075-T651-1	0/3	0/5	0/6	0/5	2/3 $\left(\begin{smallmatrix} 89, \\ 89 \end{smallmatrix}\right)$	2/2 $\left(\begin{smallmatrix} 29, \\ 50 \end{smallmatrix}\right)$
7075-T651-2	0/2	0/2	2/2 $\left(\begin{smallmatrix} 47, \\ 25 \end{smallmatrix}\right)$	2/2 $\left(\begin{smallmatrix} 10, \\ 11 \end{smallmatrix}\right)$	2/2 $\left(\begin{smallmatrix} 10, \\ 27 \end{smallmatrix}\right)$	2/2 $\left(\begin{smallmatrix} 6, \\ 6 \end{smallmatrix}\right)$
AZ74.61	---	---	0/2	0/2	0/2	0/2
AZ74.61-A	---	0/1	0/2	---	0/1	0/1
7075-T73	---	0/1	0/2	---	0/2	0/1
X7080-T7	---	1/1 (44) <sup>b</sup>	0/2	---	0/2	0/1
7079-T611-A	---	0/1	0/2	---	0/2	1/1 (5)
7079-T611-G	---	0/1	0/2	---	0/2	0/1
7079-T6-G	---	0/1	2/2 $\left(\begin{smallmatrix} 4, \\ 89 \end{smallmatrix}\right)$	---	2/2 $\left(\begin{smallmatrix} 2, \\ 2 \end{smallmatrix}\right)$	1/1 (1)
7575	---	---	0/2	2/2 $\left(\begin{smallmatrix} 89, \\ 37 \end{smallmatrix}\right)$	1/2 (42)	2/2 $\left(\begin{smallmatrix} 28, \\ 44 \end{smallmatrix}\right)$
7578	---	---	0/2	0/2	1/2 (83)	1/2 (83)
7178-T7651	---	---	0/2	0/2	0/2	0/2

<sup>a</sup>3.5% NaCl solution.

<sup>b</sup>Poorly anodized

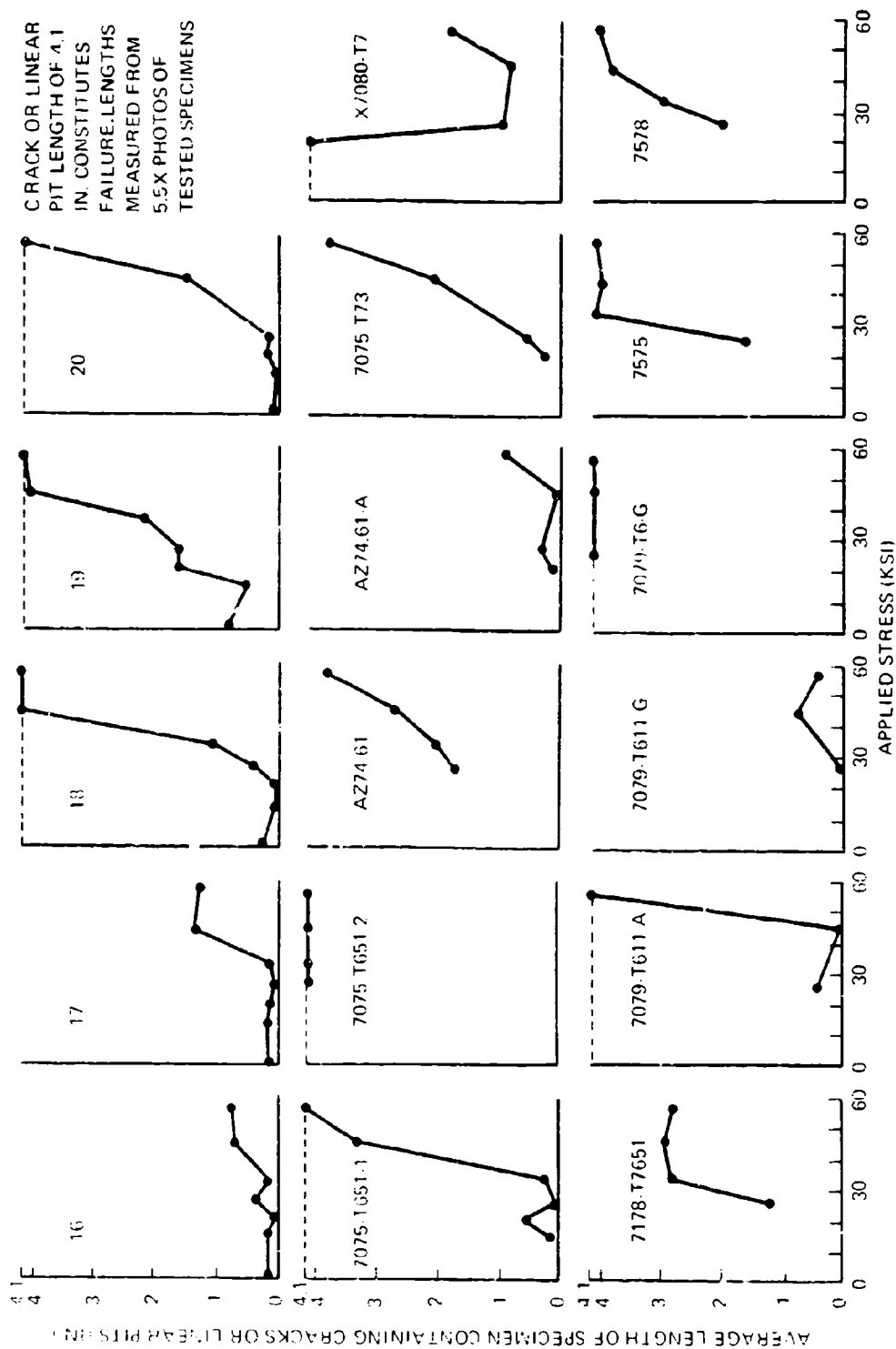


Figure 20. Extent of Cracking and Pitting on Phase II and Comparison Alloy Tested by Alternate Immersion in 3.5-Percent Sodium Chloride Solution

## (2) 20-KSI Specimens

None of the 38 specimens stressed to 20 ksi failed in alternate-immersion testing. End-of-test photographs of these specimens are shown in Appendix IV. Again there was little difference between the surface appearances of alloys 16 and 17. Some general pitting was apparent. Alloy 20 was slightly more heavily pitted and alloy 19 much more heavily pitted than alloys 16 and 17. Alloy 18 was virtually unattacked. The two heats of 7075 showed some general corrosion, and 7075-T651-1 showed some linear pitting.

Cross sections through the pitted or cracked areas of these specimens showed the following:

Alloy 16	Very shallow pitting; depth less than 0.001 in.
Alloy 17	Pitting, sharp intergranular cracks; depth 0.018 in.
Alloy 18	No pitting or cracking
Alloy 19	Pitting, sharp intergranular cracks; depth 0.025 in.
Alloy 20	Rounded pits, blunt intergranular protrusions; depth 0.008 in.
7075-T651-1	Rounded pits, blunt intergranular protrusions; depth 0.010 in.
7075-T651-2	Sharp intergranular cracking

## (3) 26-KSI Specimens

Four failures occurred in the 58 specimens stressed to 26 ksi. Both 7075-T651-2 specimens and both 7079-T6-G specimens failed at this level. Time-sequence and cross-section photographs are shown in Figs. 21 through 37 for a heavily damaged specimen from each of the Phase II and comparison alloys. The end-of-test photographs for the remaining 26-ksi specimens are shown in Appendix IV.

Observation of the surfaces and cross sections produced the following findings:

Alloy 16	Ranged from no attack to moderate linear pitting
Alloy 17	Minor pitting
Alloy 18	Linear pitting, sharp intergranular cracking; depth 0.035 in.
Alloy 19	General pitting and linear pitting, blunt intergranular protrusions; depth 0.006 in.

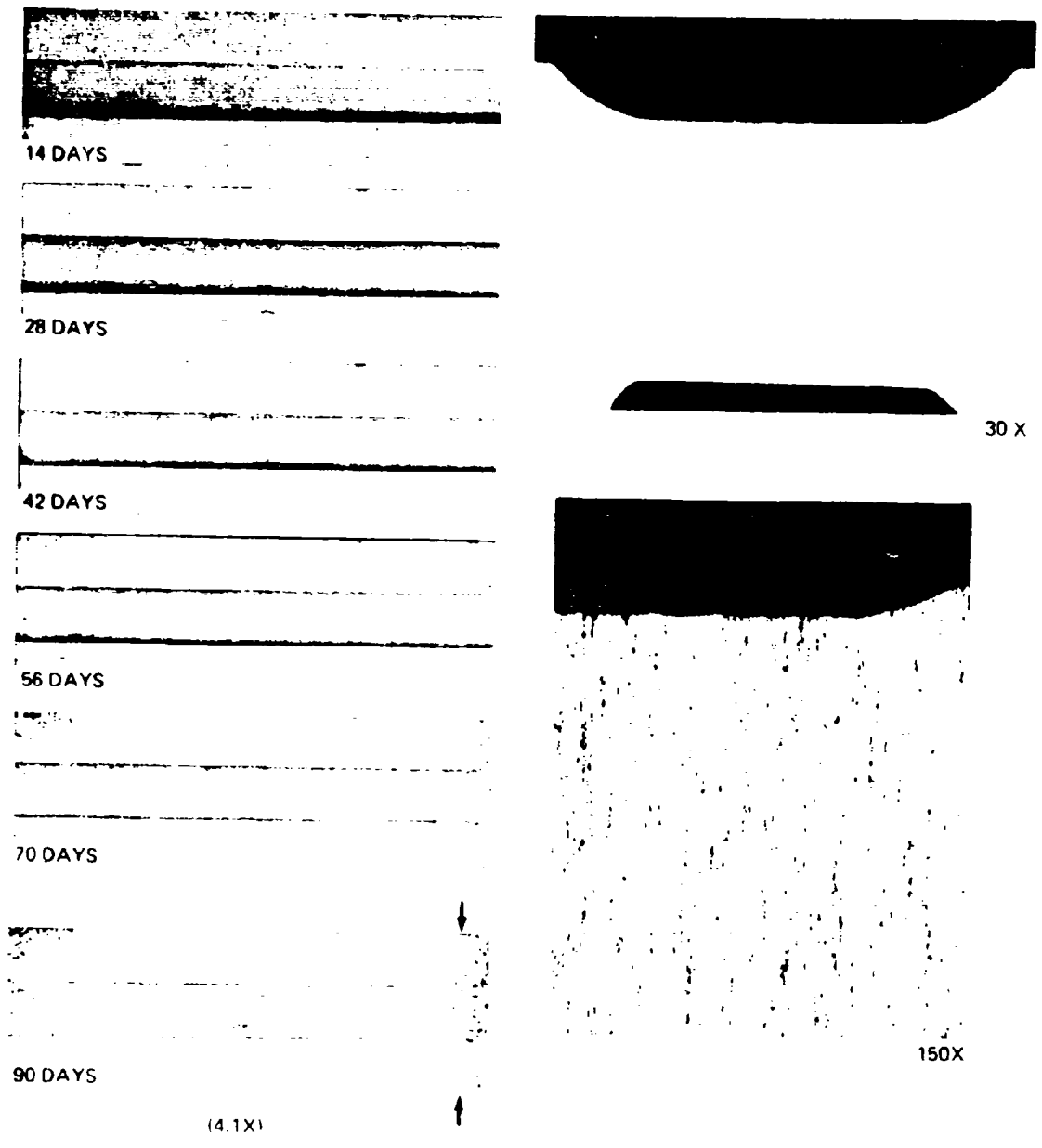


Figure 21. Time-Sequence and Cross-Section Photographs of 16-2 S at 26 KSI



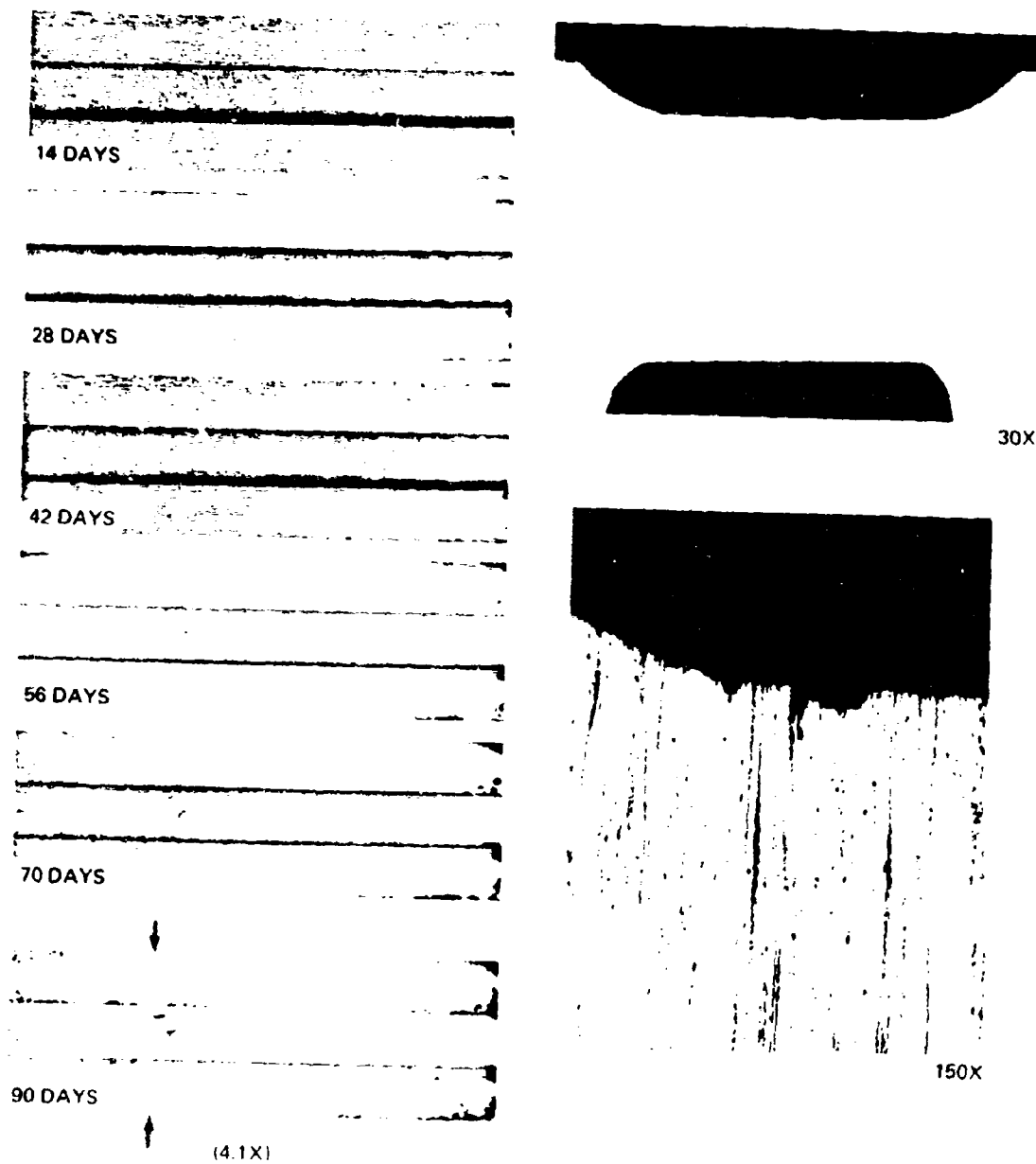


Figure 22. Time-Sequence and Cross-Section Photographs of 17-16 at 26 KSI

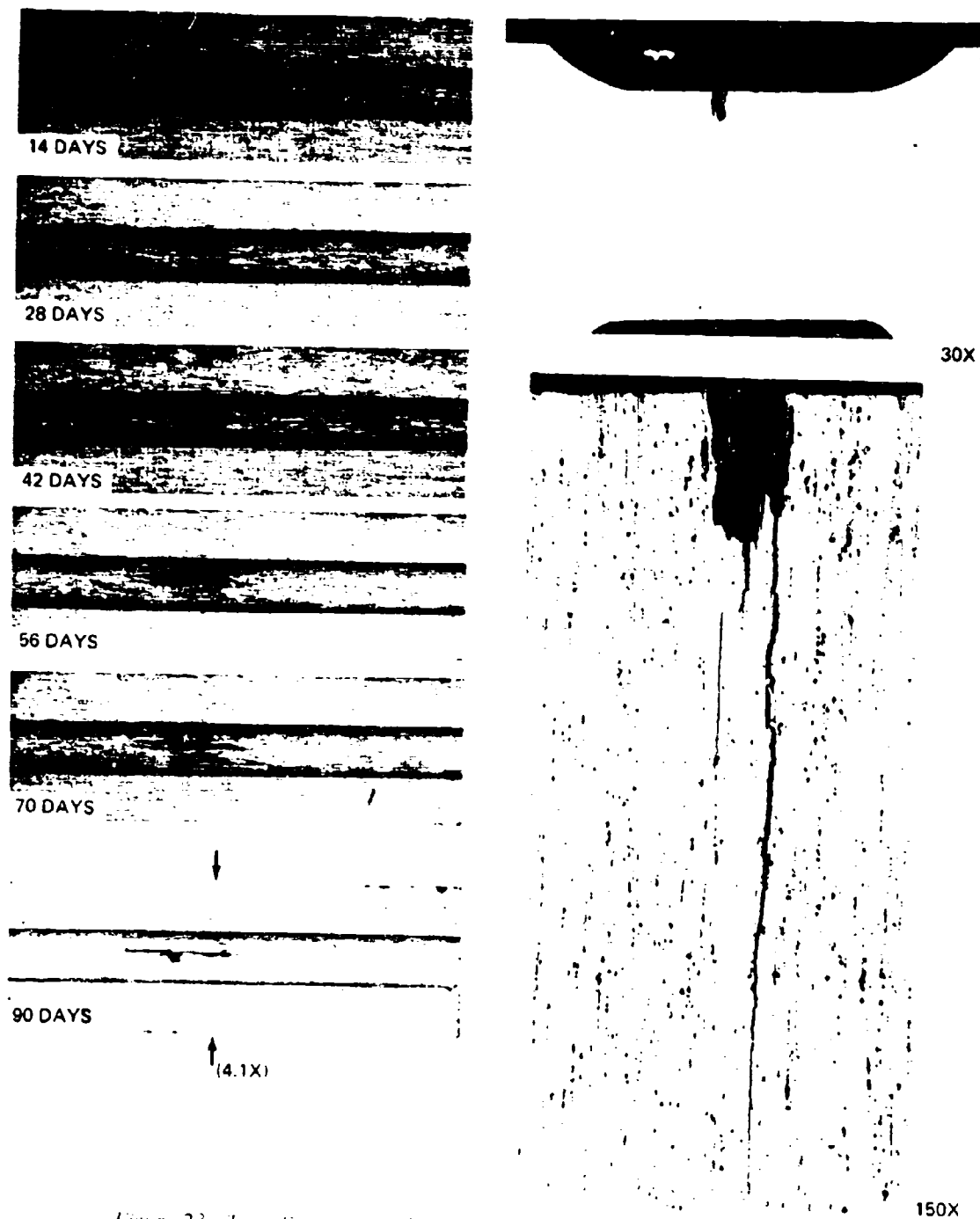


Figure 23. Time-Sequence and Cross-Section Photographs of 18-S at 26 KSI

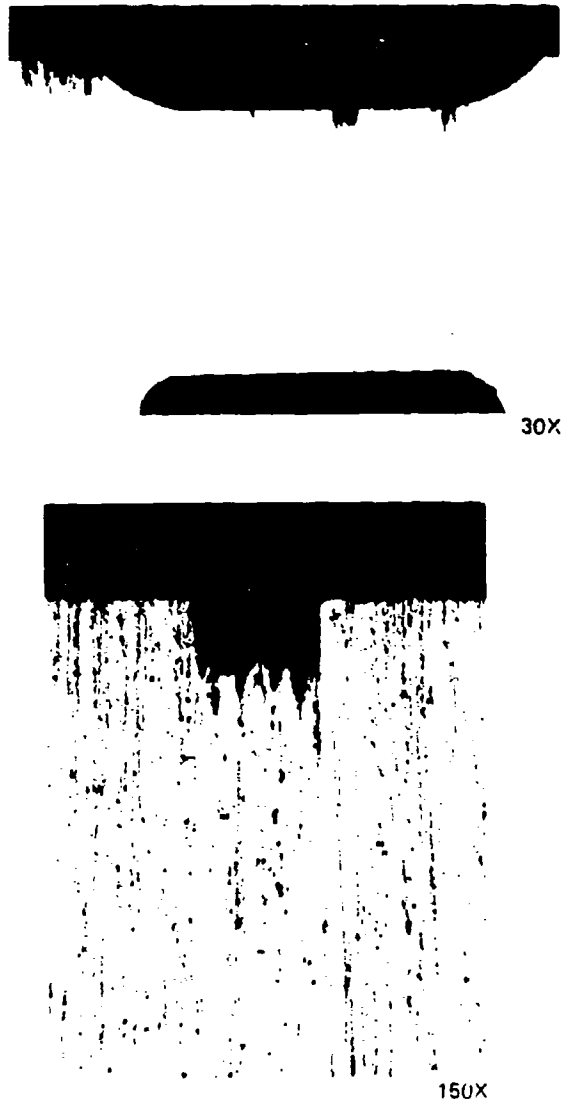
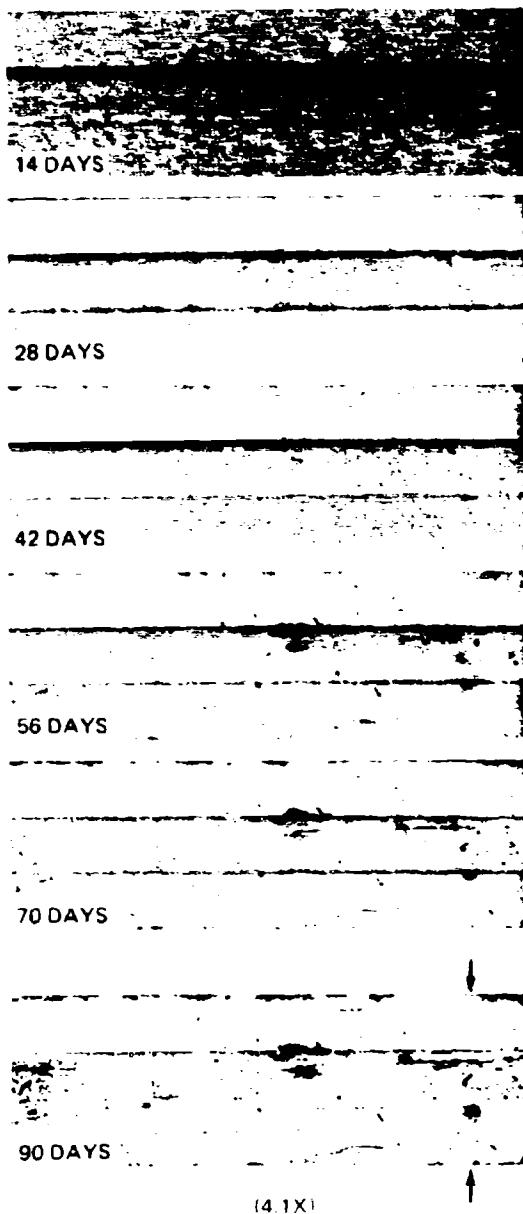
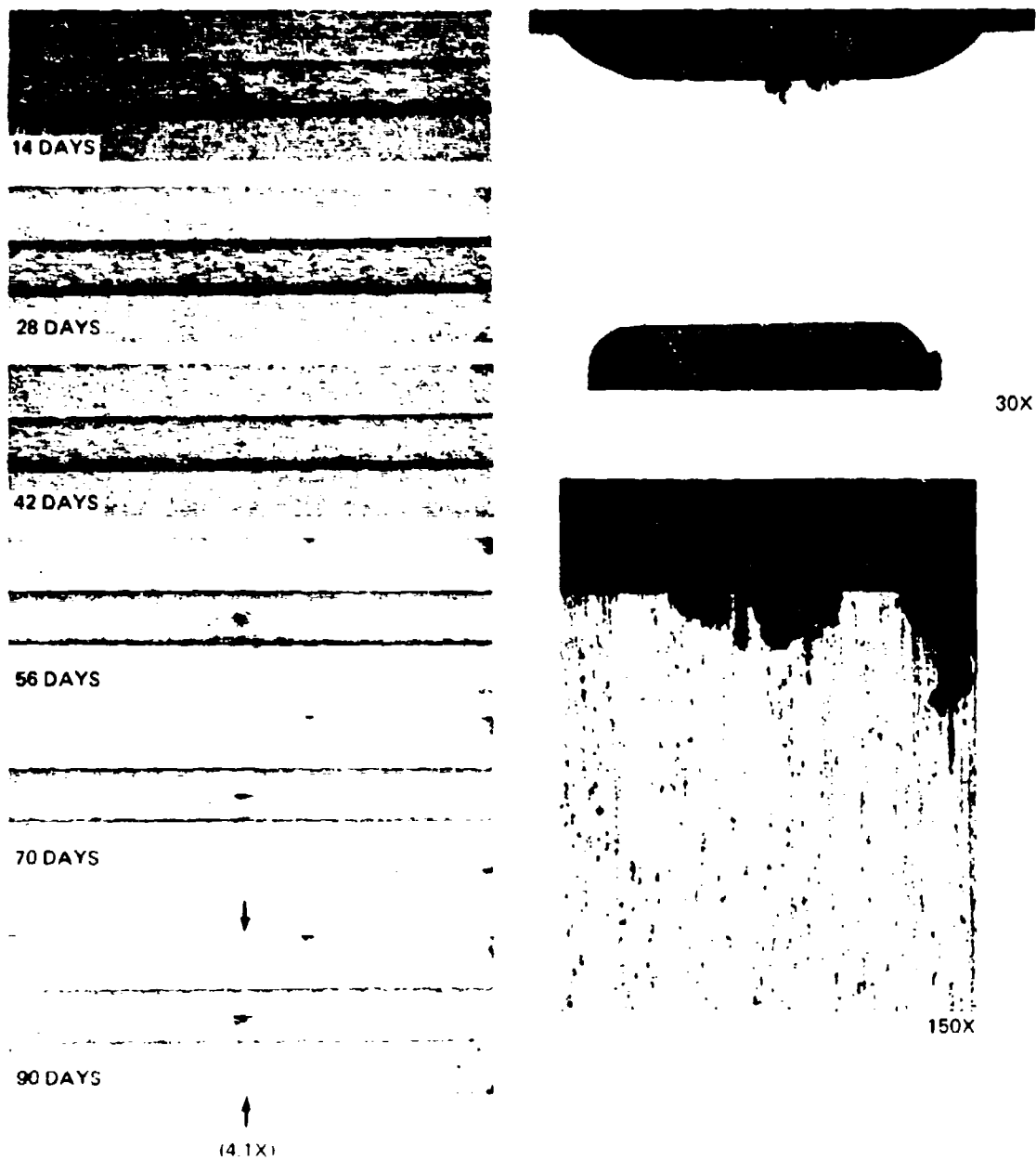
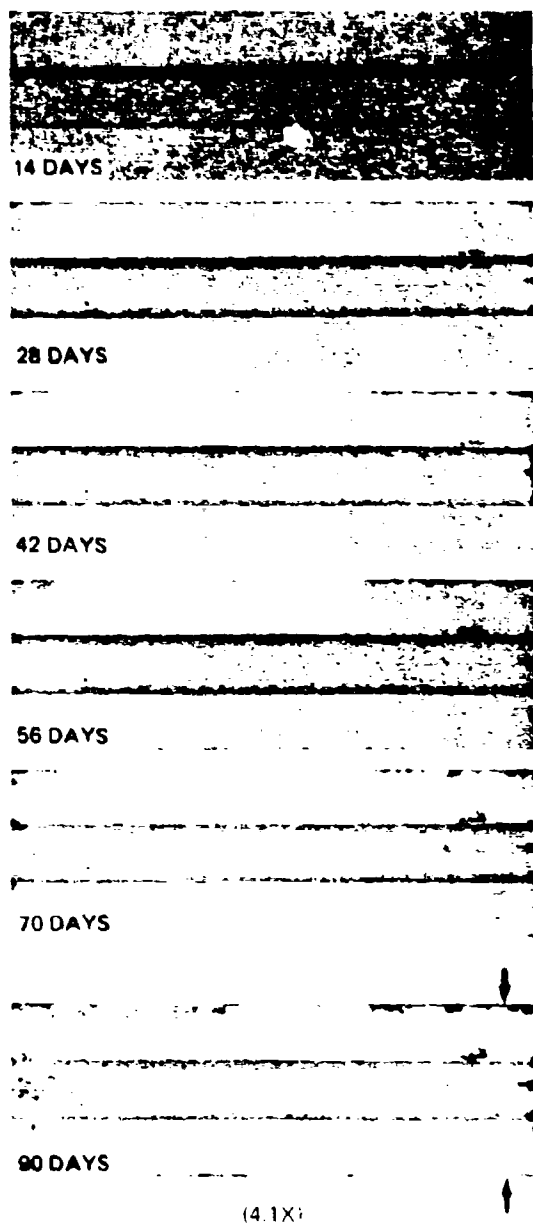


Figure 24. Time-Sequence and Cross-Section Photographs of 19-5 at 26 KSI



*Figure 25 Time Sequence and Cross-Section Photographs of 26-11 at 26 KSI*



30X



150X

*Figure 26. Time-Sequence and Cross-Section Photographs of 7075-T651-1-23 at 26 KSI*



Figure 27. Time-Sequence and Cross-Section Photographs of 7075-T6S1-2-11 at 26 KSI

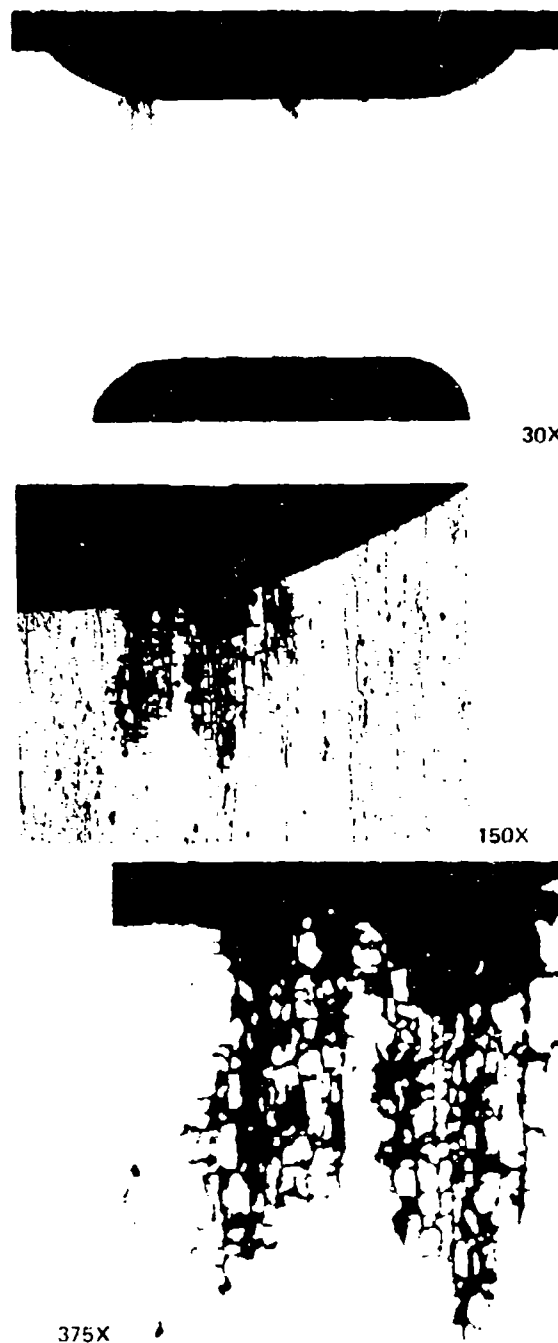
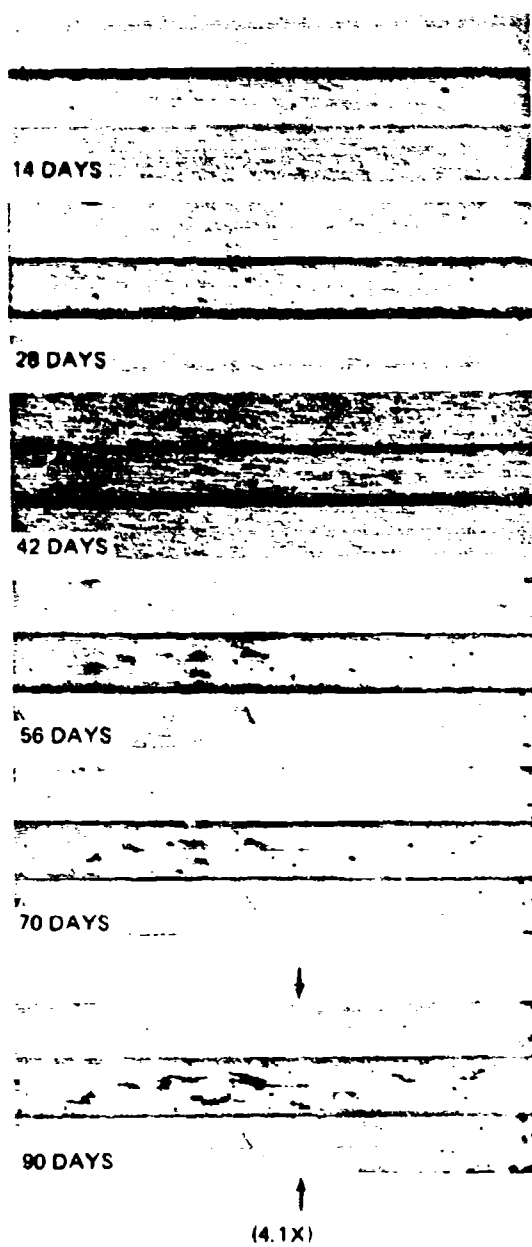


Figure 28. Time-Sequence and Cross-Section Photographs of AZ74-61 (2-2) at 26 KSI

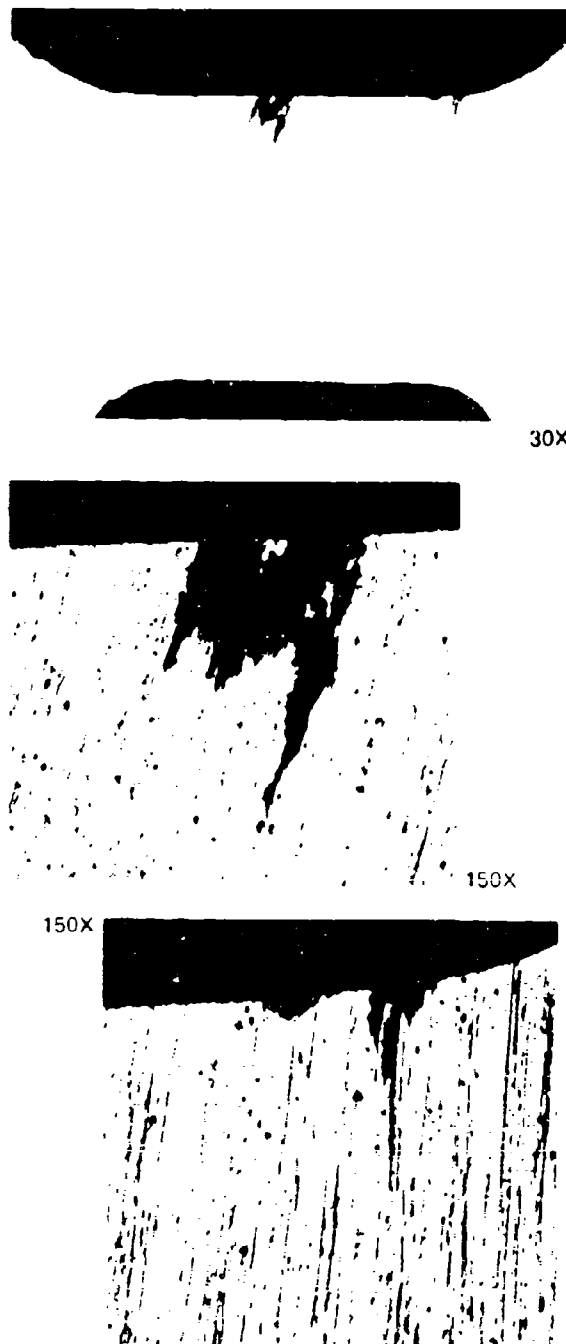
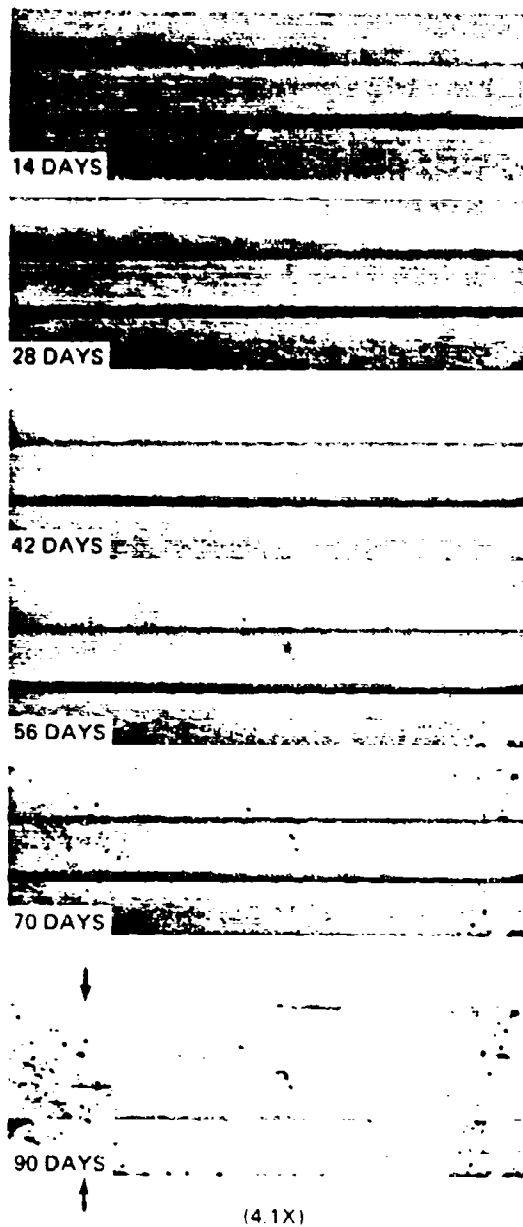


Figure 29 Time-Sequence and Cross-Section Photographs of AZ7461 (A-7) at 26 KSI



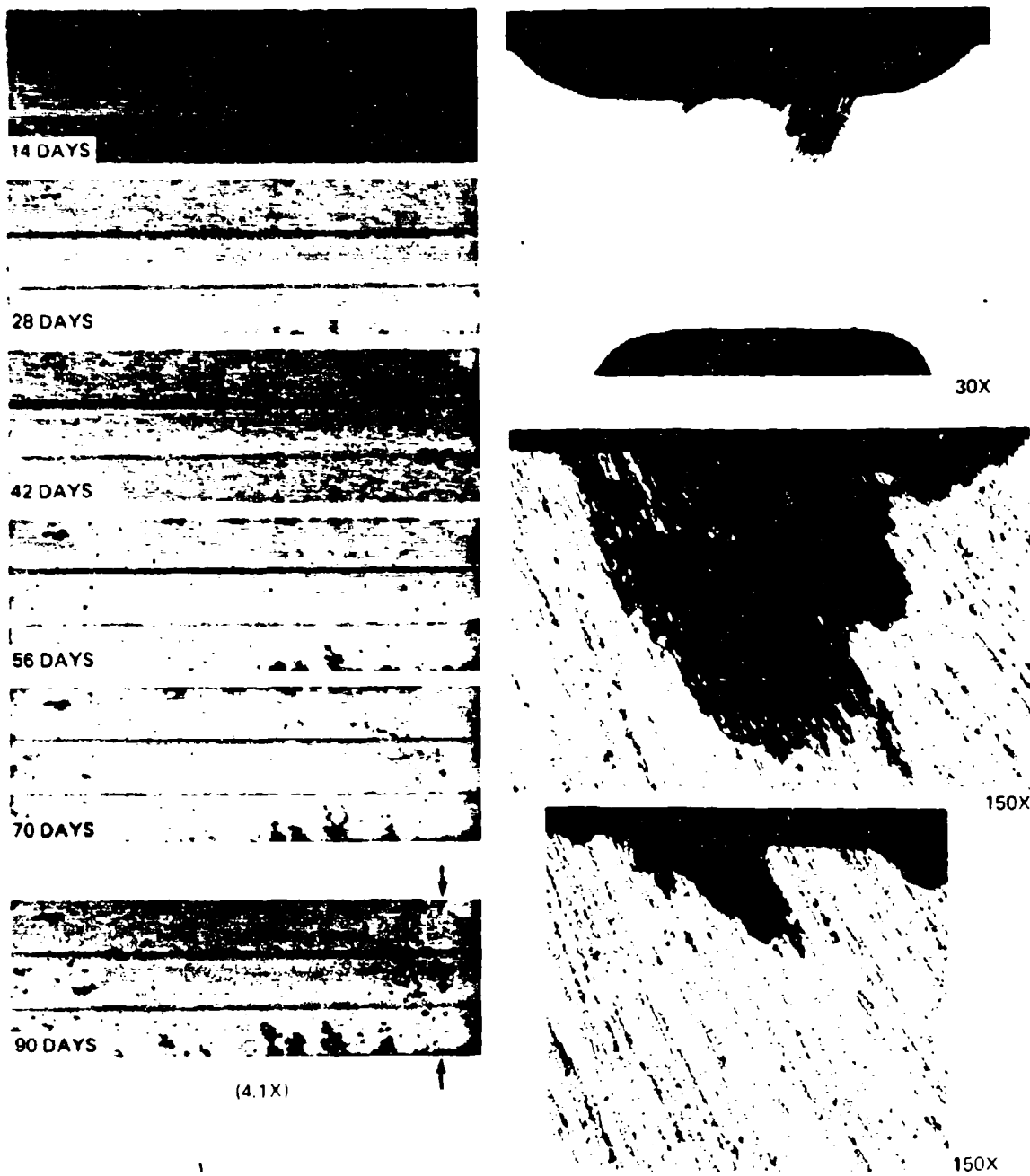


Figure 30 Time-Sequence and Cross-Section Photographs of 7075-T73 (B-7) at 26 KSI

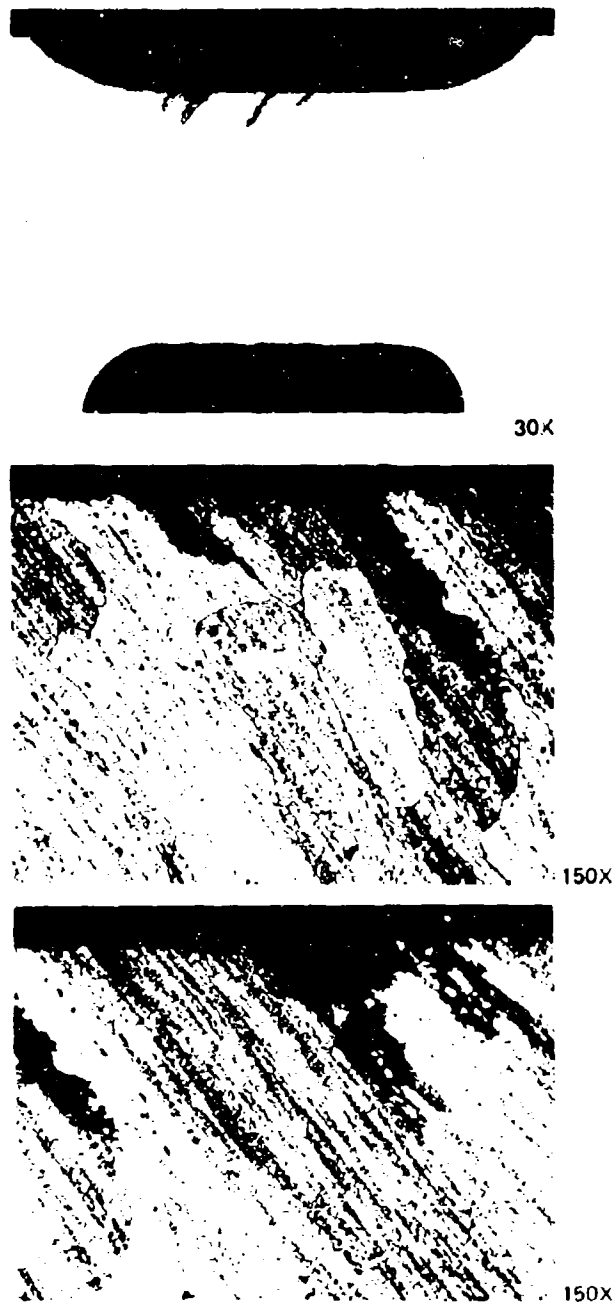
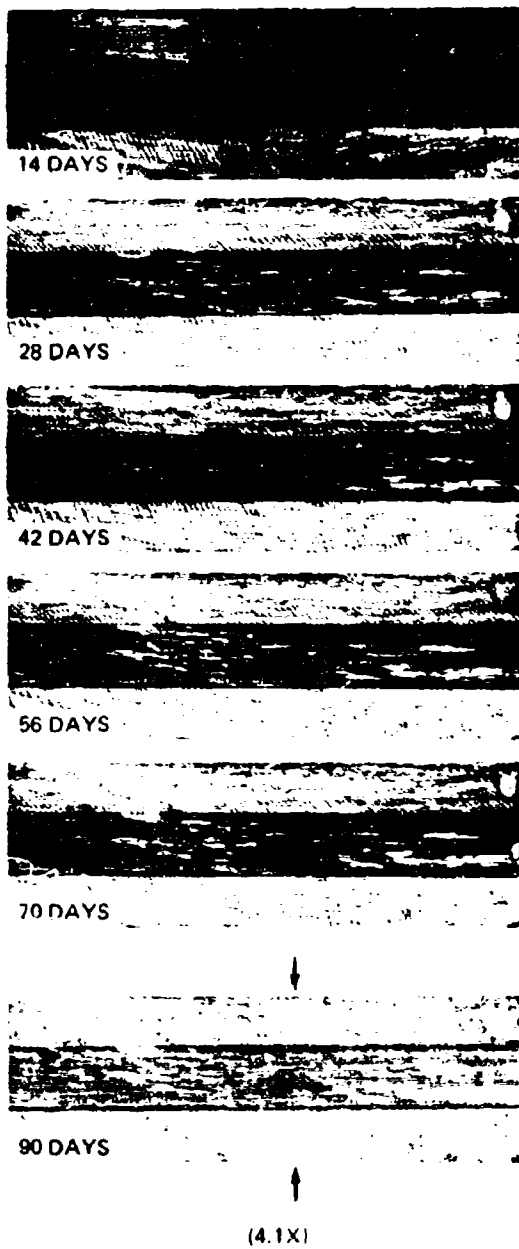
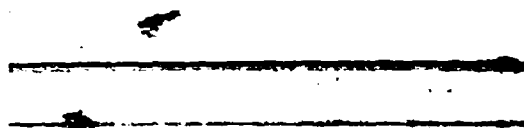
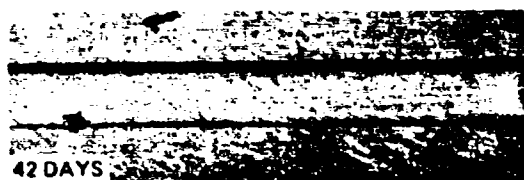
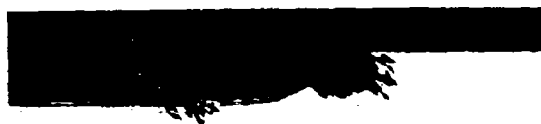


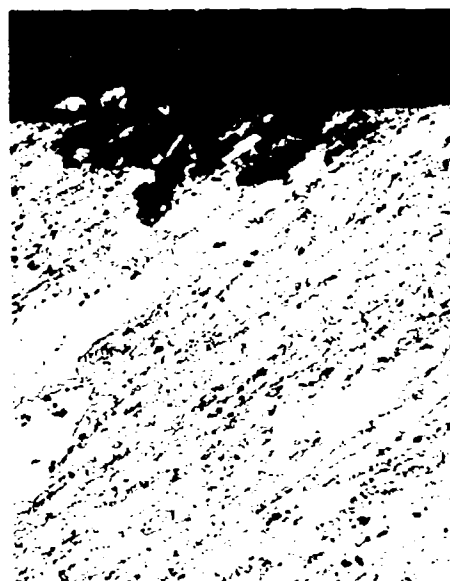
Figure 31. Time-Sequence and Cross-Section Photographs of X70S0-T7 (D-S) at 26 KSI



(4.1X)

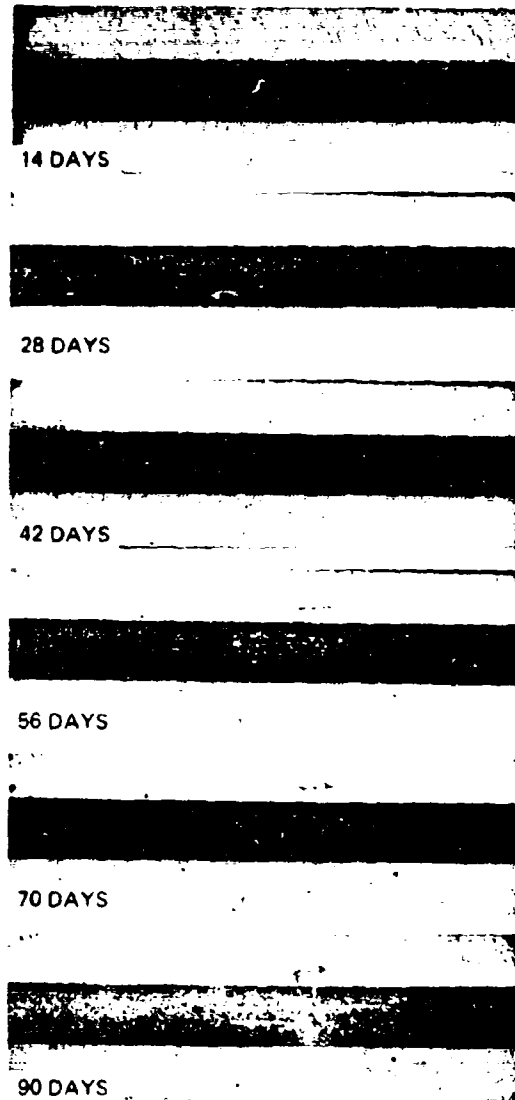


30X



150X

Figure 32. Time-Sequence and Cross-Section Photographs of 7079-T611-A (C-7) at 26 KSI



(4.1X)

*Figure 33. Time-Sequence Photographs of 7079-T611-G (F-9) at 26 KSI*

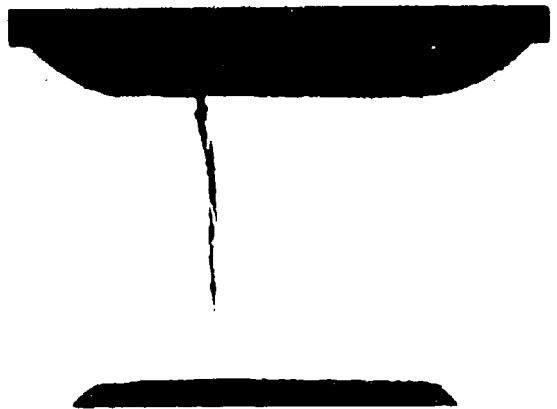
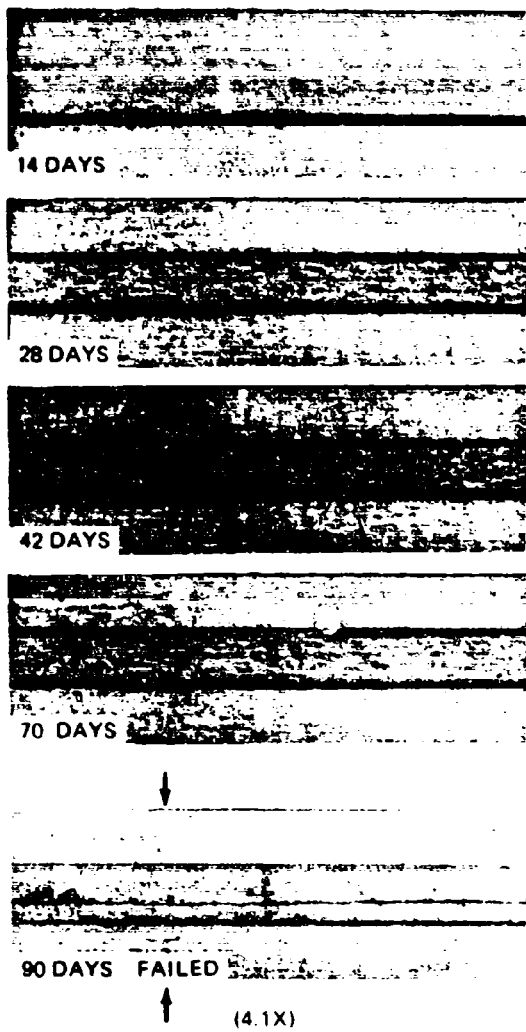
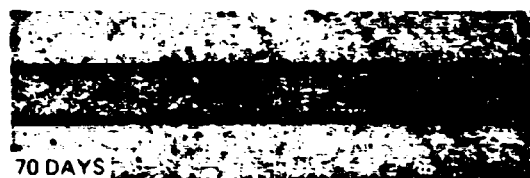
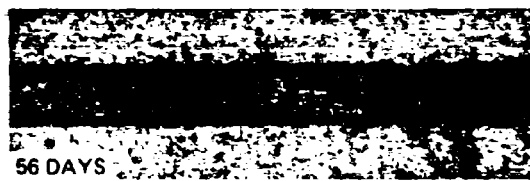
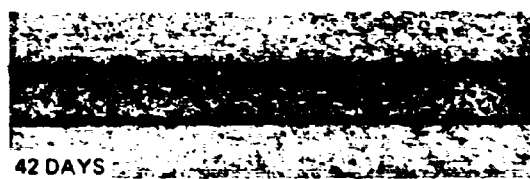


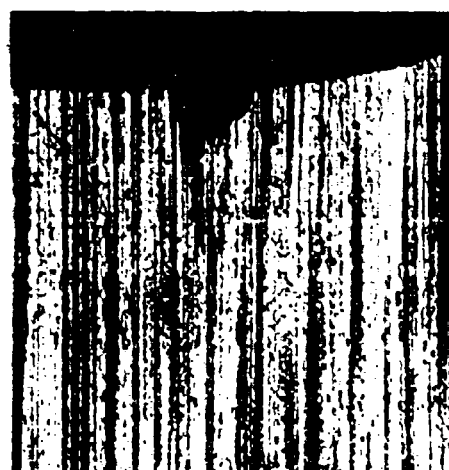
Figure 34. Time-Sequence and Cross-Section Photographs of 7079-T6-G (E-9) at 26 KSI



(4.1X)



30X

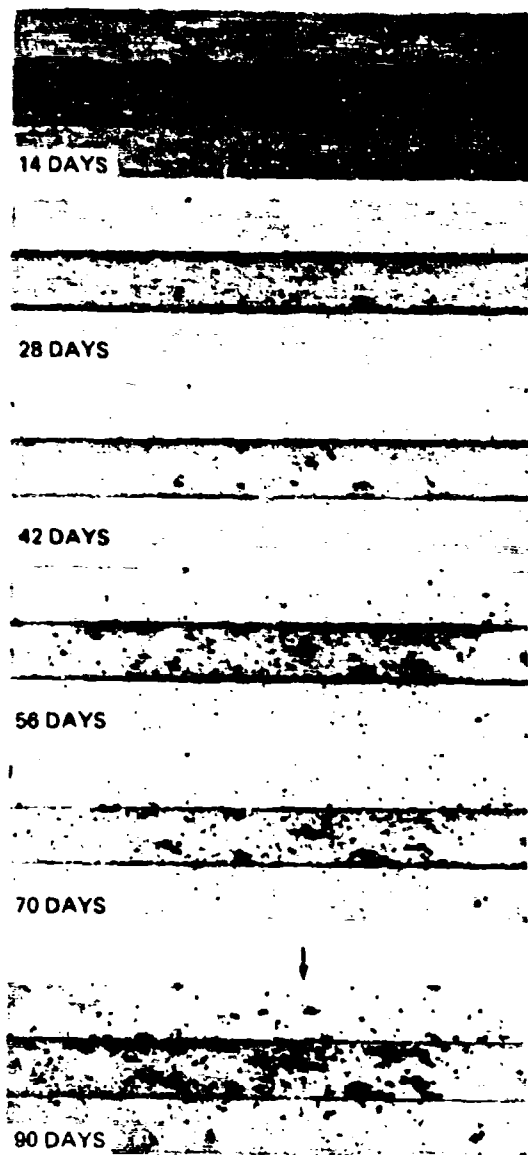


150X



375X

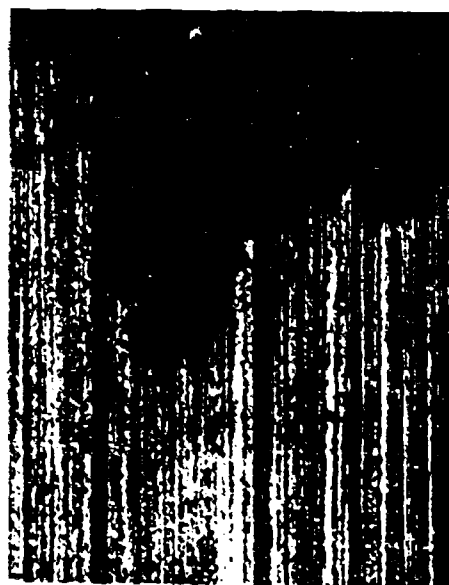
Figure 35 Time-Sequence and Cross-Section Photographs of 75-75-S at 26 KSI



(4.1X)



30X



150X

Figure 36. Time-Sequence and Cross-Section Photographs of 7578-S at 26 KSI

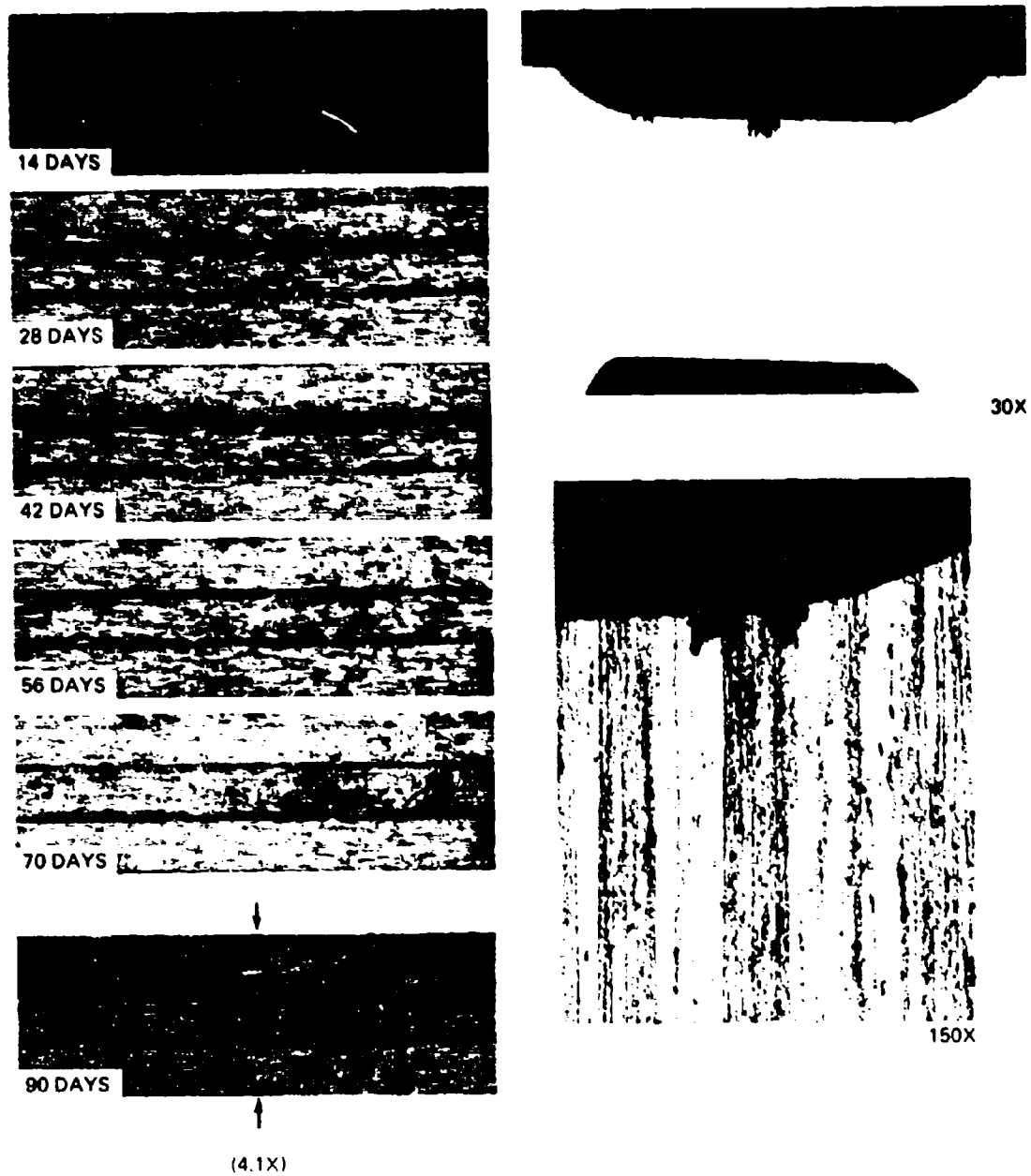


Figure 37. Time-Sequence and Cross-Section Photographs of 2178-T7651-I at 26 KSI



Alloy 20	Moderate pitting and linear pitting, blunt intergranular protrusions; depth 0.008 in.
7075-T651-1	Minor pitting, sharp intergranular cracking; depth 0.035 in.
7075-T651-2	Extensive sharp intergranular cracking; failed
AZ74.61	Pitting and linear pitting, intergranular attack, subgrain boundary branch cracking; depth 0.006 in.
AZ74.61-A	Pitting and linear pitting, blunt intergranular protrusions
7075-T73	Rounded pits, very blunt intergranular protrusions; depth 0.016 in. Grain flow was not normal to stress axis
X7080-T7	Pitting and linear pitting, intergranular attack, subgrain dislodgement
7079-T611-A	General pitting; depth 0.008 in. Grain flow was not normal to stress axis
7079-T611-G	Little attack, not sectioned. Grain flow was not normal to stress axis
7079-T6-G	Extensive sharp intergranular cracking; failed
7575	Moderate pitting and linear pitting, intergranular attack, subgrain boundary branch cracking; depth 0.006 in.
7578	Heavy pitting and linear pitting; depth 0.013 in.
7178-T7651	Moderate pitting and linear pitting, blunt intergranular protrusions; depth 0.005 in.

Additional comments are:

- (a) Alloys AZ74.61 and X7080-T7 contained extensive substructures.
- (b) In alloys AZ74.61 and X7080-T7 the primary cracks were continually blunted by a strong tendency for the crack front to branch along the subgrain boundaries.
- (c) Alloy X7080-T7 possessed a relatively large grain size and anodized with a surface appearance different from that of the other alloys.
- (d) Crack propagation in 7079-T6-G was extremely rapid.

(4) 32-KSI Specimens

Seven failures occurred in the 40 specimens stressed to 32 ksi, as follows:

Alloy 16	One (damaged during anodizing) of five
Alloy 18	One of five
Alloy 20	One (damaged during anodizing) of five
7075-T651-2	Two of two
7575	Two of two

Time-sequence and cross-section photographs of a heavily pitted or cracked specimen of each Phase II alloy are shown in Figs. 38 through 44. End-of-test photographs for all other 32-ksi specimens are shown in Appendix IV. Observations of the surface and cross sections produced the following findings:

Alloy 16	Minor linear pitting, sharp intergranular cracking; depth 0.023 in.
Alloy 17	Minor pitting and linear pitting, blunt intergranular protrusions; depth 0.008 in.
Alloy 18	Minor pitting, sharp intergranular cracking; depth 0.049 in.
Alloy 19	Moderate pitting and linear pitting, intergranular protrusions; depth 0.018 in.
Alloy 20	Minor pitting and linear pitting, blunt intergranular protrusions; depth 0.010 in.
7075-T651-1	Minor pitting, sharp intergranular cracking; depth 0.010 in.
7075-T651-2	Extensive sharp intergranular cracking; failed

(5) 44-KSI Specimens

Twelve failures occurred in the 39 specimens stressed to 44 ksi, as follows:

Alloy 18	Three of three
Alloy 19	One of three
7075-T651-1	Two of three
7075-T651-2	Two of two
7079-T6-G	Two of two
7575	One of two
7578	One of two

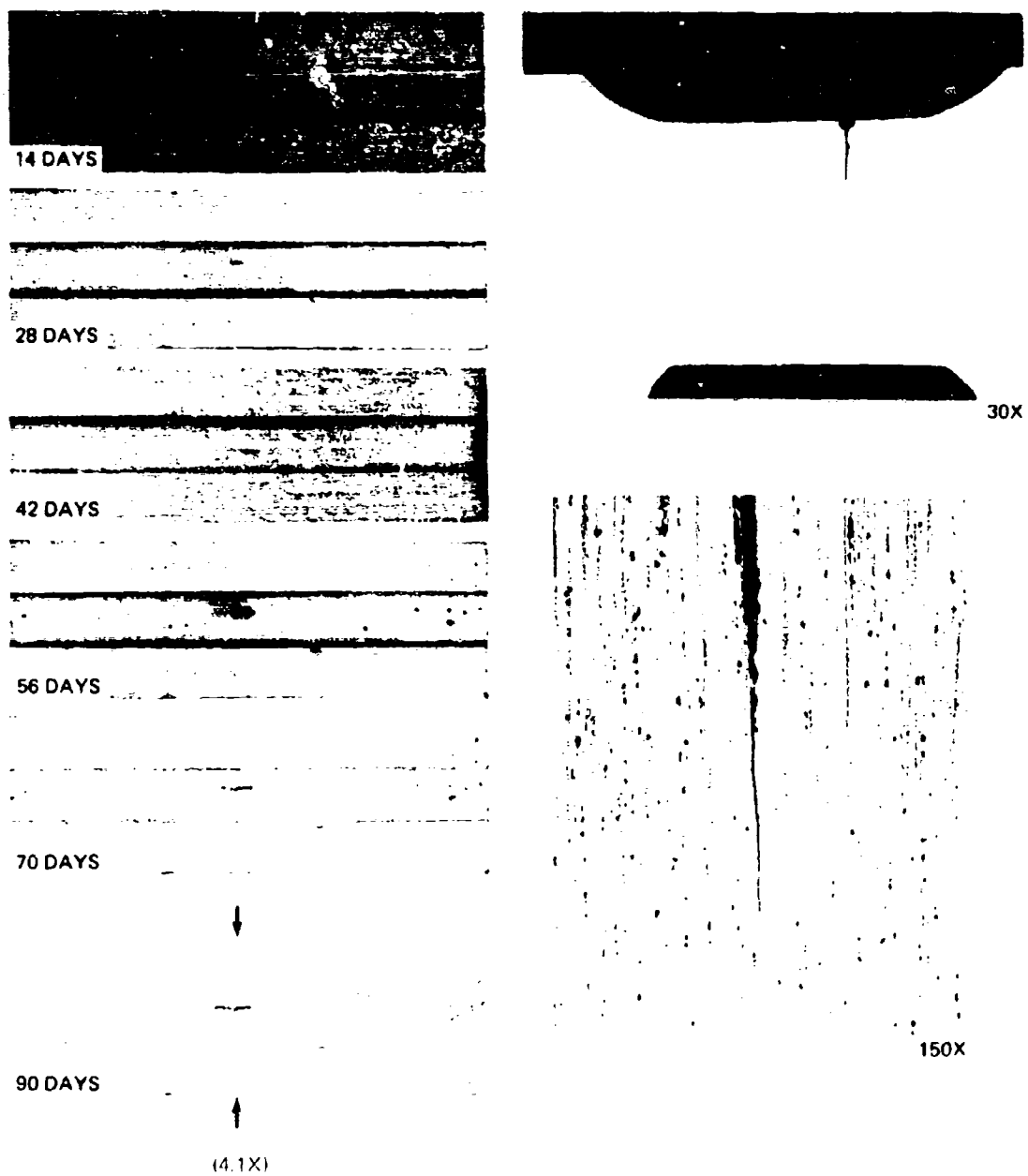


Figure 38. Time-Sequence and Cross-Section Photograph of 16-19 at 32 KSI

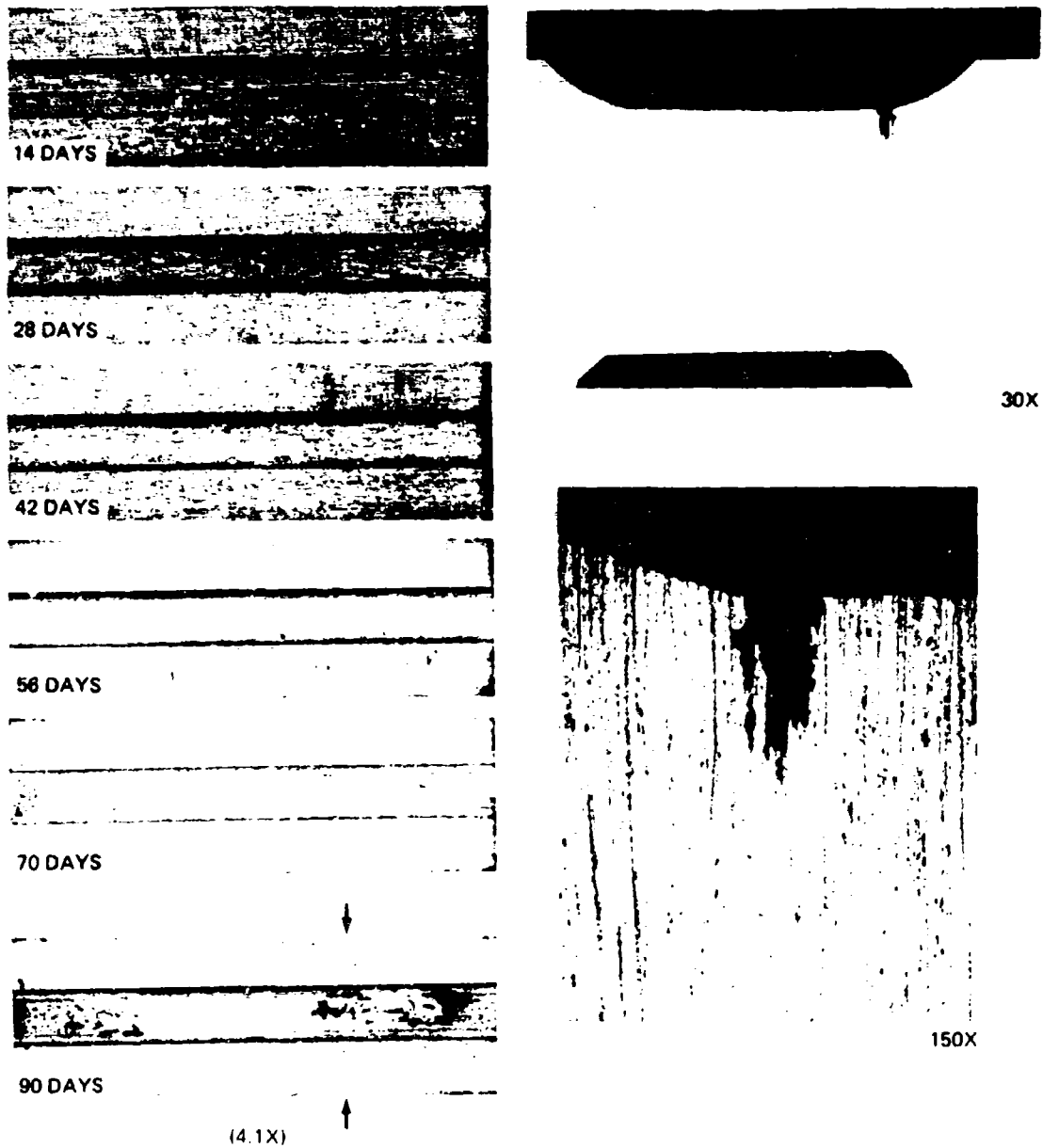


Figure 39. Time-Sequence and Cross-Section Photographs of 17-21 at 32 KSI

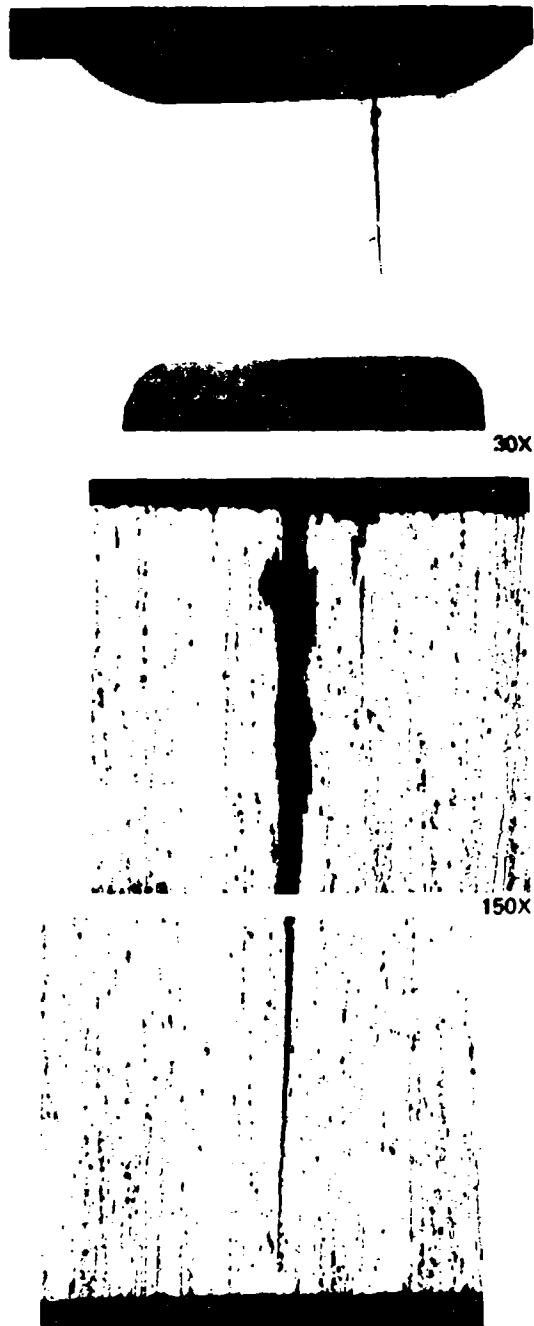
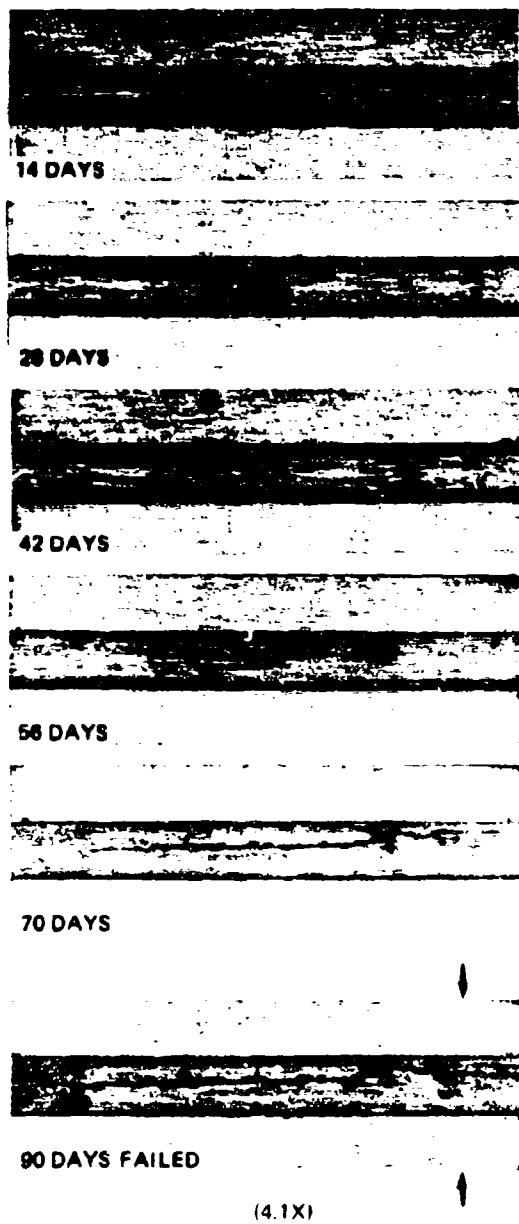
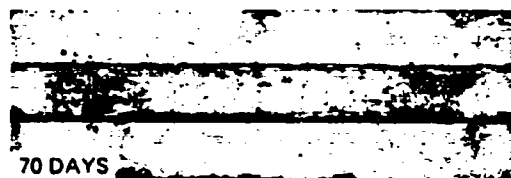
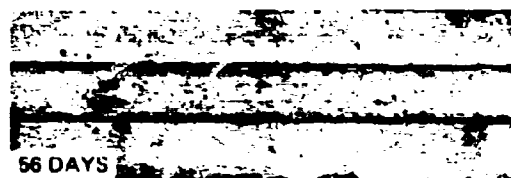
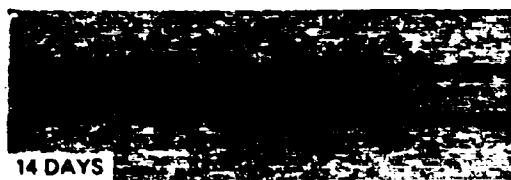


Figure 40. Time-Sequence and Cross-Section Photographs of 18-3 at 32 KSI 150X



(4.1X)



30X



150X

Figure 41. Time-Sequence and Cross-Section Photographs of 19-3 at 32 KSI

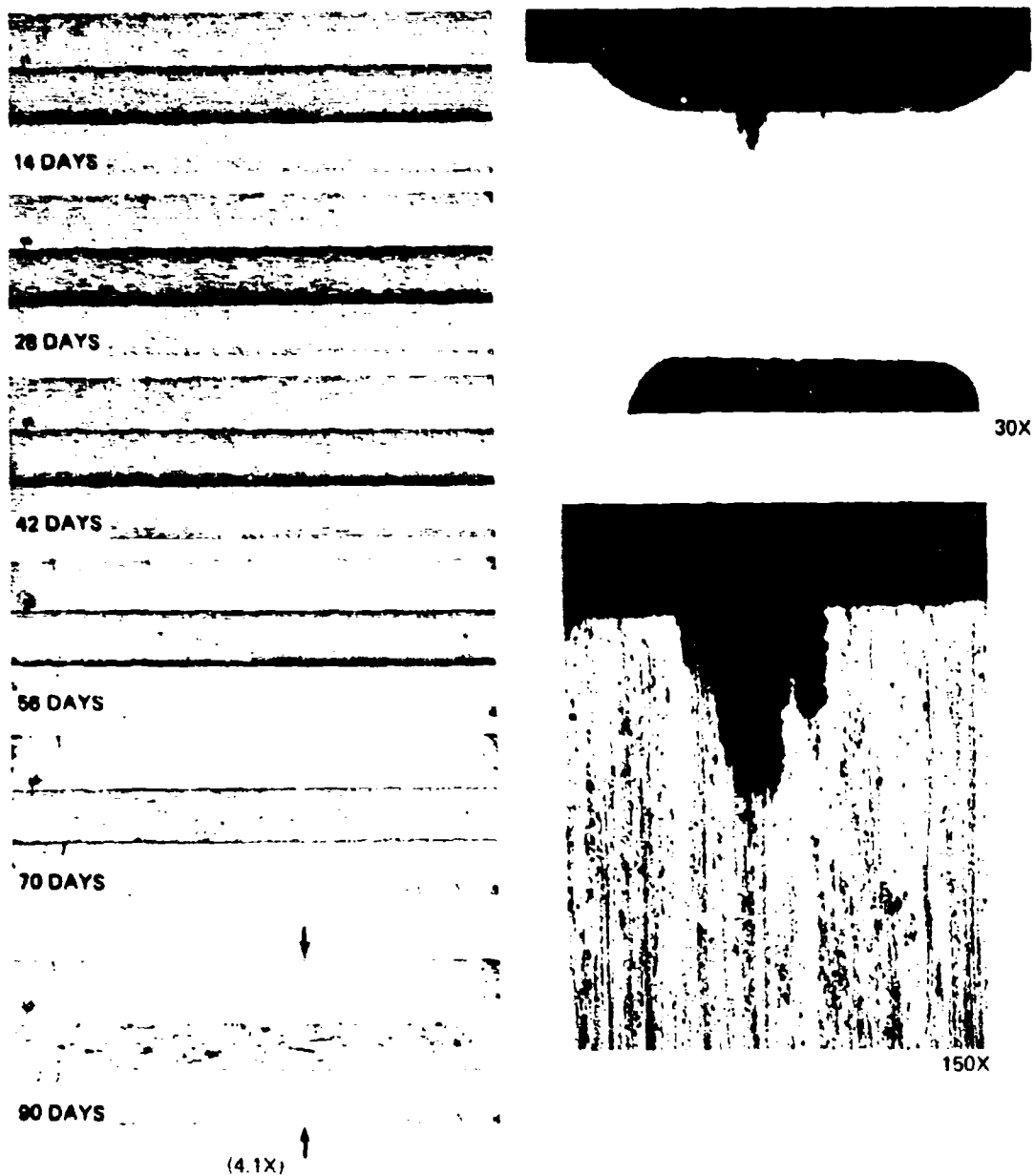


Figure 42. Time-Sequence and Cross-Section Photographs of 20-21 at 32 KSI

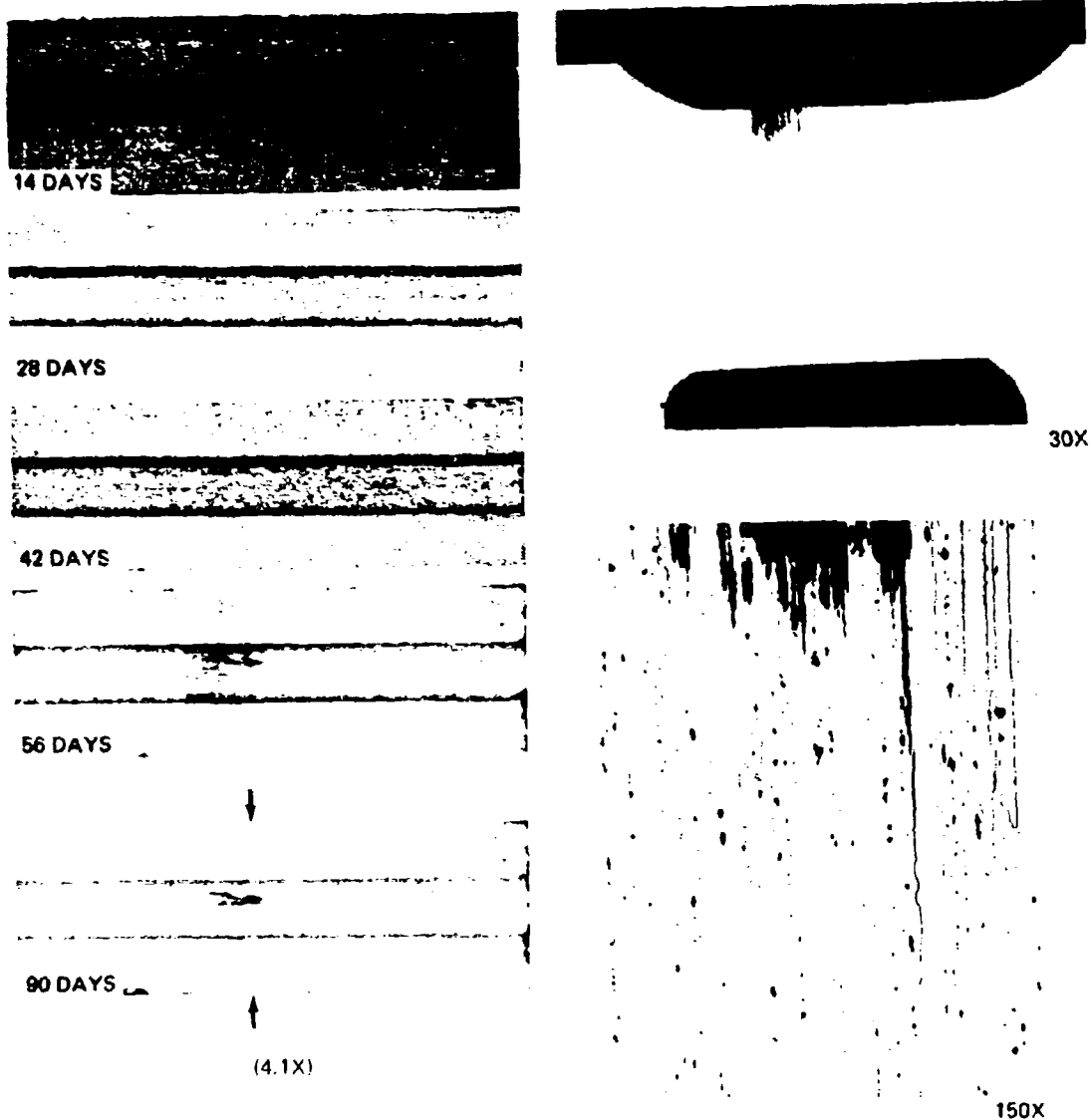
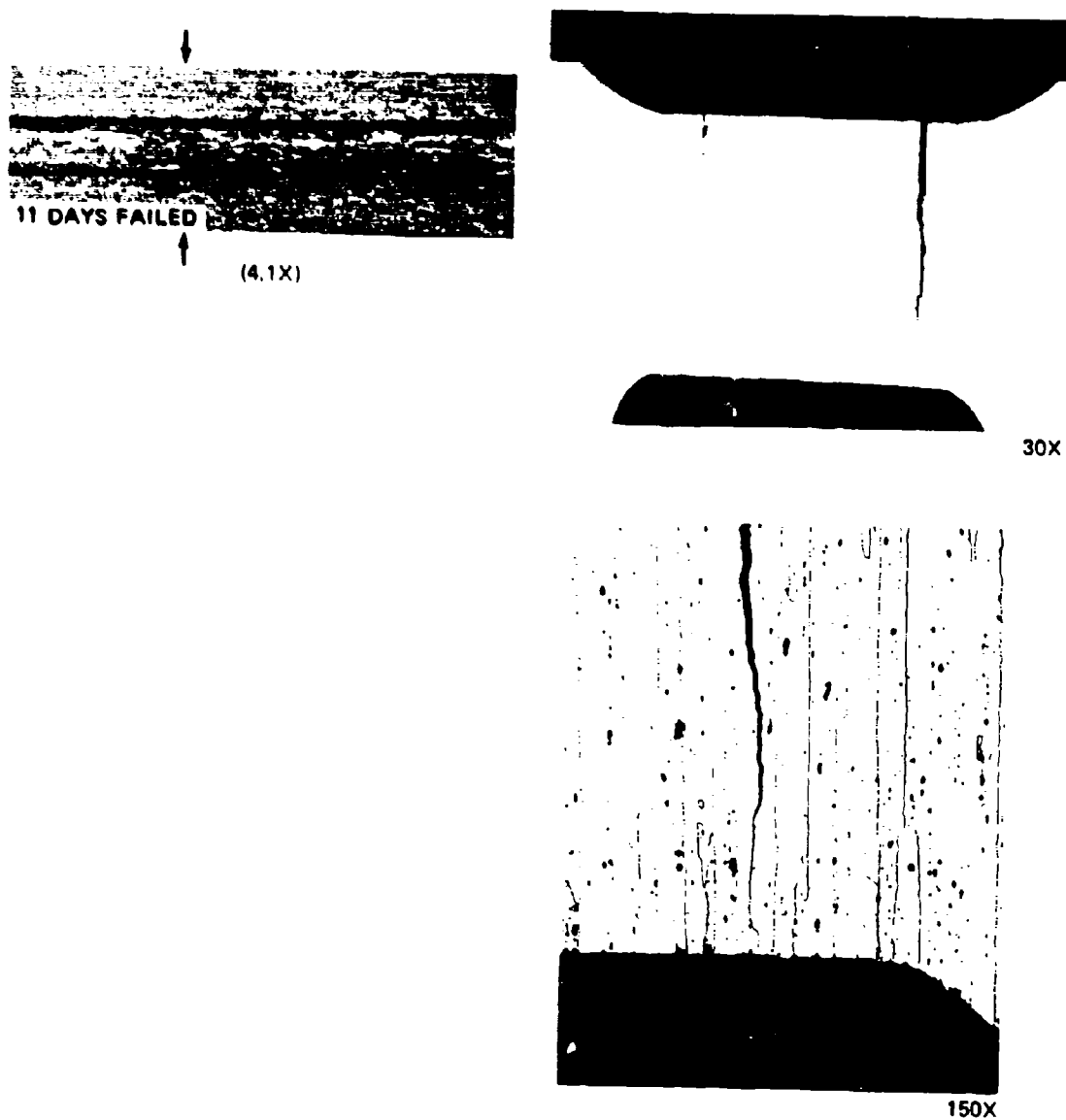


Figure 43. Time-Sequence and Cross-Section Photographs of 7075-T651-I-19 at 32 KSI





*Figure 44. Time-Sequence and Cross-Section Photographs of 7075-T651-2-9 at 32 KSI*

Time-sequence and cross-section photographs of a heavily pitted or cracked specimen of each Phase II alloy are shown in Figs. 45 through 51. End-of-test photographs for the other 44-ksi specimens are shown in Appendix IV.

All Phase II alloys exhibited sharp intergranular cracking. The extent of cracking was less for alloys 16, 17, and 20 than for 18, 19, and 7075-T651-1. For the comparison alloys, trends established at lower stress levels continued. Note that 7079-T6-G developed sharp stress-corrosion cracks after only 2 days in test.

#### (6) 56-KSI Specimens

Fourteen failures occurred in the 28 specimens stressed to 56 ksi, as follows:

Alloy 18	Two of two
Alloy 19	Two of two
Alloy 20	One of two
7075-T651-1	Two of two
7075-T651-2	Two of two
7079-T611-A	One of one
7079-T6-G	One of one
7575	Two of two
7578	One of two

End-of-test photographs for the 56-ksi specimens are shown in Appendix IV. Cracking in Phase II alloys was sharply intergranular. There was little difference in the extent or nature of cracking between alloys 16 and 17, and both were less severely cracked than alloys 18, 19, 20, and 7075-T651-1.

Alloys 7075-T651-2, 7079-T611-A, and especially 7079-T6 failed quickly. All specimens experienced a higher degree of cracking and pitting at this high stress level.

#### (7) Unstressed Specimens

For comparison one anodized, unstressed rectangular specimen of each Phase II alloy was placed in the alternate-immersion test with the stressed specimens. End-of-test photographs for these specimens are shown in Fig. 52. Residual stresses in the commercial 7075-T651-1 were high enough to cause stress-corrosion cracking. Much of the cracking shown in the end-of-test photograph occurred in the first 5 days of exposure. Cross sections through the 7075-T651-1 specimen showed the cracking to be sharply intergranular to a depth of at least 0.050 in.

Alloy 19 (high copper) showed more pitting than the other unstressed specimens. This increased tendency toward pitting was also evident on the stressed specimens. Except for the attack around the edges of the specimens where the anodized layer is less effective, there was little difference in surface appearance among the other Phase II alloys.

#### (8) Posttest Cracking

After the completion of alternate-immersion testing, the stressed specimens were stored in the laboratory, still in the stressed condition. Later observations revealed that a number of the

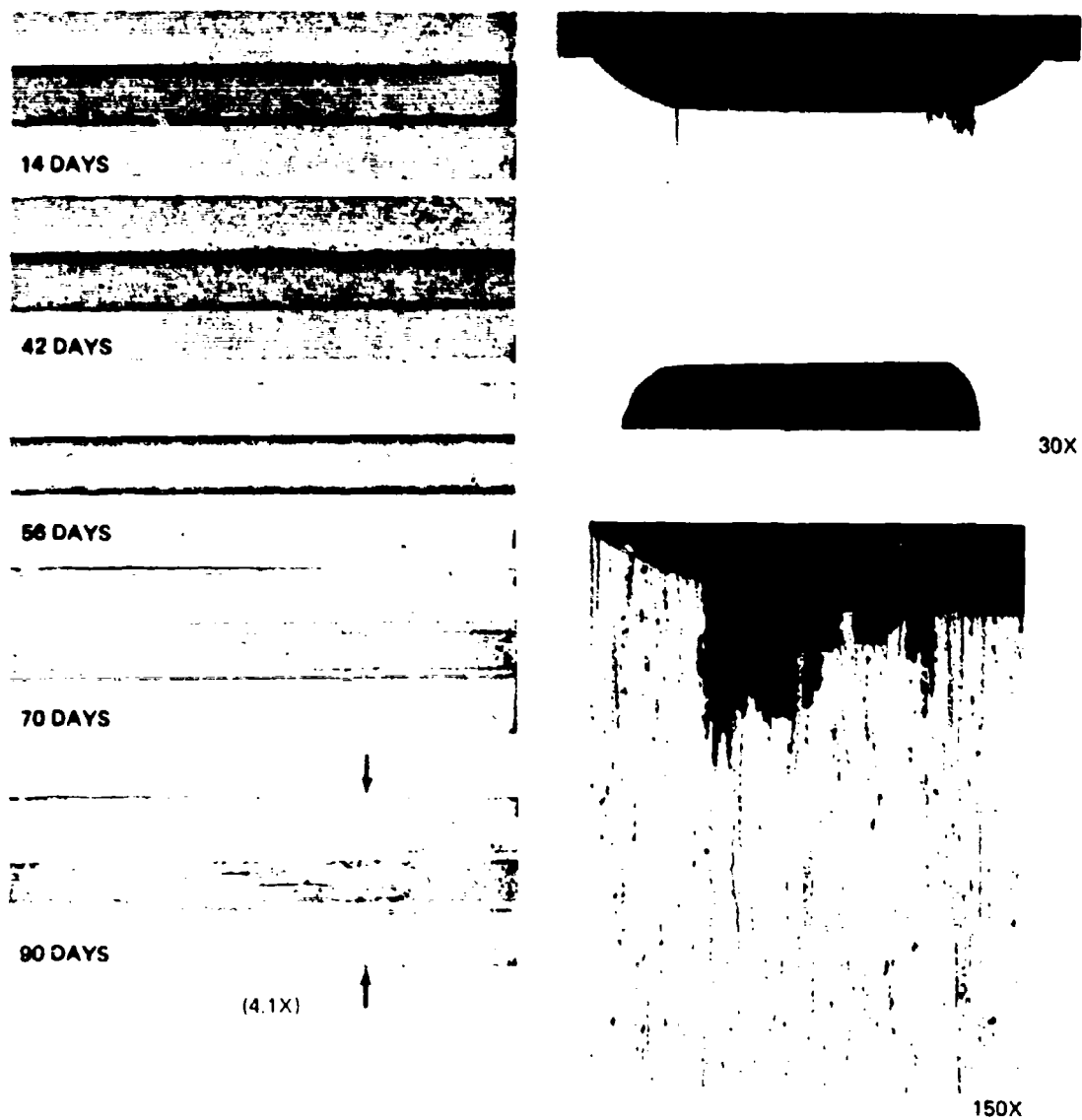


*Figure 45. Time-Sequence and Cross-Section Photographs of 16-6 at 44 KSI*

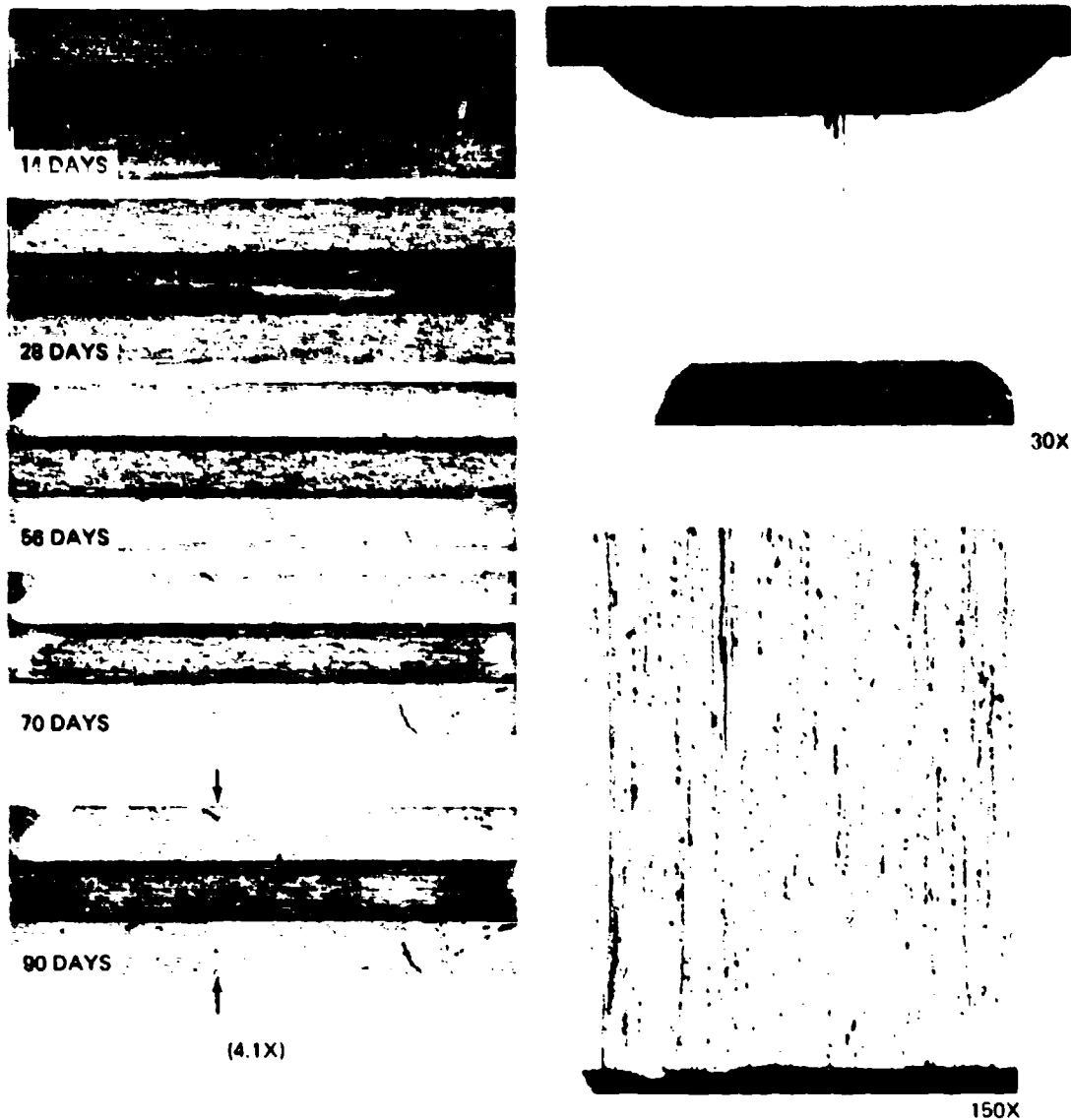
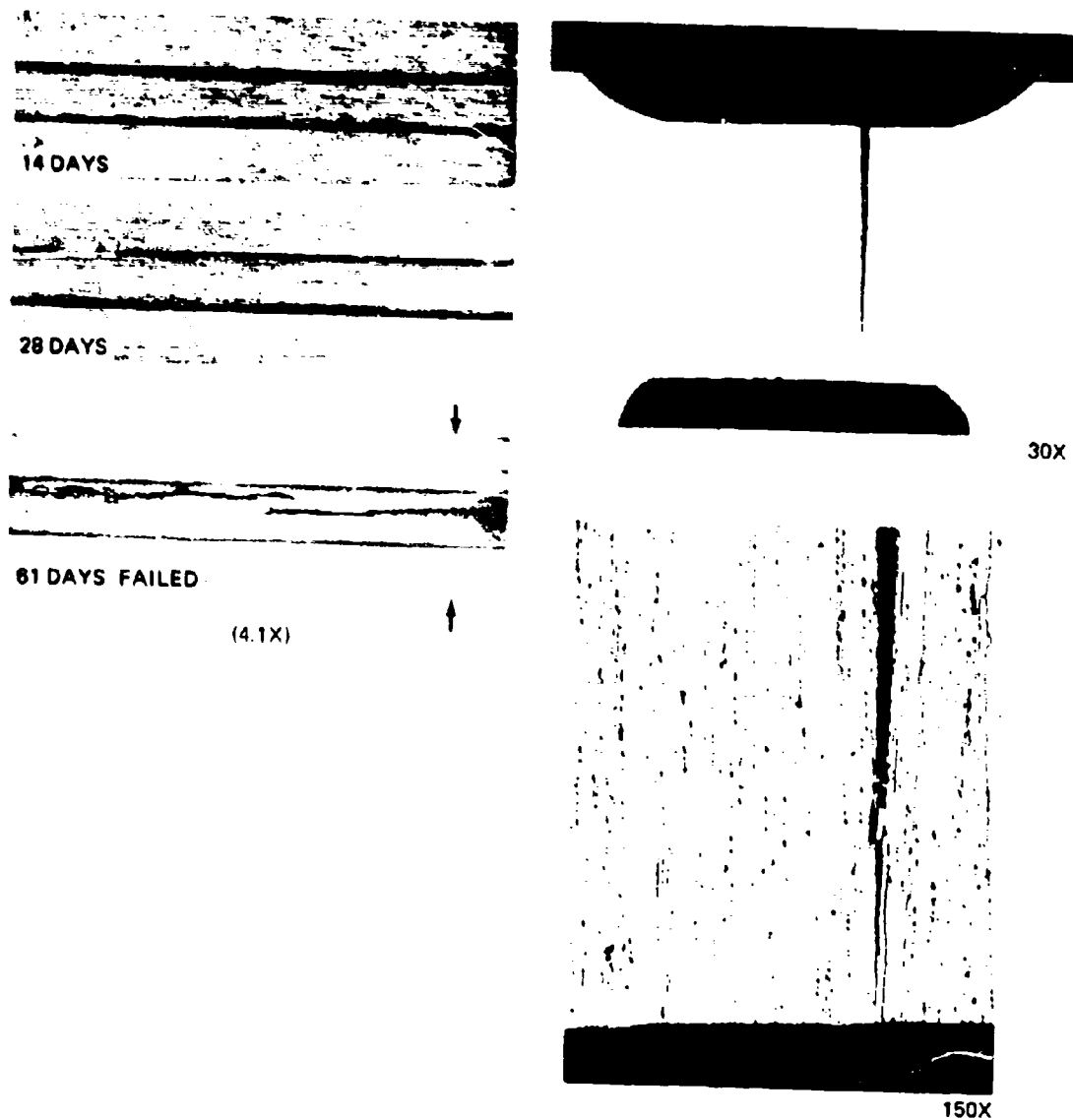


Figure 46. Time-Sequence and Cross-Section Photographs of 17-13 at 44 KSI



*Figure 47 Time-Sequence and Cross-Section Photographs of 1S-6 at 44 KSI*

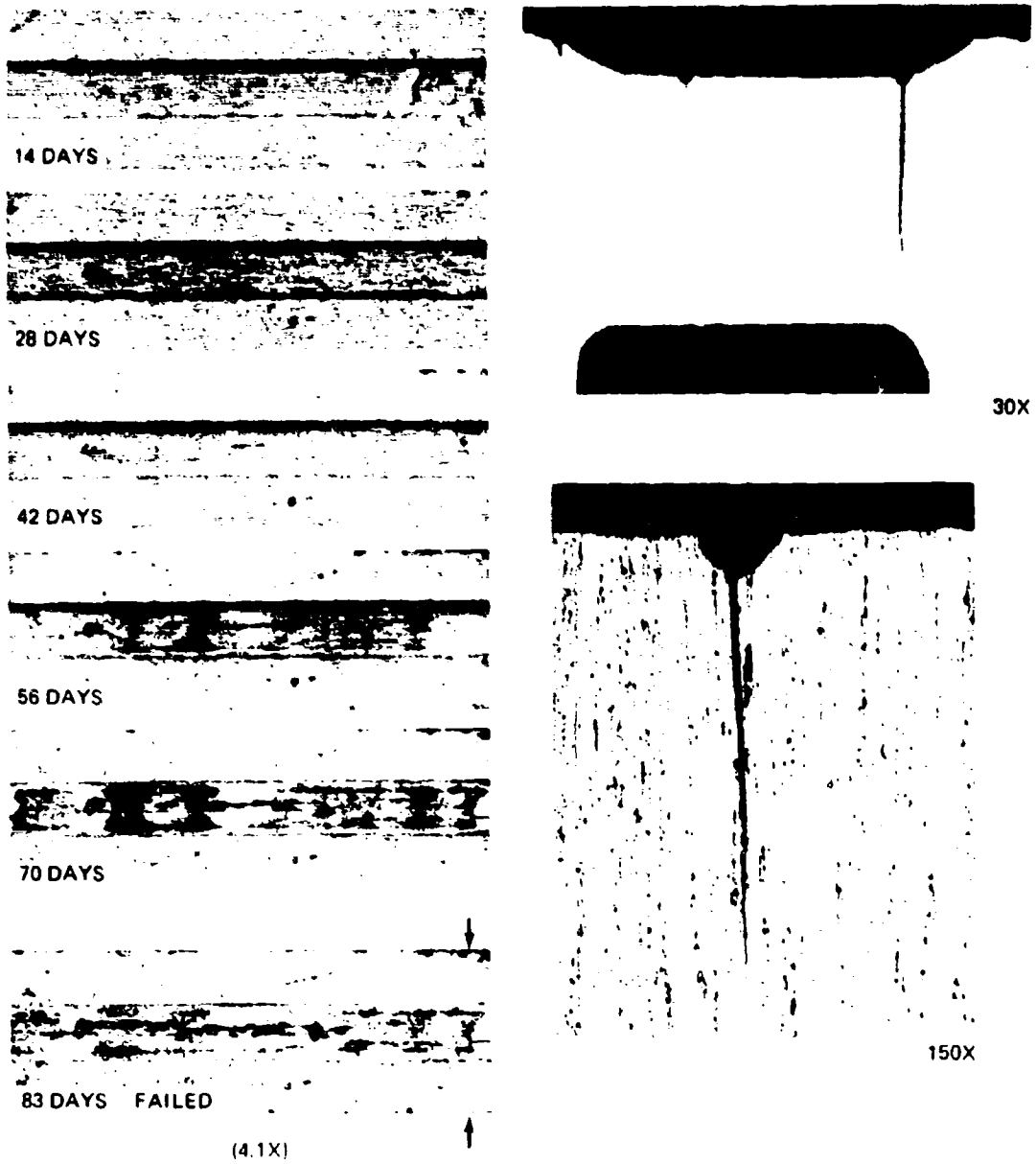
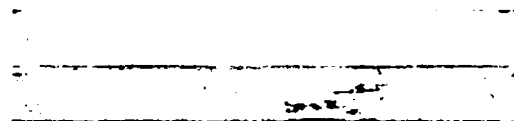
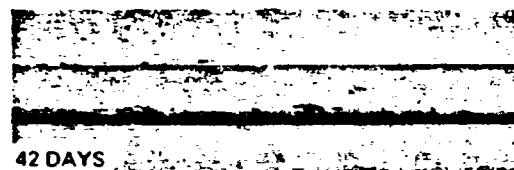
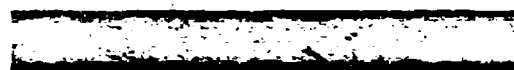
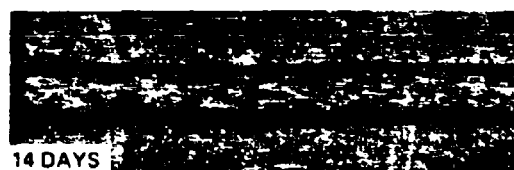


Figure 48. Time-Sequence and Cross-Section Photographs of 19-10 at 44 KSI



90 DAYS

(4.1X)



30X



150X

Figure 49. Time-Sequence and Cross-Section Photographs of 20 13 at 44 KSI

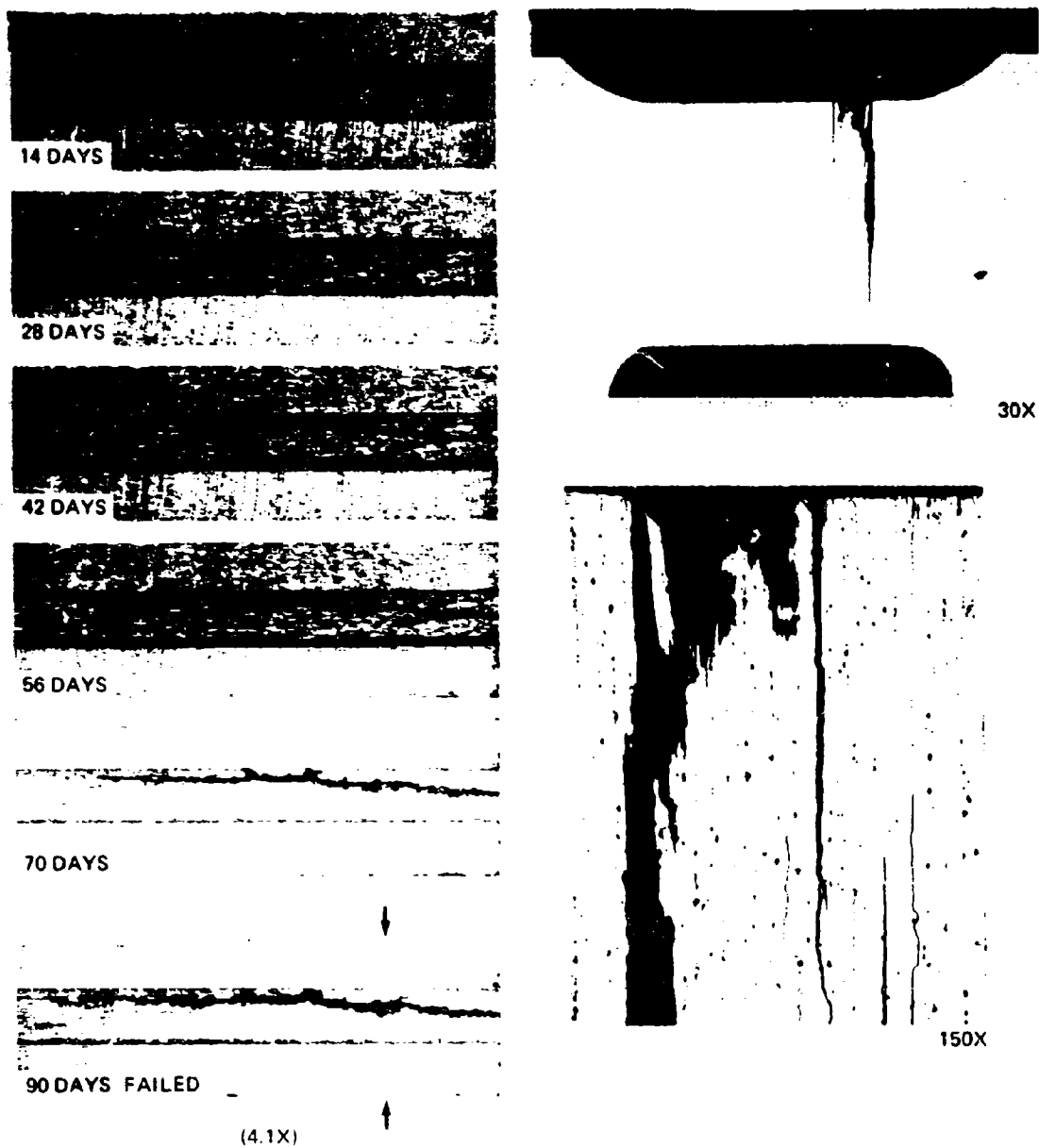
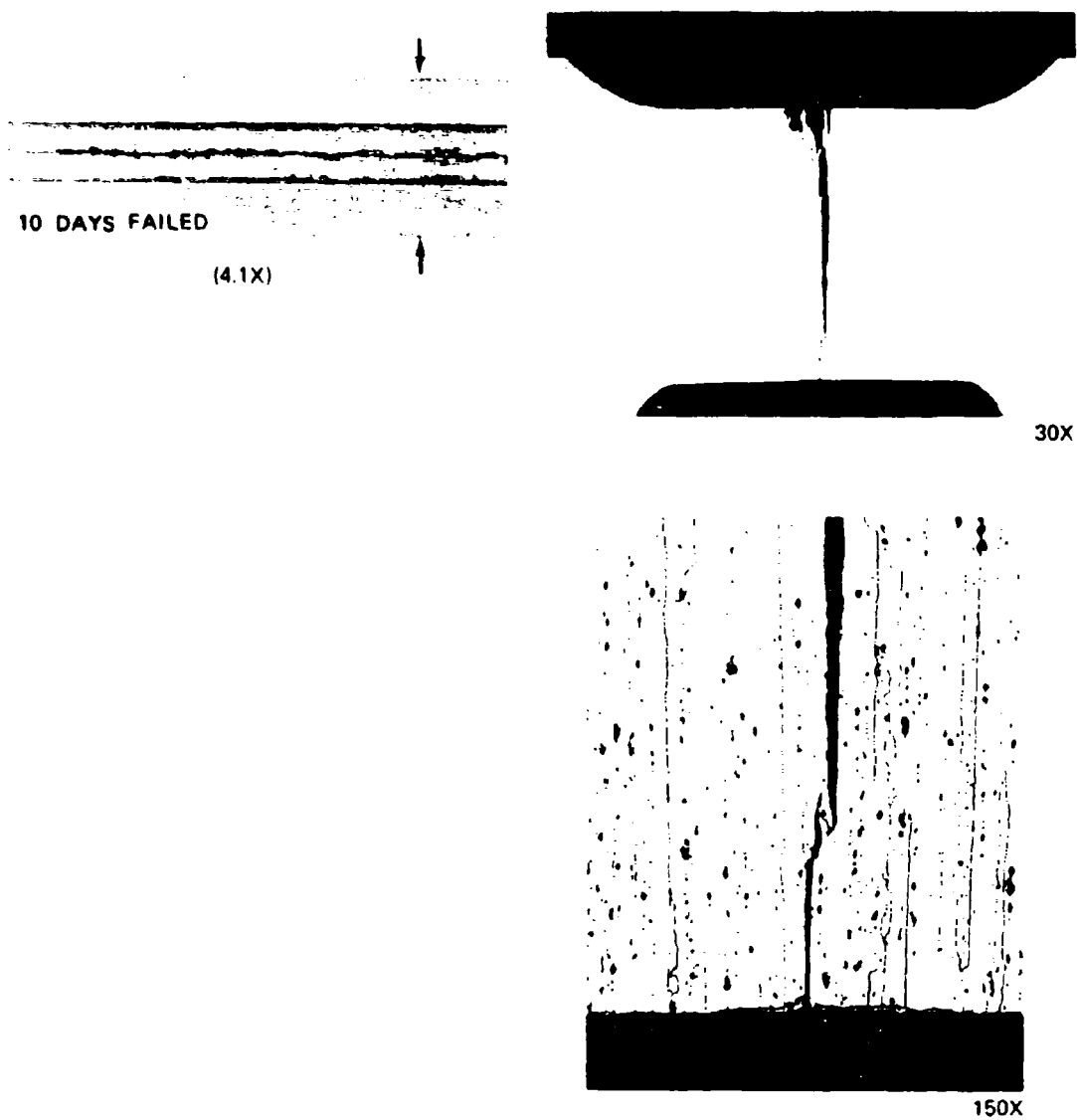


Figure 50. Time-Sequence and Cross-Section Photographs of 7075-T651-I-13 at 44 KSI



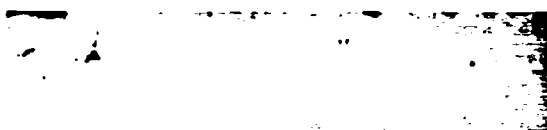


*Figure 51. Time-Sequence and Cross-Section Photographs of 7075-T651-2-S at 44 KSI*

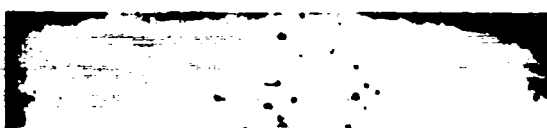
ALLOY 16



ALLOY 17



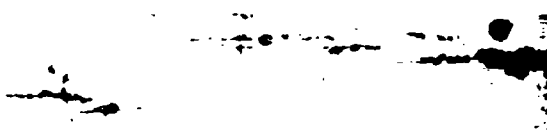
ALLOY 18



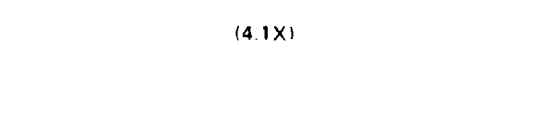
ALLOY 19



ALLOY 20



7075-T651-1



(4.1X)

*Figure 52. Photographs of Unstressed Phase II Alloy Coupons after 90 Days*

cracked specimens cracked even further in this laboratory environment. The specimens had a residual coating of sodium chloride. Additional cracking occurred on alloys 16 and 17 at 56 ksi, alloys 18 and 19 at 26 ksi and higher, alloy 20 at 44 ksi, and 7075-T651-1 at 32 ksi and higher. This additional cracking at any given stress level was less severe on alloy 19 than on any other Phase II alloy, and more severe on alloy 18 than on any other Phase II alloy.

#### (9) Crack and Linear-Pit Growth Rates

Growth rates along the length of the test section of each stress-corrosion specimen were measured from the time-sequence photographs. When cracking or linear pitting occurred in more than one location, only one was used to calculate the growth rate. The crack or linear pit selected for measurement was isolated wherever possible to minimize the complicating effects of nearby parallel cracks.

The average growth-rate data for cracking and linear pitting are shown in Table V. The complete data for each specimen are shown in Appendix III. Three items are evident from the data:

1. The growth rates generally increase with increasing stress level for alloys 18, 19, 20, 7075-T651-1, 7075-T651-2, and 7079-T6-G.
2. The growth rates do not increase smoothly with increasing stress level for Phase II alloys 16 and 17 and for the overaged comparison alloys AZ74.61, 7075-T73, X7080-T7, 7575, 7578, and 7178-T7651. This results from a greater tendency for the cracks to blunt in these alloys and to slow or to stop growing along the length of the test section.
3. The only alloys having growth rates greater than 0.001 in./hr at the 56-ksi stress level are 7079-T6-G, 7079-T611-A, 7075-T651-2, and 19. The fastest growth rate observed was 0.038 in./hr for 7079-T6-G. At the lower stress levels of 26, 32, and 44 ksi, only alloys 7075-T651-2 and 7079-T6-G showed growth rates greater than 0.001 in./hr; 7079-T6-G still had the highest growth rates (0.013 to 0.015 in./hr).

#### b. Testing of Double-Cantilever Beam (DCB) Specimens

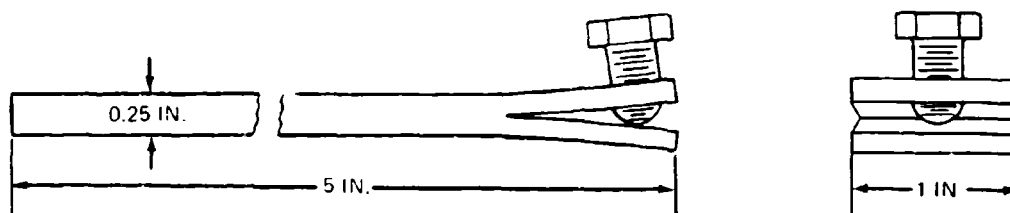
The DCB specimen is currently used at Boeing and the Naval Research Laboratories (4) to measure  $K_{IC}$ ,  $K_{ISCC}$ , and stress-corrosion crack growth rates as a function of stress intensity level in high-strength aluminum alloys. This specimen was developed by Ripling, Mastovoy, and Patric (5), and was initially used to measure the fracture toughness of adhesive joints. Gilman (6) used a similar specimen to obtain direct measurement of surface energy in ionic crystals. More recently this specimen was used to measure the plane-strain fracture toughness of several high-strength materials (7, 8).

Two DCB specimens with dimensions of 5 by 1 by 0.25 in. (Fig. 53) were fabricated from each Phase II alloy to test whether  $K_{IC}$  and  $K_{ISCC}$  could be determined from the 0.25-in.-thick Phase II alloy material. The usual thickness of a DCB specimen at Boeing is 1 in. Because of the thinness of the Phase II specimens, fracture of the arms during stressing was a problem; therefore, the specimens were loaded to a deflection of only 0.080 in. At

Table V. Comparative Growth Rates of Stress-Corrosion Cracks or Linear Pits

Alloy	Average growth rate $\left(\frac{\text{thousandths in.}}{\text{hr}}\right) *$					
	14 ksi	20 ksi	26 ksi	32 ksi	44 ksi	56 ksi
16	0.027	---	0.114	0.020	0.082	0.057
17	0.057	0.019	---	0.075	0.095	0.095
18	---	---	0.046	0.187	0.498	0.723
19	0.067	0.108	0.153	0.168	0.147	1.57
20	0.057	0.027	0.030	0.055	0.073	0.244
7075-T651-1	0.037	0.037	0.010	0.047	0.229	0.527
7075-T651-2	0.035	---	1.16	3.85	3.42	5.17
AZ74.61	---	---	0.061	0.052	0.067	0.107
AZ74.61-A	---	---	0.113	---	---	0.063
7075-T73	---	0.046	0.043	---	0.099	0.089
X7080-T7	---	---	0.091	---	0.043	0.070
7079-T611-A	---	---	---	---	---	6.2
7079-T611-G	---	---	---	---	0.067	---
7079-T6-G	---	---	13.1	---	15.0	38.8
7575	---	---	0.088	0.356	0.221	0.249
7578	---	---	0.025	0.073	0.075	0.058
7178-T7651	---	---	0.077	0.097	0.055	0.149

\*Measured parallel to groove direction from time sequence photographs.



NOTE:

DEFLECTION (MEASURED AT LOADING POINTS) = 0.080 IN. ON ALL ALLOYS ( $K \approx 20 \text{ KSI} \sqrt{\text{IN}}$ )

Figure 5.3. Double-Cantilever Beam (DCB) Specimen for Stress-Corrosion Testing

this deflection plane-strain fracture (pop-in) did not occur and the DCB specimens were not precracked. In contrast, the 1-in.-thick specimen is deflected until pop-in occurs, thus allowing  $K_{IC}$  to be calculated and causing a sharp crack to be present at the start of stress-corrosion testing.

Three times a day the notch tip area of each specimen was covered with 3.5-percent sodium chloride solution to provide the corrosive environment. (The steel bolt used to load the specimen was not in contact with the solution.) Crack-length-vs.-time data for these specimens are plotted in Fig. 54. The fastest crack growth rates occurred in 7075-T651-1, 18, and 19. Average rates for the three alloys at a crack length of 0.9 in. were:

7075-T651-1	0.0028 in./hr
Alloy 18	0.0031 in./hr
Alloy 19	0.0003 in./hr

Cracking in alloy 19 is slower than in 7075-T651-1 and 18, whereas in the data of Table V it is faster. These growth rates are higher than any shown in Table V for 7075-T651-1 and 18, and lower than any shown in Table V for alloy 19.

The growth rates for 7079-T6-G in Table V are much higher than for alloys 7075-T651-1 and 18 in the DCB configuration. This indicates that 7079 has by far the highest stress-corrosion crack growth rates. This rapid growth rate for 7079 has been confirmed using 5-by-1-by-1-in. short-transverse DCB specimens of 7079-T651 from 1-in.-thick plate. Growth rates as high as 0.1 in./hr have been measured for this alloy at  $K$  levels of about 20 ksi  $\sqrt{\text{in.}}$ . Audible "pops" are heard periodically during this rapid crack growth, indicating that crack growth is discontinuous.

#### c. Industrial-Environment Testing

To evaluate the behavior of the Phase II alloys in an industrial environment, 60 specimens of the configuration shown in Fig. 19 were tested outdoors: two each at 20 ksi, three each at 26 ksi, two each at 32 ksi, two each at 44 ksi, and one each unstressed (Appendix III). Comparison alloys tested outdoors were AZ74.61, six specimens; 7575, two specimens; 7578, two specimens; and 7178-T76, two specimens. All comparison alloys were stressed to 26 ksi. After 160 days in test, no cracks have been observed on any of the specimens. These specimens will be left in test for several more months.

#### d. Exfoliation Testing

Exfoliation corrosion testing of 3-by-5-by-0.25-in. panels of each Phase II alloy and several other commercial alloys were conducted in a salt-fog cabinet, using 5-percent sodium chloride solution buffered to pH 3 with acetic acid. Test procedures were those described in Ref. 9. After two weeks of testing, none of the Phase II alloys showed any signs of exfoliation corrosion. Some other alloys (2014-T6, X2021, and slowly quenched 7075-T651) showed mild to severe exfoliation attack.

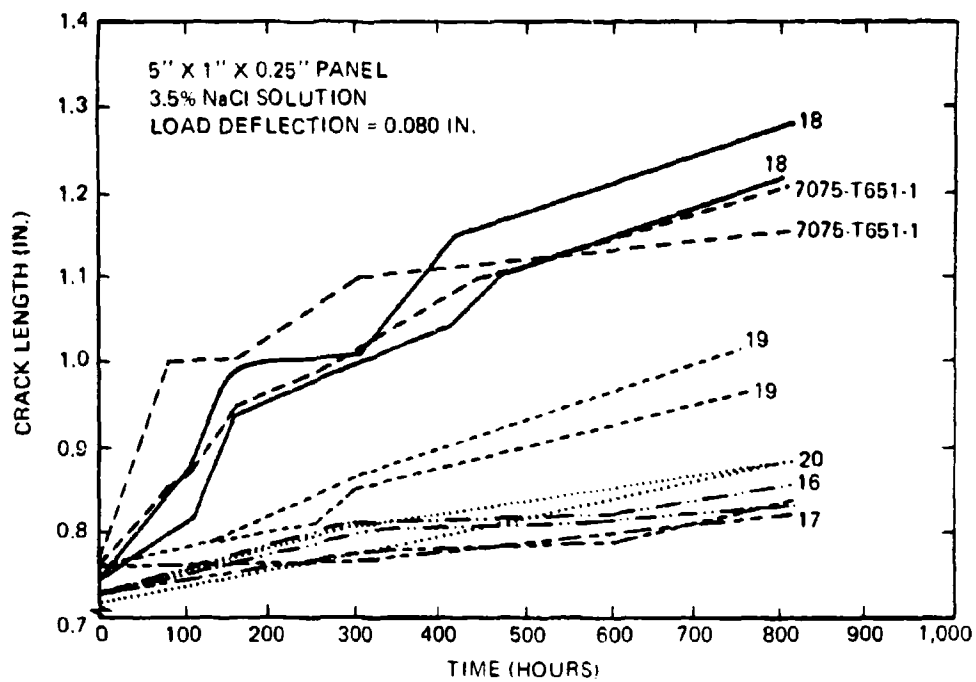


Figure 54. Stress-Corrosion Crack Propagation Curves for DCB Specimens

## SECTION IV

### DISCUSSION

The high-strength 7000-series aluminum alloys in current use, particularly 7075-T6 and 7079-T6, have an unfortunate susceptibility to stress corrosion cracking and thus are subject to random service fractures. One goal of aluminum alloy development then is to significantly reduce the incidence of these random fractures without materially affecting the product performance. What constitutes a significant reduction and how performance is affected are engineering judgments.

The T73 heat treatment for alloy 7075 produces a very high stress-corrosion resistance and is used in applications where near-immunity is required. However, this immunity is achieved with about 14 percent reduction in minimum allowable mechanical properties.

It has been proposed that AZ74.61, a silver-bearing alloy, could offer both the stress-corrosion resistance of 7075-T73 and the high strength of 7075-T6. This study has shown that AZ74.61 has good stress-corrosion resistance, but its mechanical properties are similar to those of 7075-T73. It does not appear that the minimum properties of 7075-T6 can be guaranteed for AZ74.61.

Two alloys, 7178-T7651 and 7001-T75, with higher mechanical properties than either 7075-T73 or AZ74.61 possess a stress-corrosion resistance adequate to meet the goals of this contract. However, these alloys have a disadvantage shared by both 7075-T73 and AZ74.61: They contain chromium and are quench sensitive. The higher copper content in 7001, 7178, and 7075 further increases the quench sensitivity of these alloys. In addition, the very high alloy content in 7001-T75 results in low fracture toughness.

The new low-copper, chromium-free X7080-T7 is a quench-insensitive alloy that offers good stress-corrosion resistance (but less than 7075-T73) and strength comparable to that of 7075-T73.

There is a need for a stress-corrosion-resistant alloy with the strength of 7075-T6. This alloy must have fatigue and fracture toughness properties equal to or better than those for 7075-T6, and should offer stress-corrosion resistance substantially greater than that of 7075-T6 and 7079-T6. The alloy that will meet the goals of this contract is not commercially available. These goals can be met by a chromium-free, silver-free, zirconium-bearing, medium-copper alloy with a zinc and magnesium content intermediate between those of 7075 and 7178. One of the alloys studied in Phase II of this contract contained zirconium in place of chromium, but the alloy also contained silver. This alloy, without silver, is the alloy recommended for further development. Its nominal composition is 6.4% Zn, 2.55% Mg, 1.1% Cu, 0.1% Mn, 0.15% Zr.

The remainder of this discussion considers the following engineering and technical points that led to the recommendation of this alloy composition:

- The effect of silver additions
- Meeting the stress corrosion goal

- Meeting the mechanical property goal
- Controlling quench sensitivity
- Maintaining fracture toughness
- Maintaining fatigue properties

## 1. THE EFFECT OF SILVER ADDITIONS

Patents filed by Rosencranz in 1958 (10, 11) stated that silver additions improved stress-corrosion resistance in a range of wrought Al-Zn-Mg alloys. In 1960, Polmear (12, 13) found that silver additions stimulated the precipitation of the  $M'$  phase in high-purity Al-Zn-Mg alloys, so that it was very evenly dispersed. Precipitation occurred even in the grain boundary regions, where precipitate-free zones were observed in high-purity silver-free alloys. Polmear suggested that this effect of silver should lead to increased resistance to stress-corrosion cracking; this increased resistance was verified in limited laboratory tests on sheet materials. He also suggested that the microstructural changes induced by silver would provide increased shatter resistance (higher toughness) under ballistic impact.

Later work by Polmear (14) showed that similar microstructural changes occurred with silver additions to certain high-strength commercial Al-Zn-Mg alloys. In addition, high strengths could be obtained at higher than normal aging temperatures. He suggested that the higher aging temperatures would also improve stress-corrosion resistance by reducing residual quenching stresses. Preliminary tests indicated that silver slightly improved the unnotched fatigue properties of a forged commercial silver-bearing alloy; Polmear suggested that this was due to the increased microstructural stability of alloys containing silver. It was also reported that silver additions increased the quench sensitivity of these high-strength aluminum alloys (14, 15).

These early studies indicated that several beneficial effects could be achieved by adding silver to high-strength Al-Zn-Mg commercial alloys. Some of these effects are:

- Increased stress-corrosion resistance
- Improved mechanical properties at higher than normal aging temperatures ( $> 250^{\circ}\text{F}$ )
- Improved fracture toughness
- Improved fatigue properties

It was recognized that silver additions could increase quench sensitivity. Subsequent work has been involved with evaluating the expected beneficial effects.

### a. Stress-Corrosion Resistance

It was recently reported (16) that the presence of silver makes no difference in the short-transverse stress-corrosion threshold stress in 7075-type alloys thermally treated to develop equal strength. This investigation was conducted with 2-in.-thick plate.

A more favorable view of increasing stress-corrosion resistance with silver additions was recently published by Elkington and Turner (17). These investigators evaluated the effects of silver on strength and stress-corrosion resistance by using a base alloy with two different copper contents and with and without manganese and chromium. The material was in the form of 3-in. plate. The alloys were quenched at various rates, held 5 days at room temperature, and aged 12 hr at  $275^{\circ}\text{F}$ . The silver-bearing alloys were also tested after aging 6 hr at  $329^{\circ}\text{F}$ .



It was reported that the silver addition produced marked improvement in stress-corrosion resistance, as did the addition of chromium, a slower quenching rate, and an increase in aging temperature. The investigators concluded that an attractive combination of stress-corrosion resistance and tensile properties could be obtained with an alloy containing 6% Zn, 2.5% Mg, 1.35% Cu, 0.5% Mn, and 0.3% Ag, aged 6 hr at 329°F.

The alloy proposed by Elkington and Turner is very similar to the chromium-free, manganese-bearing X7080 comparison alloy of this study (X7080-T7), with the exception of the silver addition. The composition of the X7080-T7 was 5.88% Zn, 2.3% Mg, 0.86% Cu, and 0.38% Mn; the heat treatment is proprietary.

Both alloys possess good stress-corrosion resistance. Elkington and Turner reported that four out of five short-transverse stress-corrosion specimens of their alloy were unbroken after 100 days at 90 percent of the 0.1-percent yield stress in a rural environment. One specimen broke in 97 days (17). They did not report whether cracks were present on the unfailed specimens. The test specimens were loaded in four-point bending under constant load (Black test).

Comparison data on X7080-T7 obtained at Boeing in an industrial environment (specimen shown in Fig. 19) show that no failures have occurred after 450 days in test for three specimens stressed between 40 and 60 ksi. All three specimens have shown intergranular cracking, however. Cracking, but not failure, also occurred on the X7080-T7 specimens tested in the 3.5-percent alternate-immersion facility. These cracks grew very slowly, and no failures of X7080-T7 occurred during the 90-day exposure. From this information it appears that X7080-T7 and Elkington and Turner's proposed alloy are similar with respect to stress-corrosion resistance.

One aspect of the current program was to evaluate the effect of silver on the stress-corrosion resistance of the step-aged Phase II base alloy. The results show no consistent differences between the stress-corrosion performance of alloy 16 and alloy 17 in the T6 + 10 hr at 320°F heat treatment. Both alloys were equally resistant to stress-corrosion cracking.

On the basis of these results it does not appear that a silver addition to an alloy provides improved stress-corrosion resistance over that of a similar alloy without silver when both alloys are overaged.

#### b. Mechanical Properties

During Phase I, silver additions to a 7075-type alloy aged at 320°F after a 4-day room-temperature delay were found to increase the strength several percent over that of a similar silver-free alloy. However, it has been shown (18) that silver has a greater strengthening effect on 7075-type alloys than on more highly alloyed alloys of the Phase II type. In addition, the degree of strengthening due to silver noted in Phase I may not be realistic because the Phase I alloys were not step-aged. Optimum mechanical properties may require step aging, especially for the silver-free alloy.

Alloy 17 possessed a longitudinal yield strength 1.5 ksi greater than that of alloy 16. This small strengthening effect of silver on the Phase II base alloy might have been even smaller had the optimum room-temperature delay time been used for alloy 16. Rosencranz (19) reported a substantial effect of room-temperature delay time on the strength of silver-free alloys

of the AZ74 type when aged at 320°F. When these silver-free alloys were room-temperature aged for 15 to 48 hr, strengths were as much as 9 ksi below those which could be attained with a 15-day room-temperature delay. The final age in this case was 10 hr at 320°F. The same effect for other silver-free alloys (7075-T6, 7178-T6) is well known, and data (3) indicate that the difference between optimum and reduced yield strengths for 7178-T6 and 7075-T6 can be as high as 3 ksi. For 7178 the highest strengths are obtained with a minimum delay between quenching and aging. This is also true for 7075, but delays of 4 to 30 hr are more detrimental than longer delays. At higher aging temperatures, this difference (1 to 3 ksi) between optimum and reduced yield strengths would probably increase.

In silver-bearing alloys of the AZ74 type, Rosencranz found that room-temperature delay time had little effect on tensile properties when the alloys were aged at 320°F. Thus the tensile properties of the silver-bearing Phase II alloys are typical (room-temperature delay time probably has little effect), but the tensile strength of base alloy 16 is not optimum and may be slightly below that possible with shorter or longer room-temperature delay times. Had the base alloy been given a longer or shorter room-temperature delay time before the aging treatment, the small strength advantage of the silver addition would have been reduced.

In the comparison alloy tests, the commercial silver-bearing alloy AZ74.61 showed good stress-corrosion resistance but did not offer a strength advantage over the silver-free 7075-T73 alloy. In another study, however, James (20) reported a substantial strength advantage for AZ74.61 over 7075-T73. This discrepancy apparently involves the question of minimum allowable properties versus mechanical properties from random samples. There is no indication at present that the minimum allowables for AZ74.61 will be as high as those of 7075-T6, but they may be higher than those of 7075-T73.

#### c. Quench Sensitivity

Using cooling-rate data from Ref. 3, the average cooling rate in the center of the boiling-water-quenched X7080 comparison alloy was 0.8°F per second between 750° and 550°F. A comparison with cooling-rate data for Elkington and Turner's proposed silver-bearing alloy is shown below:

	<u>Cooling rate</u>	<u>0.2-percent yield strength</u>
X7080-T7	0.8°F/sec	61.9 ksi (transverse)
Elkington and	0.8°F/sec	36 ksi (short-transverse)
Turner's	36°F/sec	59.5 ksi (short-transverse)
alloy	180°F/sec	68 ksi (short-transverse)

The fact that Elkington and Turner measured average cooling rates from 779° to 383°F instead of from 750° to 550°F makes little difference in this comparison.

The X7080-T7 has a strength advantage for cooling rates below 36°F per second. This cooling rate is equivalent to that in the center of 2.0-in.-thick plate quenched in 75°F water.

The Elkington and Turner alloy had higher strength than X7080-T7 when rapidly quenched. This can be attributed to its higher zinc, magnesium, and copper content, and to a small strengthening effect of silver at the higher cooling rates. This alloy's increased quench sensitivity is due to the silver addition and to its slightly higher manganese and copper content.

An increased quench sensitivity was also noted in the Phase II alloys with silver additions. Alloy 18 was more quench sensitive than the silver-free X7080-T7. Quench sensitivity also increased with higher copper content in the Phase II alloys.

It has been shown that the detrimental effects of silver on quench sensitivity are less severe in low-magnesium alloys (21). Polmear, however, has reported that cracking is a problem in larger ingots with reduced magnesium contents (22).

The increased quench sensitivity of the silver-bearing, chromium-free alloys is detrimental because slow quenching offers three important advantages. First, residual stresses due to quenching are reduced significantly; second, parts can be heat treated in thick sections with minimum distortion during subsequent machining; third, slow cooling rates are beneficial to stress-corrosion resistance (17, 23).

#### d. Fracture Toughness

Alloys 17 and 18 possessed the best toughness-strength combinations. The silver addition in alloy 17 had a beneficial effect on  $K_{IC}$ ; despite a higher strength for alloy 17, it is tougher than alloy 16. With alloy 16 as a reference point and using the average slope of the curves in Figure 55 (-3.5 ksi  $\sqrt{\text{in.}}$  per 1 ksi  $F_{TY}$ ), alloy 17 is 11 percent tougher than expected.

The Royal Armament Research and Development Establishment (RARDE) in England has also found silver to be valuable in increasing resistance of sheet to shatter under ballistic impact (24). Shatter under ballistic impact is particularly severe if the sheet is in tension during impact. RARDE measured the susceptibility to shatter by means of a Charpy impact test at liquid nitrogen temperature (-196°C). A 0.3-percent silver content was found to promote freedom from shatter in both low- and high-copper versions of DTD 687B (5.7% Zn, 2.6% Mg, 0.45% or 1.2% Cu, 0.12% Cr, 0.30% Mn). In these tests the alloys were aged to peak strength at temperatures from 230° to 329° F.

#### e. Fatigue Properties

The slight beneficial effect of silver on fatigue-crack growth properties in distilled water was not expected on the basis of previous work (25). That work showed silver to have a slight detrimental effect, but was conducted on T6-temper alloys with lower zinc and magnesium content and higher copper content than the Phase II alloys.

Polmear (22) has conducted other tests on silver-free and silver-bearing alloys, using notched and unnotched fatigue specimens from the short-transverse and longitudinal directions of 3-in.-thick plate. Silver significantly increased the unnotched fatigue endurance limit at  $10^8$  cycles of a low-copper alloy (5.7% Zn, 2.7% Mg, 0.5% Cu, 0.2% Cr) in the short-transverse direction. However, in a higher-copper alloy (5.7% Zn, 2.7% Mg, 1.35% Cu, 0.2% Cr) silver produced no change in the endurance limit at  $10^8$  cycles in either the notched or unnotched condition.

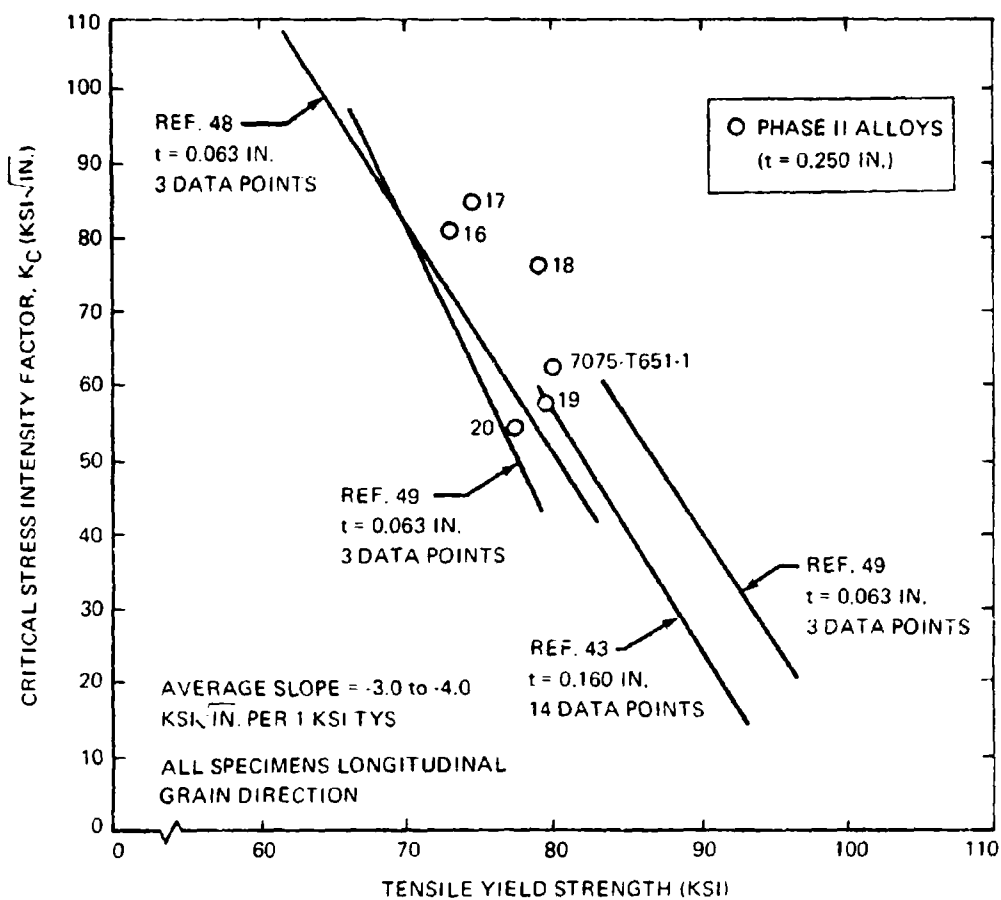


Figure 55. Fracture Toughness Parameter  $K_{IC}$  Versus Tensile Yield Strength for Several 7000-Series Aluminum Alloys

Rotating-beam fatigue tests on the silver-bearing alloy AZ74.61 (6% Zn, 2.3% Mg, 0.85% Cu, 0.2% Cr, 0.4% Ag) have shown no increase in endurance limit over that for similar silver-free Al-Zn-Mg alloys (26).

DiRusso has studied the effects of silver on chromium-bearing and zirconium-bearing 7075 (5.7% Zn, 2.5% Mg, 1.8% Cu, 0.18% Cr or Zr) in the form of extruded bar and rolled sheet (27, 28). He also found little difference in fatigue properties between silver-free and silver-bearing alloys.

f. Economic Considerations

The current price of silver is more than \$1.80 per troy ounce. To add 0.3 weight percent silver to a wrought Al-Zn-Mg alloy would cost more than \$0.08 per pound, assuming that production, processing, and handling costs of the silver-bearing alloy do not also increase.

Increased cost can be justified either by (1) reducing service problems (i.e. stress-corrosion cracking) or (2) increasing strength (i.e. reducing structural weight). It has already been shown that silver additions do not increase the stress-corrosion resistance for overaged alloys.

It is not uncommon to set a value on a pound of weight saved; this figure is often \$50.00 per pound or higher. It can be shown that silver additions are economically justified if the minimum mechanical properties allowables are raised by 1 ksi, even assuming that 3 lb of alloy are required to produce a 1-lb as-machined part.

Will silver additions raise the minimum mechanical property allowables by 1 ksi? It appears that this would be the case in rapidly quenched thin sections. However, since silver increases quench sensitivity, it is more likely that, for thick sections, a silver addition could actually lower the allowables.

Since neither improved stress-corrosion resistance nor higher mechanical properties result (for thick sections), the addition of silver does not appear justified.

g. Summary

Silver additions to the Phase II base alloy produced several beneficial effects, i.e. (1) greater fracture toughness, (2) lower fatigue-crack growth rates, and (3) a slight strength increase in thin, rapidly quenched sections. The addition of silver to the recommended alloy does not appear warranted, however, on the basis of:

- (1) The small extent of the beneficial effects
- (2) The similar stress-corrosion performance of the silver-free and silver-bearing overaged Phase II alloys
- (3) The problem of quench sensitivity in thick sections.

## 2. MEETING THE STRESS-CORROSION GOAL

Hunter et al. (29) state that "if a part is to fail, a crack must initiate, and if conditions conducive to crack initiations are maintained, failure almost certainly will result. Thus, it is the initiation of the crack, and the factors related to initiation, that determines whether a part will survive or fail."

We agree with this statement, but two important factors must be considered from an engineering point of view: (a) virtual immunity (e.g. in 7075-T73) can only be achieved with a considerable reduction of mechanical properties; (b) the vast majority of 7075-T6 and 7079-T6 parts perform satisfactorily in service. The results of this program indicate that Phase II alloys 16 through 20 in the step-aged condition would all perform better in service than 7075-T6. The superior performance of these alloys would be expected whether considering an electrochemical model or a coplanar slip model.

Sprowles and Brown (16) relate the superior resistance to intergranular attack and stress corrosion in overaged 7075-T73 to electrochemical effects, in particular to a reduction in the amount of copper in solid solution in the grain bodies. This reduction occurs during the second high-temperature aging step of the T73 heat treatment. The net result is that the grains and grain boundaries attain the same potential. This conclusion is based in part on the work of Hunter, Frank, and Robinson as reported by Sprowles and Brown (16) and Fink and Wiley (30). Hunter, Frank, and Robinson found selective corrosion along grain margins in thin films of slowly quenched ( $45^{\circ}\text{F/sec}$ ) 7075-T6 sheet. This selective corrosion left grain boundary precipitates unattacked. Fink and Wiley suggested that the grain margins would be anodic because of the partial depletion of the solid solution of copper at the grain edges, thereby causing the grain margins to become anodic to the grain bodies and to the precipitated constituent in the grain boundaries. These observations were in accord with those reported by Brown (16) on the effect of artificial aging on the electrochemical potential of rapidly quenched 7075. Brown reported that aging at  $250^{\circ}\text{F}$  caused the potential of the 7075 to shift about 75 mV in the cathodic direction after 24 to 36 hr. Additional aging at  $250^{\circ}\text{F}$  caused little change. If after aging 24 hr at  $250^{\circ}\text{F}$  the alloy was aged 8 hr at  $350^{\circ}\text{F}$ , Brown found that the potential shifted about 35 mV in the anodic direction. As Brown pointed out, these changes in potential indicate the precipitation of zinc from solid solution at the lower temperature and of copper at the higher temperature. The second aging step thus reduces the copper in solid solution in the grain bodies, with the result that the grains and grain boundaries attain the same potential.

However, changes other than electrochemical changes also occur with overaging. The coherency, size, and volume fraction of the hardening precipitates change during aging. Speidel (31, 32, 33) and Holl (34) have shown by thin-foil analysis of deformed high-strength aluminum alloys that these changes alter the mode of dislocation movement. Coplanar slip with pile-ups at grain boundaries has been observed in the alloys susceptible to stress-corrosion cracking, whereas the more overaged alloys exhibit slip bands containing curved dislocations and dislocation loops and tangles. These authors postulate that the pile-ups at grain boundaries occurring in the susceptible alloys can cause intercrystalline fracture in the manner proposed by Robertson and Tetelman (35) and Stroh (36). Slip line evidence showing dislocation pile-ups at a cracked grain boundary of an Al-7.5Zn-2.4Mg alloy has been obtained by Brummer et al. (37).

No cracks have occurred in alloys 16 through 20 in the industrial environment after 160 days at 20, 26, 32, and 44 ksi. The performance of alloy 18 in the alternate-immersion tests and in the double-cantilever beam (DCB) stress-corrosion configuration was somewhat inferior to that of alloys 16, 17, 19, and 20. However, additional overaging is proposed for the recommended alloy (alloy 18 without silver); its stress-corrosion resistance should be significantly greater than that of alloy 18. Overaging is definitely the method to achieve increased stress-corrosion resistance. Even the highly susceptible alloy 7079 can be made highly resistant to stress-corrosion cracking with sufficient overaging: The 7079-T611-G comparison alloy (highly overaged as evidenced by its high electrical conductivity, Table I) possessed excellent stress-corrosion resistance, but its yield strength was the lowest of any alloy tested. The silver-bearing alloy 7578 is another example. This alloy is very similar to alloy 20 except for its higher aging temperature (T6 + 8 hr at 340° F). The corrosion attack consisted of very blunt pitting (Fig. 36), similar to that which occurred on the 7075-T73 (Fig. 30). The higher aging temperature also resulted in lower mechanical properties for the 7578, and the strength of this alloy was comparable to that of AZ74.61, AZ74.61-A, and 7075-T73.

Thus the degree of overaging must be the minimum required to impart the desired level of stress-corrosion resistance. Aging curves indicate that the time at 320° F. can be doubled for alloy 18 without lowering properties below those of 7075-T6. Since silver influences strength only slightly, the recommended alloy should be overaged approximately 20 hr at 320° F.

a. Composition Effects

Other factors that may influence stress-corrosion resistance are summarized below.

(1) Minor Element Additions

The effects of silver, boron, cerium, yttrium, and zirconium on stress-corrosion resistance were evaluated in Phases I and II. It is apparent that the effects of thermal treatment far outweigh the individual elemental effects. An additional comment on the effect of silver is that alloys with high silver contents (e.g. 7578) show a high density of pitting attack. This effect was also noted in Phase I (1).

(2) Copper Content

Another possible explanation for the difference in performance between 7075-T73 and 7178-T7651 as compared to X7080-T7 is their different copper contents. The higher copper contents in the former two alloys may have contributed to their tendency to pit rather than to crack as the X7080-T7 did. However, alloys 17 and 18 contained the same copper content. In this case, the lower rate of overaging noted in alloy 18 certainly contributed to the greater extent of cracking in this alloy. It should also be noted that higher copper contents increase quench sensitivity.

(3) Manganese, Chromium, and Zirconium

The manganese-bearing and zirconium-bearing alloys may not be as resistant to stress-corrosion cracking as similarly aged chromium-bearing alloys (7075-T73, 7178-T7651). For example, no specimens of alloy 18 failed at stress levels of 26 ksi or below (the goal was 25 ksi

threshold), but cracks did develop in three of the six specimens of this alloy at 26 ksi. The manganese-bearing, stress-corrosion-resistant X7080-T7 comparison alloy also developed sharp intergranular cracks at the 26-ksi stress level.

One possible explanation for the poorer performance of the manganese- and zirconium-bearing alloys is the fact that the thin-foil analysis showed a much lower density of intermetallics in the manganese-bearing X7080-T7 and the zirconium-bearing alloy 18 than in the chromium-bearing alloys 17, 7075, and 7178. Speidel (31) has suggested that the intermetallic particles formed by chromium, manganese, and zirconium are either bypassed by dislocations or act as dislocation sources when the material is stressed, thus reducing the effective stress concentration at grain boundaries that results from coplanar slip and pile-ups in susceptible alloys. The much greater density of intermetallics observed in the chromium-bearing alloys could therefore be more effective in reducing the extent of dislocation pile-ups at grain boundaries.

However, the same effect of reducing pile-ups has been shown by Speidel (31, 32, 33) and Holl (34) to occur by overaging these alloys until a large fraction of the hardening precipitates are bypassed rather than sheared. Therefore, even if manganese- and zirconium-bearing alloys are slightly inferior, overaging in these alloys should maintain a high level of immunity.

#### b. Other Metallurgical Effects

##### (1) Substructure, Quench Rate, and Grain Orientation

The improved stress-corrosion resistance of the recommended alloy after additional overaging may be further increased if slower quenching rates are used. This expectation is based on the work of Elkington (23). He showed that slower quenches or prolonged aging after slow quenching increased the stress-corrosion life of DTD 5034 (5.2-6.2% Zn, 2.2-3.2% Mg, 0.3-0.7% Cu, 0.18-0.5% Cr + Mn) by increasing the amount of subboundary precipitation. He also showed that the amount of substructure in DTD 5034 could be increased by varying the amount of working. Increased substructure resulted in increased stress-corrosion resistance.

Would alloy 18 have performed better if it had been boiling-water quenched (more subboundary precipitation) rather than cold-water quenched? It appears that the answer is yes. None of the Phase II alloys showed any heavy subboundary precipitation, as evidenced by the difficulty in observing the subboundaries in etched samples of these alloys. However, subboundaries were clearly visible in the more resistant AZ74.61 and X7080-T7 comparison alloys. The larger amount of subboundary precipitates in these alloys is probably due to the slower quenching rate. Also, in the case of X7080-T7, the alloy was almost certainly more highly overaged than any of the Phase II alloys. This conclusion is based on the high electrical conductivity of the X7080-T7 and the electron microscopy study.

The increased subboundary precipitation in the AZ74.61 and X7080-T7 was a factor in the good performance of these alloys in the stress-corrosion test. Both heats of AZ74.61 and the X7080-T7 showed definite intergranular attack even at the 26-ksi stress level, but the cracks propagated very slowly. Primary cracks were continually blunted because of a tendency for the attack to branch out along the subgrain boundaries (Figs. 28 and 31). The attack dislodged entire subgrains along the primary grain boundary, resulting in a blunted crack and retarding the preferential propagation of any one crack.



The better than expected performance of alloy 7079-T611-A (Fig. 32) resulted at least in part from the grain structure and grain flow orientation at the parting plane of the forging from which the specimens were taken, and not from an inherently resistant structure (which can only be achieved by overaging).

## (2) Fabrication History

The difference in stress-corrosion resistance between the two heats of 7075-T651 indicates that the pile-up theory by itself is not enough to explain stress-corrosion susceptibility. This follows from the fact that in two different heats of 7075-T651 with similar chemistry, heat treatment, and grain structure, similar dislocation arrangements (restricted slip and pile-ups at grain boundaries) would be expected and thus could not account for the differences in stress-corrosion performance. On the other hand, differences in local chemistry along grain boundaries of the two heats of 7075-T651 might explain the differences in their performance. These chemistry differences could result from differences in starting ingot size, homogenization time and temperature, and time-temperature-fabrication history. Some work has been reported on the effect of various homogenization temperatures on the composition gradients across grain boundaries (38).

To determine if the difference in stress-corrosion performance could be accounted for by differences in composition across grain boundaries, a microprobe analysis was made at low angles across grain boundaries in the two heats of 7075-T651. The analysis was for zinc, magnesium, and copper. Although slight variations in copper content from point to point were noted, no consistent differences in composition at the grain boundaries were detected. The reason for the different performances in the two heats of 7075-T651 is not clear at this time.

## (3) Resistance to Exfoliation

None of the overaged Phase II alloys were susceptible to exfoliation corrosion. This would be expected on the basis of the electrical conductivities of the Phase II alloys. Rotsell (39) has shown that susceptibility to exfoliation becomes negligible when the alloys are overaged to electrical conductivities of about 35 percent IACS or greater. His findings are based on studies of 7075, 7178, and 7001.

## 3. MEETING THE MECHANICAL PROPERTY GOAL

Since all the Phase II alloys except alloy 20 were located in the center of a proposed composition range, their mechanical properties must be considered typical, not minimum. To obtain some idea of the minimum mechanical properties of the proposed alloy, a value must be subtracted from the typical values obtained for alloy 18. Subtracting 7 ksi from the tensile properties observed for alloy 18 is reasonable in estimating the minimum longitudinal properties. Therefore, the minimum yield strength for the recommended alloy with a heat treatment of T6 + 10 hr at 320° F should be about 72 ksi (79 ksi - 7 ksi). This calculation assumes that eliminating silver from the proposed alloy will have as little an effect on strength as was observed between alloy 16 and 17. Since additional overaging is suggested for the recommended alloy, the 72 ksi value must be reduced further. Based on the aging curves for alloy 18, the proposed aging treatment of T6 + 20 hr at 320° F would not lower the minimum strength of the recommended alloy below that of 7075-T6 for comparable forms and thicknesses.

#### 4. CONTROLLING QUENCH SENSITIVITY

The phase II base alloy met the stress-corrosion and strength goals of the contract. However, the presence of chromium results in a quench-sensitive alloy. It would be an obvious advantage to be able to eliminate or replace chromium without sacrificing strength, fracture toughness, fatigue life, or stress-corrosion resistance. Chromium can be replaced with manganese (e.g. X7080), and Panseri and DiRusso (40) have shown that zirconium may substitute for chromium in promoting subgrain formation and in inhibiting recrystallization of 7075 during solution treatment.

Bryant (41) has shown that chromium additions make an alloy more quench sensitive than do manganese additions. DiRusso (2) has shown that chromium additions make an alloy more quench sensitive than do zirconium additions. DiRusso postulates that chromium cannot maintain a high concentration of vacancies at slower quenching rates and that the effect is a reduction in the number of nucleation centers (assuming that nucleation requires solute atom-vacancy clusters). The resulting less dense and coarser hardening precipitates cause lower strength. DiRusso proposes that zirconium maintains a high concentration of vacancies even at low quenching rates because of a high interaction energy of the zirconium with vacancies.

Robinson and Hunter, according to Sprowls and Brown (16), have stated that chromium accelerates zone growth. This effect is reported to be due to chromium atoms that remain in solid solution and increase retention of vacancies during quenching. This view seems to conflict with DiRusso's.

Bryant (41) states that chromium and manganese increase quench sensitivity by nucleating preferential precipitation during quenching so that a portion of the solute is not available for subsequent age hardening.

Bryant discusses two possibilities to account for the behavior of chromium and manganese. First, the chromium and manganese atoms in supersaturated solution may form clusters that provide sites for precipitate nucleation. The slow diffusion rates of the chromium and manganese permit this supersaturation at levels far above the equilibrium solid solubility. Second, the recrystallization-inhibiting properties of these two elements result in the formation of a stable dislocation substructure, which persists throughout solution treatment and provides nuclei for the preferential precipitation of solute during the quench. The fact that chromium has a more marked effect on quench sensitivity than manganese is attributed by Bryant to the slower diffusion rate of chromium and its greater ability to inhibit recrystallization.

Zirconium will be used in place of chromium in the recommended alloy. The alloy will thus be less quench sensitive.

#### 5. MAINTAINING FRACTURE TOUGHNESS

Fracture toughness properties for all Phase II alloys were comparable to those for 7075-T651. One of the Phase II alloys contained the highest zinc + magnesium content in the proposed chemistry range. This alloy possessed higher strength than the Phase II base alloy and provided a measure of the minimum fracture toughness to be expected. In the 7000-series high-strength aluminum alloys, the fracture toughness parameter  $K_{IC}$  decreases approximately 3.5 ksi  $\sqrt{\text{in.}}$  per 1 ksi increase in tensile yield strength, as shown in Fig. 55. (The  $K_{IC}$  values

plotted in Fig. 55 do not take slow growth into account.) Most of the data in Fig. 55 are for thicknesses of 0.063 in. and 0.160 in., but  $K_C$  is a function of thickness. With their greater thickness (0.250 in.), the Phase II alloys would be expected to lie on a curve to the left of the curve in Fig. 55. Using data from Kaufman and Holt (42), a decrease in  $K_C$  of about 20 ksi  $\sqrt{\text{in.}}$  for 7075-T6 would be expected going from 0.063 in. to 0.250 in. thickness. Despite the greater thickness of the Phase II test material, alloys 16 through 20 (including the high zinc + magnesium alloy) were within the scatter band for 0.063-in. material.

Analysis of the fracture toughness data for alloy 18 shows that the replacement of chromium with zirconium had an additional beneficial effect; alloy 18 is about 10 percent tougher than expected, using alloy 17 as the reference point. These comparisons use  $K_C$  and not  $G_C$  values;  $G_C = K_C^2/E$ .

In both strength and toughness, alloy 18 possesses the most attractive combination of properties. It contains silver, which the previous analysis has shown has a beneficial effect on toughness. Removal of the chromium intermetallics from the alloy has resulted in fewer nucleating sites for the coalescence of microvoids, thereby increasing toughness. This was evident from the fractographs comparing the fractured Charpy specimens from alloy 18 with the other Phase II alloys. The dimple size for alloy 18 was much larger. Data from a current Boeing alloy development program (25) show that in a high-zinc/magnesium-ratio alloy containing both silver and chromium, the addition of zirconium increased toughness and strength. Since chromium intermetallics were present in the latter alloy, zirconium must increase the toughness of an alloy just as silver did. The high toughness of alloy 18 is due partly to the silver addition, partly to the zirconium addition, and partly to the removal of the chromium intermetallics.

Alloy 20 (high zinc and magnesium) had the lowest toughness-strength relationship as expected, but this toughness is within the range of toughness values reported for 7075-T651. The high copper in alloy 19 also decreases toughness below that expected, using alloy 17 as the reference point. A higher-volume fraction of the S phase ( $\text{CuMgAl}_2$ ) may be responsible for this behavior.

The lowest fracture toughness to be expected in any 7000-series alloy depends not only on the heat treatment and the zinc, magnesium, and copper contents, but also on the iron and silicon content. An analysis of the effects of iron and silicon at constant strength levels (43, 44) has shown that the intermetallics resulting from iron ( $\text{Al}_7\text{Cu}_2\text{Fe}$ ) and silicon ( $\text{Mg}_2\text{Si}$ ) are detrimental to fracture toughness. Therefore, the minimum toughness shown for alloy 20 could be further lowered if increased iron and silicon are allowed in the recommended alloy. Data from Ref. 43 indicate that the toughness of alloy 20 will decrease by about 5 ksi  $\sqrt{\text{in.}}$  if 0.2 weight percent iron is present. Increasing silicon content has the complicating effect of decreasing the magnesium available for strengthening by tying up more magnesium in  $\text{Mg}_2\text{Si}$  particles. This competing reaction decreases the strength, thus tending to increase toughness at the same time that the increased-volume fraction of  $\text{Mg}_2\text{Si}$  is tending to decrease toughness. The results from Ref. 44 indicate that in a material of the alloy 20 composition, 0.2 percent silicon will lower strength and increase the amount of  $\text{Mg}_2\text{Si}$  in such a manner that the resulting toughness changes only slightly. Therefore, the lowest toughness one might expect for alloy 20 with 0.2% Fe and 0.2% Si is about 49 ksi  $\sqrt{\text{in.}}$  (54 ksi  $\sqrt{\text{in.}}$  - 5 ksi  $\sqrt{\text{in.}}$  due to increased iron). The resulting yield strength of the alloy in this case (44) would be about 72 ksi (77 ksi - 5 ksi) owing to the increased silicon content.

If the strength of alloy 20 is increased to that of 19 and 7075-T651-1 by moving along a slope of  $-3.5 \text{ ksi } \sqrt{\text{in.}}$ , as in Fig. 55, it can be seen that alloys 19 and 20 both have lower toughness than the 7075-T651-1. This occurs despite a slightly higher iron content in the 7075-T651-1. This finding substantiates previous findings that the alloy with the lowest total alloy content (in this case the 7075-T651-1) has the highest fracture toughness for a given yield strength. As another example, alloys of the types 7075-T651, 7178-T76, and 7001-T75 are all of similar strength. The most highly alloyed of the three, 7001-T75, has the lowest fracture toughness. This discussion leads to an important point in aluminum alloy development: Any alloy of the 7075, 7178, or 7001 type, or even one more highly alloyed, can be overaged to obtain adequate stress-corrosion resistance, and if highly alloyed will possess high strength after the overaging treatment. The fracture toughness, however, will decrease with increasing total alloy content, even if the alloys are all overaged to the same strength. In addition to the toughness decrease with increasing total alloy content, the quench sensitivity increases.

The preceding discussion considers the parameter  $K_{IC}$  for a given thickness and in one grain direction. The same general effects of composition and heat treatment apply to the plane-strain fracture toughness parameter  $K_{IQC}$ .

Another parameter that can assume tremendous importance in thick sections is grain orientation. For example, extremely low toughness values have been observed across the parting plane of a 7079-T6 die forging (45). These data were obtained by using precracked Charpy specimens and relating  $W/A$  values to the fracture toughness parameter  $G_C$  as shown in Fig. 56. These data are for the longitudinal grain direction and represent very-high-strength to medium-strength 7000-series aluminum alloys. All the phase II alloys fall within the scatter band, and the same trends observed on longitudinal center-notched panels are exhibited by the longitudinal precracked Charpy specimens. The correlation between  $W/A$  and  $G_C$  is quite good for the lower toughness values, but becomes uncertain at the higher toughness values (lower strengths).

All Phase II alloys had higher  $W/A$  values than 7575, 7578, and 7178-T76, despite the fact that these alloys have lower strengths than any of the Phase II alloys. Charpy data indicate a  $K_{IC}$  of about  $41 \text{ ksi } \sqrt{\text{in.}}$  for 7178-T7651 at a yield strength of 71.5 ksi. The Phase II alloy with the lowest toughness had a  $K_{IC}$  of  $54.1 \text{ ksi } \sqrt{\text{in.}}$  at a yield strength of 77.3 ksi. The lower-strength comparison alloys X7080-T7 and AZ74.61 were tougher than the other comparison alloys and the Phase II alloy.

An interesting possibility is that overaging may increase short-transverse fracture toughness. The short-transverse delaminations in the 7075-T651-1 fractures were intergranular, indicating that the material cannot sustain high stresses in the short-transverse direction without cracking along grain boundaries. Since these intergranular fractures are brittle, little energy is absorbed and the toughness is low. The important point is that overaging markedly reduces this tendency for short-transverse delamination.

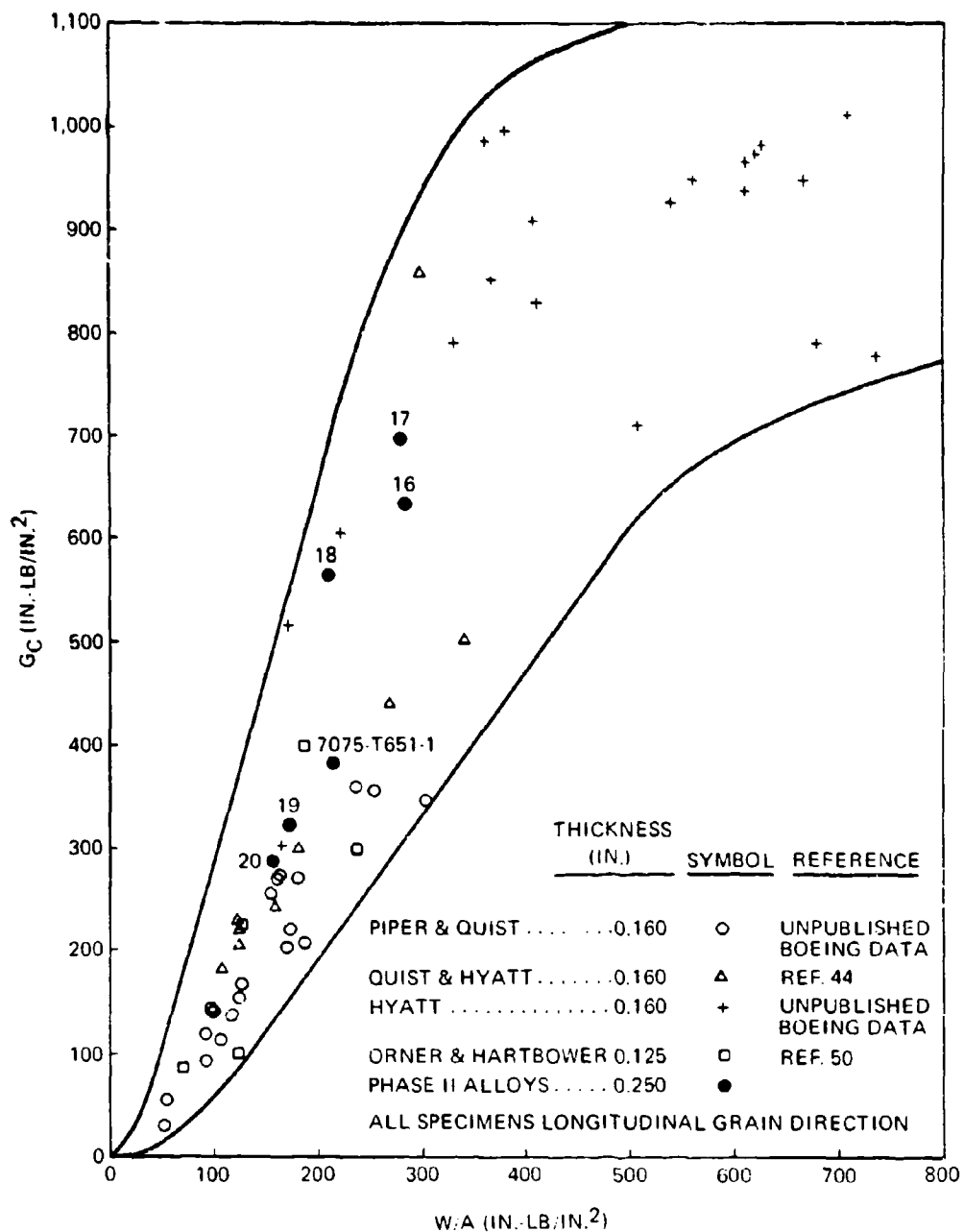


Figure 56. Correlation Between Precracked Charpy V-Notch Impact Data and  $G_c$  for Several 7000-Series Aluminum Alloys

## 6. MAINTAINING FATIGUE PROPERTIES

The most significant finding from the fatigue evaluation of the Phase II alloys was that all the overaged alloys (16, 17, 18, 19, 20) outperformed the peak-strength 7075-T651-1 in distilled water. The overaged alloys were more resistant to the environmentally induced acceleration of fatigue cracking, as evidenced by the preponderance of ductile striations on the fracture surfaces. Fatigue-crack growth data obtained in distilled water are comparable to data obtained in high-humidity air (46). High-humidity environments are common in service, and the fatigue growth data obtained in distilled water are significant.

The slight detrimental effect of increased copper content on fatigue-crack growth properties in distilled water was unexpected. Previous work on T6-temper alloys showed high copper content to be beneficial in reducing crack growth rates in distilled water and in decreasing the amount of brittle striations (25). Thus, generalizations concerning the effects of various chemical composition changes cannot be extrapolated from one base chemistry to another. Zinc/magnesium ratio, strength level, and heat-treat condition also play important roles.

The additional overaging proposed for the recommended alloy should help further to slow the fatigue-crack growth rates in humid environments.

Fatigue-crack growth data are not available for the comparison alloys. Notched fatigue data on axial fatigue specimens of the chromium-free X7080-T7 have been obtained (47), and the results indicate lower than expected endurance limits (5 ksi at  $10^7$  cycles at  $K_t$  values of 2.4 and  $R = -1.0$ ). The significance of these data with respect to the recommended alloy is not known, and further work is indicated.

## 7. THE RECOMMENDED ALLOY

The recommended alloy chemistry is as follows:

<u>Zn</u>	<u>Mg</u>	<u>Cu</u>	<u>Mn</u>	<u>Cr</u>	<u>Zr</u>	<u>Ti</u>	<u>Fe</u>	<u>Si</u>
5.9- 6.9%	2.2- 2.9%	0.7- 1.5%	0.05- 0.15%	0.05% max	0.10- 0.25%	0.10% max	0.20% max	0.20% max

These composition ranges are typical for commercially available high-strength Al-Zn-Mg-Cu alloys, and the basic chemistry is in a range in which alloys have been successfully produced. Thus this alloy appears to be commercially feasible.

The alloy's strength is governed primarily by the zinc, magnesium, and copper contents and by the aging treatment. With the given alloy content and a two-step aging treatment, minimum mechanical properties equivalent to those of 7075-T6 should be produced.

With chromium and silver removed, this alloy will be relatively quench insensitive. High mechanical properties will thus be produced in thick sections and at slow quenching rates.

A high stress-corrosion resistance will be achieved by overaging. In addition, quenching stresses will be reduced, leading to an improvement in in-service stress-corrosion performance.

The fracture and fatigue properties will be better than those of 7075-T6. The zirconium addition (and removal of chromium) will increase toughness. Short-transverse toughness will be improved by overaging, as will fatigue-crack growth characteristics.

## SECTION V

### CONCLUSIONS

1. All Phase II alloys had longitudinal 0.2-percent yield strengths above 70 ksi, had stress-corrosion resistance superior to that of 7079-T6 and 7075-T6, and met the contract's stress-corrosion goals. Fatigue and fracture toughness properties were comparable to those of current high-strength commercial alloys.
2. In the Phase II base alloy, the silver addition increased longitudinal yield strength only 2 percent and had no measurable effect on transverse strength. The silver increased fracture toughness, reduced fatigue-crack growth rates in distilled water, increased quench sensitivity, and had no measurable effect on the alloy's short-transverse stress-corrosion resistance in the overaged condition.
3. The beneficial effects conferred upon the Phase II base alloy by the addition of silver are not great enough to warrant the use of silver in a production alloy of the Phase II base composition.
4. Removing chromium and adding zirconium to the Phase II base alloy with silver increased longitudinal and transverse yield strength by 6 percent, increased fracture toughness, and increased fatigue-crack growth rates. The reduced rate of overaging in this alloy (alloy 18), shown by its slow rate of decrease in hardness, its slow rate of increase in electrical conductivity, and its less overaged microstructure, resulted in greater susceptibility to stress-corrosion cracking for the aging treatment used (T6 + 10 hr at 320°F). Doubling the aging time at 320°F or increasing the aging temperature 10°F will increase stress-corrosion resistance without lowering the yield strength below contract goals. Slower quenching may make longer or high-temperature overaging unnecessary. Alloy 18 was far less quench sensitive than any other Phase II alloy. Without silver it will be even less quench sensitive. If the removal of silver from this alloy has no more effect than the removal of silver from the chromium-bearing Phase II base alloy, the recommended alloy (item 15) possesses by far the most attractive combination of properties that can be realized from this study.
5. Increasing the copper content of the Phase II base alloy with silver increased longitudinal yield strength 7 percent, decreased fracture toughness, decreased fatigue crack growth in dry air at low  $K_{Ic}$  levels, and increased fatigue crack growth in distilled water at low  $K_{Ic}$  levels. The high copper content increased quench sensitivity and increased the density of pitting attack in 3.5-percent sodium chloride.
6. The increased zinc + magnesium content in the Phase II base alloy with silver increased longitudinal yield strength 4.5 percent and decreased fracture toughness to the lowest value observed. This value was within the range for commercial high-strength aluminum alloys. The increased zinc + magnesium content increased fatigue-crack growth rates in distilled water and dry air and had very little effect on stress corrosion performance.
7. Stress-corrosion-crack growth rates for the 7075-T651-2 and 7079-T6-G comparison alloys were ten to 100 times greater than for any of the overaged Phase II alloys or other comparison alloys.



8. The chromium-free, silver-free comparison alloy X7080-T7 was the most quench insensitive of all alloys tested. The stress-corrosion cracks in this alloy grew very slowly and at the same rate as those in the Phase II alloys 16, 17, and 20.
9. The comparison alloys AZ74.61 and 7075-T73 had similar strengths and stress-corrosion resistance. The strength advantage of AZ74.61 over 7075-T73, if it exists, is small, and AZ74.61 cannot meet 7075-T6 minimum strength properties. [Two phenomena may explain why only 10 hr overaging at 320°F was enough for AZ74.61, whereas 24 to 30 hr at 320°F was required for 7075-T73: (a) AZ74.61 has a low copper content and thus tends to overage more rapidly. (b) An extensive subgrain structure and subgrain boundary precipitate in most of the AZ74.61 forgings examined causes branching of the main stress-corrosion crack; this leads to blunting of the crack tip. The same effect was seen in the chromium-free X7080-T7. Slow quenching rates are partly responsible for this behavior.]
10. The 7178-T7651 had the highest strength of the ten comparison alloys, and the lowest precracked Charpy toughness values of any alloy tested.
11. The chromium-free alloys 18 (containing zirconium) and X7080-T7 (containing manganese) had lower densities of small intermetallics than the chromium-bearing alloy. This accounted for the large ductile dimples on alloy 18 toughness specimens.
12. Overaging treatments decreased the short-transverse delamination or "splitting" during fracture of longitudinal center-notched panels.
13. All overaged Phase II alloys had better fatigue-crack growth properties in distilled water than did the peak-aged 7075-T651.
14. None of the Phase II alloys were susceptible to exfoliation corrosion.
15. The results of this program indicate that an alloy with the following nominal composition will best meet the goals of this contract: 6.40% Zn, 2.55% Mg, 1.10% Cu, 0.15% Zr, 0.10% Mn. This alloy when aged to T6 + 20 hr at 320°F or T6 + 10 hr at 330°F will be stronger than X7080-T7 and as quench insensitive as X7080, and as strong as and tougher than 7178-T7651. It will be far superior to 7178-T7651 in thick-section properties and far superior to 7075-T6 and 7079-T6 in stress-corrosion resistance. The allowable chemistry range for this alloy should be: 5.9-6.9% Zn, 2.2-2.9% Mg, 0.7-1.5% Cu, 0.10-0.25% Zr, 0.05-0.15% Mn, 0.05% max Cr, 0.10% max Ti, 0.20% max Fe, 0.20% max Si.
16. The ease with which all the Phase II alloys were cast and fabricated indicates that the recommended alloy is commercially feasible.

## SECTION VI

### RECOMMENDATIONS FOR FURTHER WORK

The recommended alloy is thus far only a "paper alloy"; it has been neither produced nor tested, but holds promise of meeting the goals of the program in production quantities.

To complete the development of this alloy, it is necessary to accomplish the following tasks:

1. Produce pilot plant heats of the alloy in various ingot sizes and forms;
2. Complete the determination of the optimum heat treatment;
3. Perform verification mechanical, fracture, and stress-corrosion tests;
3. Establish design allowables data.

A recommended course of action is as follows:

1. Cast two or three large ingots of the proposed alloy (preferably different heats).
2. Fabricate the material into:
  - a. Extrusions (rod or bar)
  - b. Forgings (hand and die with various-thickness sections up to 8 in.)
  - c. Plate (thick section)
3. Establish two-step heat treatment for optimum mechanical properties and stress-corrosion resistance. Consider:
  - a. Quenching rates
  - b. Room-temperature delay time
  - c. Time and temperature of the second step in the step-aging treatment (The first step of the step aging should be 24 hr at 250°F)
4. Verify mechanical and stress-corrosion properties in this optimum heat-treatment condition
5. Generate allowables and design data:
  - a. Mechanical properties  $F_{tu}$ ,  $F_{ty}$ , % elongation as a function of section thickness and grain direction
  - b. Stress-corrosion resistance: Threshold,  $K_{ISCC}$ , and crack growth rates

- c. Fracture toughness—Determine  $K_C$ ,  $K_{IC}$ , or  $W/A$  as a function of grain orientation and product form
- d. Fatigue properties—S-N curves, notched and unnotched; evaluate load transfer fatigue, crack growth rate, environmental effects

## REFERENCES

1. J.C. McMillan and M.V. Hyatt, Development of High-Strength Aluminum Alloys with Improved Stress-Corrosion Resistance, AFML-TR-67-180, Air Force Materials Laboratory, June 1967.
2. E. DiRusso, Further Investigations on Wrought Complex Al-Zn-Mg-Cu Alloys, Final Technical Status Report, Contract DA-91-591-EUC 3425, European Research Office, July 26, 1965.
3. Aluminum, Volume I, Properties, Physical Metallurgy and Phase Diagrams, edited by Kent R. Van Horn, ASM, 1967.
4. ARPA Coupling Program on Stress-Corrosion Cracking (Fourth Quarterly Report), Memorandum Report 1834, Naval Research Laboratories, November 1967, pp. 26-28.
5. E.J. Ripling, S. Mostovoy, and R.L. Patric, "Measuring Fracture Toughness of Adhesive Joints," Materials Research and Standards, Vol. 4, March 1964, pp. 129-134.
6. J.J. Gilman, "Direct Measurements of the Surface Energies of Crystals," J. Appl. Phys., Vol. 31, 1960, pp. 2208-2218.
7. S. Mostovoy, P.B. Crosley, and E.J. Ripling, "Use of Crack-Line-Loaded Specimens for Measuring Plane-Strain Fracture Toughness," Journal of Materials, Vol. 2, No. 3, 1967, pp. 661-681.
8. R.G. Hoagland, "On the Use of the Double Cantilever Beam Specimen for Determining the Plane Strain Fracture Toughness of Metals (67-Met-A)," Journal of Basic Engineering, Trans. ASME, Vol. 89, Series D, No. 3, September 1967.
9. B.W. Lifka and D.O. Sprowls, "An Improved Exfoliation Test for Aluminum Alloys," paper presented at the NACE 21st Annual Conference, Corrosion Principles Symposium, March 18, 1965.
10. W. Rosenkranz, British Patent No. 793, 076, 1958.
11. W. Rosenkranz, U.S. Patent No. 2,823,994, 1958.
12. I.J. Polmear, J. Inst. Metals, 1960-61, 89, 51.
13. I.J. Polmear, Nature, 1960, 186, 303.
14. I.J. Polmear, J. Inst. Metals, 1960-61, 89, 193.
15. F.G. Day, J. Inst. Metals, Vol. 95, 1967, p. 94.
16. D.O. Sprowls and R.H. Brown, "Stress Corrosion Mechanisms for Aluminum Alloys," paper presented at the International Conference on Fundamental Aspects of Stress-Corrosion Cracking, Ohio State University, September 11-15, 1967.
17. R.W. Elkington and A.N. Turner, "The Effect of Silver on the Stress-Corrosion Resistance of High-Strength Al-Zn-Mg-Cu Alloys," J. Inst. Metals, Vol. 95, 1967, pp. 294-298.

18. J.T. Vietz, K.R. Sargant, I.J. Polmear, "The Influence of Small Additions of Silver on the Aging of Aluminum Alloys: Further Observations on Al-Zn-Mg Alloys," J. Inst. Metals, Vol. 92, 1963-64, pp. 327-333.
19. W. Rosenkranz, Aluminum, 1963, 39, 290, 630, 741.
20. D. James and J. Roy, Aero. Soc., 1966, 70, 763.
21. I.J. Polmear, J. Inst. Metals, 1966, 94, 36.
22. I.J. Polmear, Report Met. 63, ARL, January 1967.
23. R.W. Elkington, J. Inst. Metals, Vol. 90, 1961-62, p. 267.
24. T. Williams, Memo 8/64, RARDE, February 1964.
25. M.V. Hyatt and W.E. Quist, "The Influence of Heat Treatment and Composition on the Stress Corrosion, Fatigue, and Fracture Properties of 7075-Type Aluminum Alloys," AFML-TR-67-329, Proceedings of the Air Force Materials Laboratory Fiftieth Anniversary Technical Conference on Corrosion of Military and Aerospace Equipment, Denver, May, 1967.
26. W. Shutz and E. Gassner, Technical Note 13/65, Laboratorium fur Betriebsfestigkeit, Darmstadt, West Germany.
27. E. DiRusso, Alluminio Nuova Metallurgia, 1964, 33, 505.
28. E. DiRusso, ibid, 1965, 34, 331.
29. M.S. Hunter, W.G. Fricke, Jr., D.L. McLaughlin, D.L. Robinson, D.O. Sprowles, and J.M. Walsh, Study of Crack Initiation Phenomena Associated with Stress Corrosion of Aluminum Alloys, First Annual Report, Contract NAS 8-20396, Alcoa Research Laboratories, September 28, 1967.
30. W.L. Fink and L.A. Wiley, "Quenching of 75S Aluminum Alloy," Metals Technology, Vol. 14, No. 5, American Institute of Mining and Metallurgical Engineers, August, 1947.
31. M.O. Speidel, "Coherent Particles and Stress Corrosion Cracking of High Strength Aluminum Alloys," AFML-TR-67-329, Proceedings of the Air Force Materials Laboratory Fiftieth Anniversary Technical Conference on Corrosion of Military and Aerospace Equipment, Denver, May 1967.
32. M.O. Speidel, "Interaction of Dislocations with Precipitates in High Strength Aluminum Alloys and Susceptibility to Stress Corrosion Cracking," paper presented at Ohio State Conference on Stress Corrosion, Columbus, September 11-15, 1967.
33. M.O. Speidel, "Interaction of Dislocations with Coherent Particles and Stress Corrosion Cracking of High-Strength Aluminum Alloys," Phys. Stat. Sol., Vol. 22, K71, 1967.

34. H.A. Holl, Corrosion, Vol. 23, 175, 1967.
35. W.D. Robertson and A.S. Tetelman, Strengthening Mechanisms in Solids, ASM, 1962, p. 217.
36. A.N. Stroth, Proc. Roy. Soc., 223, 404, 1954.
37. S.B. Brummer, R.O. Bell, F.H. Cocks, A. Cordellos, M. Krebs, and J. Russo, Study of the General Mechanism of Stress Corrosion of Aluminum Alloys and Development of Techniques for Its Detection, Fifth Quarterly Report, Contract NAS 8-20297, Tyco Laboratories, Inc., Waltham, Mass., September-November 1967.
38. V.L. Backerud, Z. Metallkde, Bd. 57 (1966) H. 4.
39. W.C. Rotsell, private communication, Harvey Aluminum (Incorporated), Torrance, Calif. January 23, 1968.
40. C. Panseri and E. DiRusso, Alluminio Nuova Metallurgia, 1961, 30, 549.
41. A.J. Bryant, "The Effect of Composition upon the Quench Sensitivity of Some Al-Zn-Mg Alloys," J. Inst. Metals, Vol. 94, 1966, pp. 94-99.
42. J.G. Kaufman and M. Holt, "Evaluation of Fracture Characteristics of Aluminum Alloys at Cryogenic Temperatures," paper presented at the Cryogenic Engineering Conference, Philadelphia, August 1964.
43. D.E. Piper, W.E. Quist, and W.E. Anderson, "The Effect of Composition on the Fracture Properties of 7178-T6 Aluminum Alloy Sheet," Application of Fracture Toughness Parameters to Structural Metals, Metallurgical Society Conferences, Vol. 31, AIME, 1966, p. 227.
44. W.E. Quist and M.V. Hyatt, "The Effect of Chemical Composition on the Fracture Properties of Al-Zn-Mg-Cu Alloys," AIAA, ASME Seventh Structures and Materials Conference Proceedings, Cocoa Beach, Florida, April 1966.
45. M.V. Hyatt, H.R. Zahn, J.C. McMillan, "Parting Plane Effects on Fracture Mode and Toughness in a 7079-T6 Die Forging," Transactions Quarterly, Vol. 59, No. 2, 1966, pp. 342.
46. J.C. McMillan, R.W. Hertzberg, "The Application of Electron Fractography to Fatigue Studies," paper presented at Seventieth Annual Meeting of ASTM, Boston, June 25-30, 1967.
47. R.V. Turley, private communication, Douglas Aircraft Division, McDonnell-Douglas, Long Beach, Calif., Nov. 3, 1967.
48. J.G. Kaufman and A.H. Knoll, Mat. Res. and Standards, Vol. 4, No. 4, 1964, p. 151.
49. J.A. Nock, Jr., and H.Y. Hunsicker, J. Metals, Vol. 15, No. 3, 1963, p. 216.
50. G.M. Orner and C.E. Hartbower, "Sheet Fracture Toughness Evaluated by Charpy Impact and Slow Bend," Welding Journal (Research Supplement), Vol. 40, 1961, p. 4055.

## APPENDIX I

### PREPARATION OF EXPERIMENTAL ALLOYS

The Phase II experimental alloys were prepared from DC ingots 3.25 in. thick by 7 in. wide by 26 in. long. After casting, each ingot was furnace stabilized at 550°F to minimize the possibility of cracking. The ingots were soaked 16 hr at 875°F and air cooled. After cropping and scalping (0.2 in. per face), ingot slices were etched. The chromium-free silver + zirconium alloy (alloy 18) had columnar grains present at the chill faces that were not entirely removed by the normal scalping. The other four alloys were uniform in structure, with a fine macro grain size.

The ingot sections were reheated to 750°F and cross-rolled to 13 in. wide. They were then rolled straightaway to 1.250 in. (56 percent hot work). After reheating to 825°F, hot rolling continued to 0.440 in. thickness. At this thickness each alloy was etched in 10 percent sodium hydroxide to remove the hot mill oxide, desmuted in nitric acid, and rinsed in hot water. The etched plates disclosed that alloy 18 had long columnar surface grains, whereas the other four alloys had extremely fine grains present at their surfaces.

The etched plates were then reheated to 825°F and hot rolled to 0.254 in. thickness (80 percent hot work at this temperature or a total of 91 percent hot work), followed by an air cool. Heat treatment began with solution treatment of the 0.254-in. plate at 860°F (a 35-min soak) followed by a quench in 60°F water. The plate material was stretcher straightened 15 hr after the quench. The material was aged 2 days at room temperature. Artificial aging at 250°F for 24 hr followed, using a 35°F/hr heat-up rate from 100°F. At the completion of the 24-hr soak, the material was air cooled. The panels were edge trimmed, then given the second-stage artificial age of 320°F for 10 hr. The heat-up rate was 35°F/hr from 250°F. The final step was an air cool from 320°F.

# APPENDIX II

## ACTUAL MECHANICAL AND FRACTURE PROPERTIES OF PHASE II ALLOYS

Table VI. Actual Mechanical and Fracture Properties of Phase II Alloys

Alloy	Grain direction	$F_{tu}$ (ksi)	$F_{ty}$ (ksi)	Elongation (% in 2 in.)	RA (%)	W/A (in. lb/in. <sup>2</sup> ) <sup>a</sup>	$K_{IC}$ (ksi $\sqrt{\text{in.}}$ ) <sup>b</sup>
16	L	80.7	72.3	11	22	295	81.9 94.4 <sup>d</sup>
	L	81.2	73.2	11	25	270	80.6 85.6 <sup>d</sup>
	T	81.4	73.3	11	27	---	---
	T	81.5	73.0	11	28	---	---
17	L	82.6	75.1	10	18	271	87.2 104.5 <sup>d</sup>
	L	81.5	73.4	11	25	287	82.0 92.1 <sup>d</sup>
	T	81.6	73.1	11	26	---	---
	T	81.5	73.0	10	27	---	---
18	L	84.4	78.6	11	23	220	82.1 86.5 <sup>d</sup>
	L	84.5	79.2	10	25	194	70.7 74.0 <sup>d</sup>
	T	83.4	77.8	11	27	---	---
	T	83.5	77.4	11	26	---	---
19	L	87.3	79.1	10	16	169	57.5 60.0 <sup>d</sup>
	L	87.8	79.9	10	20	176	(c) (c)
	T	86.6	77.8	11	29	---	---
	T	85.0	75.8	10	18	---	---
20	L	84.8	76.4	11	20	153	51.0 54.4 <sup>d</sup>
	L	85.8	78.2	10	21	153	56.8 59.7 <sup>d</sup>
	T	83.9	75.0	11	22	---	---
	T	84.1	75.7	11	21	---	---
7075-T651-1	L	84.8	79.9	13	26	221	63.6 68.2 <sup>d</sup>
	L	84.7	79.9	13	28	207	61.8 64.8 <sup>d</sup>
	T	86.2	76.2	12	21	---	---
	T	86.6	75.2	12	22	---	---

<sup>a</sup> Precracked Charpy specimens, 0.250 in. thick.

<sup>b</sup>  $K_{IC} = \sigma_g \sqrt{7a\Theta}$ ; thickness = 0.250 in.

<sup>c</sup> No load trace.

<sup>d</sup> Using crack length (2a) corrected for "slow" growth.



# APPENDIX III STRESS-CORROSION TEST DATA

Table VII. Stress-Corrosion Test Data (3.5 Percent Sodium Chloride, Alternate Immersion)

Alloy and specimen no.	Stress level (ksi)	Days to first crack or linear pit	Days to failure	Length of specimen containing cracks or linear pits (in.) <sup>a</sup>	Crack or linear pit growth rate ( $\frac{\text{thousandths in.}}{\text{hr}}$ ) <sup>b</sup>	Comments
16-0	0	21	→	0.15		
17-0	0	49	→	0.15	0.032	
18-0	0	49	→	0.25	0.028	
19-0	0	21	→	0.80	0.047	
20-0	0	70	→	0.10		
7075-T651-1-0	0	5	→	4.05	0.378	Sectioned
7075-T651-2-0	0	---	→			
16-1	14	---	→	0	---	
16-4	14	58	→	0.50	0.027	Sectioned
16-7	14	2	→	0.05		
17-1	14	---	→	0	---	
17-4	14	---	→	0	---	
17-7	14	69	→	0.73	0.057	Sectioned
18-1	14	---	→	0	---	
18-4	14	5	→	0.10	---	Sectioned
18-7	14	---	→	0	---	
19-1	14	42	→	0.40	0.038	
19-4	14	83	→	0.39	---	
19-7	14	25	→	0.60	0.095	Sectioned
20-1	14	---	→	0	---	
20-4	14	---	→	0	---	
20-7	14	70	→	0.15	0.057	Sectioned
7075-T651-1-1	14	---	→	0	---	
7075-T651-1-4	14	---	→	0	---	
7075-T651-1-7	14	58	→	0.30	0.037	Sectioned
7075-T651-2-2	14	25	→	0.90	---	
7075-T651-2-6	14	14	→	0.35	0.135	Sectioned
16-2	20	30	→	0.10	---	
16-17	20	5	→	0.15	---	Sectioned

→ Indicates no failure after 90 days.

<sup>a</sup> Measured from 5 SX photographs at failure or after 90 days if no failure occurred.

<sup>b</sup> Measured parallel to growth direction from 5 SX time-lapse photographs.

Table VII.---Continued

Alloy and specimen no.	Stress level (ksi)	Days to first crack or linear pit	Days to failure	Length of specimen containing cracks or linear pits (in.) <sup>a</sup>	Crack or linear pit growth rate (thousandths in./hr) <sup>b</sup>	Comments
16-20	20	89	→	0.03	---	
16-22	20	---	→	0	---	
16-24	20	---	→	0	---	
17-2	20	---	→	0	---	
17-17	20	23	→	0.75	0.019	Sectioned
17-20	20	37	→	0.10	---	
17-22	20	---	→	0	---	
17-24	20	---	→	0	---	
18-2	20	---	→	0	---	
18-17	20	2	→	0.05	---	
18-20	20	---	→	0	---	
18-22	20	---	→	0	---	
18-24	20	---	→	0	---	
19-2	20	69	→	1.98	0.227	Sectioned
19-17	20	19	→	1.90	0.049	
19-20	20	58	→	1.58	0.057	
19-22	20	69	→	1.77	0.114	
19-24	20	83	→	0.49	0.095	
20-2	20	5	→	0.36	---	
20-17	20	2	→	0.40	0.020	Sectioned
20-20	20	70	→	0.16	0.033	
20-22	20	80	→	0.08	---	
20-24	20	---	→	0	---	
7075-T651-1-2	20	37	→	1.10	---	Damaged in anodizing
7075-T651-1-17	20	70	→	6.10	0.038	
7075-T651-1-20	20	37	→	0.70	0.045	
7075-T651-1-22	20	5	→	0.70	---	Sectioned; damaged in anodizing
7075-T651-1-24	20	51	→	9.82	0.027	Sectioned

→ Indicates no failure after 90 days.

<sup>a</sup> Measured from 5,5X photographs at failure or, after 90 days if no failure occurred.

<sup>b</sup> Measured parallel to groove direction from 5,5X time sequence photographs.

Table VII. -- Continued

Alloy and specimen no.	Stress level (ksi)	Days to first crack or linear pit	Days to failure	Length of specimen containing cracks or linear pits (in.) <sup>a</sup>	Crack or linear pit growth rate ( $\frac{\text{thousandths in.}}{\text{hr}}$ ) <sup>b</sup>	Comments
7075-T651-2-5	20		→	0	---	Sectioned
7075-T651-2-10	20	6	→	0.5	---	
AZ74.61 A-5	20	9	→	0.15	---	
7075-T73 B-6	20	19	→	0.20	0.046	
X7080-T7 D-6	20	2	44	4.10	---	Sectioned; damaged in anodizing
7079-T611-AC-4	20	---	→	0	---	
7079-T611-G F-7	20	---	→	0	---	
7079-T6-G E-7	20	---	→	0	---	
16-5	26	---	→	0	---	Specimen lost
16-8	26	69	→	1.70	0.114	
16-11	26	---	→	0	---	
16-15	26	---	→	0	---	
16-16	26	---	→	0	---	Sectioned
16-23	26	76	→	0.15	---	
17-5	26	---	→	0	---	
17-8	26	30	→	0.04	---	
17-11	26	---	→	0	---	Sectioned
17-15	26	76	→	0.06	---	
17-16	26	76	→	0.14	---	
17-23	26	---	→	0	---	
18-5	26	56	→	0.27	0.045	Sectioned
18-8	26	2	→	1.10	0.074	
18-11	26	---	→	0	---	

→ Indicates no failure after 90 days.

<sup>a</sup> Measured from 5.5X photographs at failure or after 90 days if no failure occurred.

<sup>b</sup> Measured parallel to groove direction from 5.5X time sequence photographs.

Table VII.—Continued

Alloy and specimen no.	Stress level (ksi)	Days to first crack or linear pit	Days to failure	Length of specimen containing cracks or linear pits (in.) <sup>a</sup>	Crack or linear pit growth rate ( $\frac{\text{thousandths in.}}{\text{hr}}$ ) <sup>b</sup>	Comments
18-15	26	5	→	0.65	0.020	Sectioned
18-16	26	---	→	0	---	
18-23	26	---	→	0	---	
19-5	26	28	→	2.35	0.085	
19-8	26	5	→	1.82	0.303	
19-11	26	56	→	0.55	0.095	
19-15	26	70	→	1.32	0.151	
19-16	26	42	→	0.70	0.133	
19-23	26	89	→	0.05	---	
20-5	26	9	→	0.05	---	
20-8	26	70	→	0.19	0.057	Sectioned
20-11	26	2	→	0.18	0.010	
20-15	26	42	→	0.06	---	
20-16	26	83	→	0.28	0.038	
20-23	26	9	→	0.26	0.016	
7075-T651-1-5	26	---	→	0	---	
7075-T651-1-8	26	70	→	0.06	---	Sectioned
7075-T651-1-11	26	---	→	0	---	
7075-T651-1-15	26	---	→	0	---	
7075-T651-1-16	26	---	→	0	---	
7075-T651-1-23	26	2	→	0.15	0.010	Sectioned
7075-T651-2-7	26	10	47	4.10	0.84	
7075-T651-2-11	26	4	25	4.10	---	Sectioned
AZ74.61 1-1	26	56	→	1.42	0.045	Sectioned
AZ74.61 2-2	26	37	→	2.10	0.077	
AZ74.61 A-6	26	89	→	0.05	---	Sectioned
AZ74.61 A-7	26	70	→	0.60	0.113	

→ Indicates no failure after 90 days.

<sup>a</sup> Measured from 5.5X photographs at failure or after 90 days if no failure occurred.<sup>b</sup> Measured parallel to groove direction from 5.5X time sequence photographs.

Table VII.--Continued

Alloy and specimen no.	Stress level (ksi)	Days to first crack or linear pit	Days to failure	Length of specimen containing cracks or linear pits (in.) <sup>a</sup>	Crack or linear pit growth rate ( $\frac{\text{thousandths in.}}{\text{hr}}$ ) <sup>b</sup>	Comments
7075-T73 B-7	26	56	→	0.78	0.040	Sectioned
7075-T73 B-8	26	56	→	0.30	0.045	Not stressed in short-transverse direction
X7080-T7 D-7	26	5	→	1.30	0.151	
X7080-T7 D-8	26	9	→	0.64	0.031	Sectioned
7079-T611-A-C-5	26	2	→	0.06	---	
7079-T611-A-C-7	26	2	→	0.75	---	Sectioned
7079-T611-G-F-8	26	---	→	0	---	
7079-T611-G-F-9	26	58	→	0.10	---	Not stressed in short-transverse direction
7079-T6-G-E-8	26	2	4	4.10	15.9	
7079-T6-G-E-9	26	70	89	4.10	10.3	Sectioned
7575-1	26	70	→	0.30	---	
7575-8	26	28	→	3.07	0.088	Sectioned
7578-1	26	42	→	1.60	0.024	
7578-8	26	42	→	2.25	0.025	Sectioned
7178-T7651-1	26	25	→	1.43	0.086	Sectioned
7178-T7651-8	26	70	→	1.02	0.067	
16-3	32	13	44	4.10	---	Sectioned; damaged in anodizing
16-9	32	---	→	0	---	
16-14	32	9	→	0.20	---	
16-19	32	9	→	0.30	0.020	Sectioned
16-21	32	2	→	0.07	---	
17-3	32	---	→	0	---	
17-9	32	58	→	0.05	---	
17-14	32	---	→	0	---	
17-19	32	---	→	0	---	

→ Indicates no failure after 90 days.

<sup>a</sup> Measured from 5.5X photographs at failure or after 90 days if no failure occurred.

<sup>b</sup> Measured parallel to groove direction from 5.5X time sequence photographs.

Table VII.--Continued

Alloy and specimen no.	Stress level (ksi)	Days to first crack or linear pit	Days to failure	Length of specimen containing cracks or linear pits (in.) <sup>a</sup>	Crack or linear pit growth rate (thousandths in./hr) <sup>b</sup>	Comments
17-21	32	70	→	0.65	0.075	Sectioned
18-3	32	5	89	4.10	0.317	Sectioned
18-9	32	---	→	0	---	
18-14	32	---	→	0	---	
18-19	32	89	→	0.53	0.111	
18-21	32	9	→	0.50	0.133	
19-3	32	56	→	2.42	0.113	Sectioned
19-9	32	30	→	1.72	0.216	
19-14	32	56	→	1.59	0.162	
19-19	32	9	→	2.74	0.123	
19-21	32	5	→	2.03	0.227	
20-3	32	9	44	4.10	---	Damaged in anodizing
20-9	32	9	→	0.54	0.042	
20-14	32	9	→	0.20	---	
20-19	32	2	→	0.20	0.046	
20-21	32	58	→	1.53	0.076	Sectioned
7075-T651-1-3	32	69	→	0.15	0.108	
7075-T651-1-9	32	70	→	0.10	0.022	
7075-T651-1-14	32	76	→	0.20	---	
7075-T651-1-19	32	9	→	0.42	0.030	Sectioned
7075-T651-1-21	32	2	→	0.32	0.026	
7075-T651-2-1	32	3	10	4.10	---	
7075-T651-2-9	32	4	11	4.10	---	Sectioned
AZ74.61 1-2	32	56	→	1.77	0.063	
AZ74.61 3-1	32	30	→	2.25	0.041	
7575-4	32	9	89	4.05	0.173	
7575-6	32	5	37	4.10	0.545	
7578-4	32	9	→	3.55	0.065	
7578-6	32	14	→	2.27	0.081	

→ Indicates no failure after 90 days.

<sup>a</sup> Measured from 5.5X photographs at failure or after 90 days if no failure occurred.<sup>b</sup> Measured parallel to groove direction from 5.5X time sequence photographs.

Table VII.--Continued

Alloy and specimen no.	Stress level (ksi)	Days to first crack or linear pit	Days to failure	Length of specimen containing cracks or linear pits (in.) <sup>a</sup>	Crack or linear pit growth rate ( $\frac{\text{thousandths in.}}{\text{hr}}$ ) <sup>b</sup>	Comments
7178-T7651-4	32	56	→	2.00	0.113	
7178-T7651-6	32	28	→	3.60	0.080	
16-6	44	2	→	2.00	0.153	Sectioned
16-10	44	---	→	0	---	
16-13	44	56	→	0.10	0.010	
17-6	44	69	→	1.18	0.076	
17-10	44	51	→	1.29	0.095	
17-13	44	60	→	1.63	0.113	Sectioned
18-6	44	9	61	4.10	0.321	Sectioned
18-10	44	69	89	4.10	0.228	
18-13	44	56	83	4.10	0.945	
19-6	44	9	→	3.80	0.122	
19-10	44	2	83	4.10	0.229	Sectioned
19-13	44	37	→	4.05	0.090	
20-6	44	51	→	1.65	0.056	
20-10	44	51	→	1.39	0.076	
20-13	44	5	→	1.25	0.087	Sectioned
7075-T651-1-6	44	5	89	4.10	0.189	
7075-T651-1-10	44	5	→	1.50	0.119	
7075-T651-1-13	44	2	89	4.10	0.379	Sectioned
7075-T651-2-8	44	3	10	4.10	---	Sectioned
7075-T651-2-12	44	14	27	4.10	---	
AZ74.61 2-1	44	9	→	2.54	0.055	
AZ74.61 4-1	44	37	→	2.00	0.078	
AZ74.61 A-9	44	---	→	0	---	
7075-T73 B-9	44	5	→	2.70	0.133	
7075-T73 B-10	44	37	→	1.44	0.065	
X7080-T7 D-9	44	9	→	0.56	0.038	
X7080-T7 D-11	44	9	→	1.03	0.047	

→ Indicates no failure after 90 days.

<sup>a</sup> Measured from 5.5X photographs at failure or after 90 days if no failure occurred.<sup>b</sup> Measured parallel to groove direction from 5.5X time sequence photographs.

Table VII.—Continued

Alloy and specimen no.	Stress level (ksi)	Days to first crack or linear pit	Days to failure	Length of specimen containing cracks or linear pits (in.) <sup>a</sup>	Crack or linear pit growth rate (thousandths in./hr) <sup>b</sup>	Comments
7079-T611-A-C-8	44	80	→	0.05	---	Equiaxed grains
7079-T611-A-C-10	44	---	→	0	---	
7079-T611-G-F-10	44	56	→	1.25	0.076	Sectioned; stressed parallel to flow lines
7079-T611-G-F-11	44	70	→	0.35	0.057	Stressed parallel to flow lines
7079-T6-G-E-10	44	1	2	4.10	15.0	
7079-T6-G-E-11	44	1	2	4.10	15.0	
7575-5	44	5	→	3.70	0.022	
7575-7	44	5	42	4.10	0.419	
7578-5	44	42	→	3.6	0.087	
7578-7	44	14	83	4.0	0.063	
7178-T7651-5	44	2	→	2.95	0.060	
7178-T7651-7	44	23	→	2.93	0.050	
16-12	56	56	→	1.47	0.057	
16-18	56	56	→	0.10	---	Sectioned
17-12	56	58	→	1.33	0.113	Sectioned
17-18	56	58	→	1.23	0.076	
18-12	56	42	61	4.10	0.346	Sectioned
18-18	56	51	62	4.10	1.10	
19-12	56	2	58	4.10	1.89	
19-18	56	2	29	4.10	1.24	Sectioned
20-12	56	2	83	4.10	0.185	Sectioned
20-18	56	51	→	4.05	0.302	
7075-T651-1-12	56	2	29	4.10	0.486	Sectioned
7075-T651-1-18	56	9	50	4.10	0.567	
7075-T651-2-3	56	3	6	4.10	5.17	Sectioned
7075-T651-2-4	56	3	6	4.10	5.17	

→ Indicates no failure after 90 days.

<sup>a</sup> Measured from 5.5X photographs at failure or after 90 days if no failure occurred.<sup>b</sup> Measured parallel to groove direction from 5.5X time sequence photographs.



Table VII.-- Concluded

Alloy and specimen no.	Stress level (ksi)	Days to first crack or linear pit	Days to failure	Length of specimen containing cracks or linear pits (in.) <sup>a</sup>	Crack or linear pit growth rate (thousandths in.) <sup>b</sup> hr	Comments
AZ74.61-4-2	56	37	→	3.80	0.114	Sectioned
AZ74.61-5-1	56	23	→	3.75	0.10	
AZ74.61 A-10	56	23	→	0.91	0.063	
7075-T73 B-11	56	9	→	3.75	0.089	Sectioned
X7080-T7 D-12	56	2	→	1.70	0.070	Sectioned
7079-T611-A-C-12	56	1	5	4.10	6.2	Sectioned
7079-T611-G-F-12	56	2	→	0.50	---	Sectioned; stressed parallel to flow lines
7079-T6-G-E-12	56	1 hr	1	4.10	38.8	Sectioned
7575-2	56	5	28	3.90	0.227	Sectioned
7575-3	56	5	44	4.10	0.270	Sectioned
7578-2	56	2	83	4.10	0.089	Sectioned
7578-3	56	2	→	3.80	0.027	Sectioned
7178-T7651-2	56	42	→	3.65	0.189	
7178-T7651-3	56	44	→	2.05	0.108	

→ Indicates no failure after 90 days.

<sup>a</sup> Measured from 5.5X photographs at failure or after 90 days if no failure occurred.

<sup>b</sup> Measured parallel to groove direction from 5.5X time sequence photographs.

Table VIII. Stress-Corrosion Test Data (Industrial Environment)

Alloy and specimen no.	Stress level (ksi)	Days to first crack or linear pit	Days to failure	Length of specimen containing cracks or linear pits (in.) <sup>a</sup>	Comments
16-25	20	---	→	---	
16-28	20	---	→	---	
17-25	20	---	→	---	
17-28	20	---	→	---	
18-25	20	---	→	---	
18-28	20	---	→	---	
19-25	20	---	→	---	
19-28	20	---	→	---	
20-25	20	---	→	---	
20-28	20	---	→	---	
7075-T651-1-25	20	---	→	---	
7075-T651-1-28	20	---	→	---	
16-29	26	---	→	---	
16-31	26	---	→	---	
16-33	26	---	→	---	
17-29	26	---	→	---	
17-31	26	---	→	---	
17-33	26	---	→	---	
18-29	26	---	→	---	
18-31	26	---	→	---	
18-33	26	---	→	---	
19-29	26	---	→	---	
19-31	26	---	→	---	
19-33	26	---	→	---	
20-29	26	---	→	---	
20-31	26	---	→	---	
20-33	26	---	→	---	
7075-T651-1-29	26	---	→	---	
7075-T651-1-31	26	---	→	---	

→ Indicates no failure after 160 days. Specimens still in test.

<sup>a</sup> Measured from 5.5X photographs.

Table VIII.—Continued

Alloy and specimen no.	Stress level (ksi)	Days to first crack or linear pit	Days to failure	Length of specimen containing cracks or linear pits (in.) <sup>a</sup>	Comments
7075-T651-1-33	26	---	→	---	
AZ74.61-3-2	26	78	→	---	Anodized and stripped
AZ74.61-5-2	26	---	→	---	Anodized and stripped
AZ74.61-5-3	26	---	→	---	Anodized and stripped
AZ74.61-5-4	26	---	→	---	Anodized and stripped
AZ74.61-5-5	26	---	→	---	
AZ74.61-5-6	26	---	→	---	
7575-9	26	---	→	---	
7575-10	26	---	→	---	
7578-9	26	---	→	---	
7578-10	26	---	→	---	
7178-T7651-9	26	---	→	---	
7178-T7651-10	26	---	→	---	
16-26	32	---	→	---	
16-30	32	---	→	---	
17-26	32	---	→	---	
17-30	32	---	→	---	
18-26	32	---	→	---	
18-30	32	---	→	---	
19-26	32	---	→	---	
19-30	32	---	→	---	
20-26	32	---	→	---	
20-30	32	---	→	---	
7075-T651-1-26	32	---	→	---	
7075-T651-1-30	32	---	→	---	
16-27	44	---	→	---	
16-32	44	---	→	---	
17-27	44	---	→	---	
17-32	44	---	→	---	

→ Indicates no failure after 160 days. Specimens still in test.

<sup>a</sup> Measured from 5.5X photographs.

Table VIII.--Concluded

Alloy and specimen no.	Stress level (ksi)	Days to first crack or linear pit	Days to failure	Length of specimen containing cracks or linear pits (in.) <sup>a</sup>	Comments
18-27	44	---	→	---	
18-32	44	---	→	---	
19-27	44	---	→	---	
19-32	44	---	→	---	
20-27	44	---	→	---	
20-32	44	---	→	---	
7075-T651-1-27	44	---	→	---	
7075-T651-1-32	44	---	→	---	
16-0	0	---	→	---	
17-0	0	---	→	---	
18-0	0	---	→	---	
19-0	0	---	→	---	
20-0	0	---	→	---	
7075-T651-0	0	---	→	---	

→ Indicates no failure after 160 days. Specimens still in test.

<sup>a</sup> Measured from 5.5X photographs.

APPENDIX IV  
END-OF-TEST PHOTOGRAPHS



16-1



18-1



16-7



18-7



16-4



18-4



17-4



18-1



17-1



19-4



17-7



18-7

(4.1X)

14 KSI  
90 DAYS

(4.1X)

20-1

7075-T651-1-4

20-4

7075-T651-1-7

20-7

7075-T651-2-2

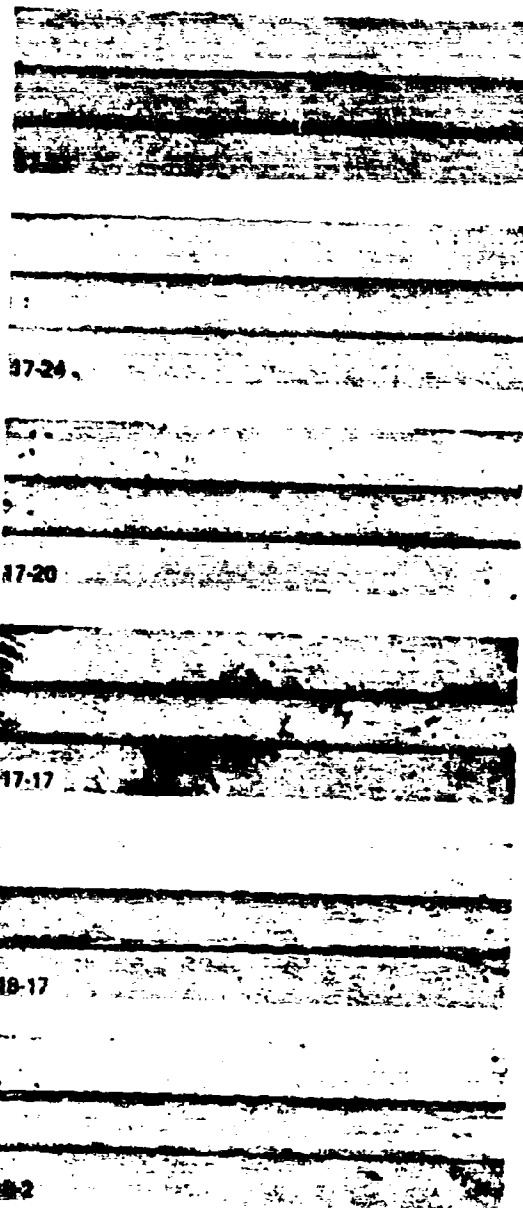
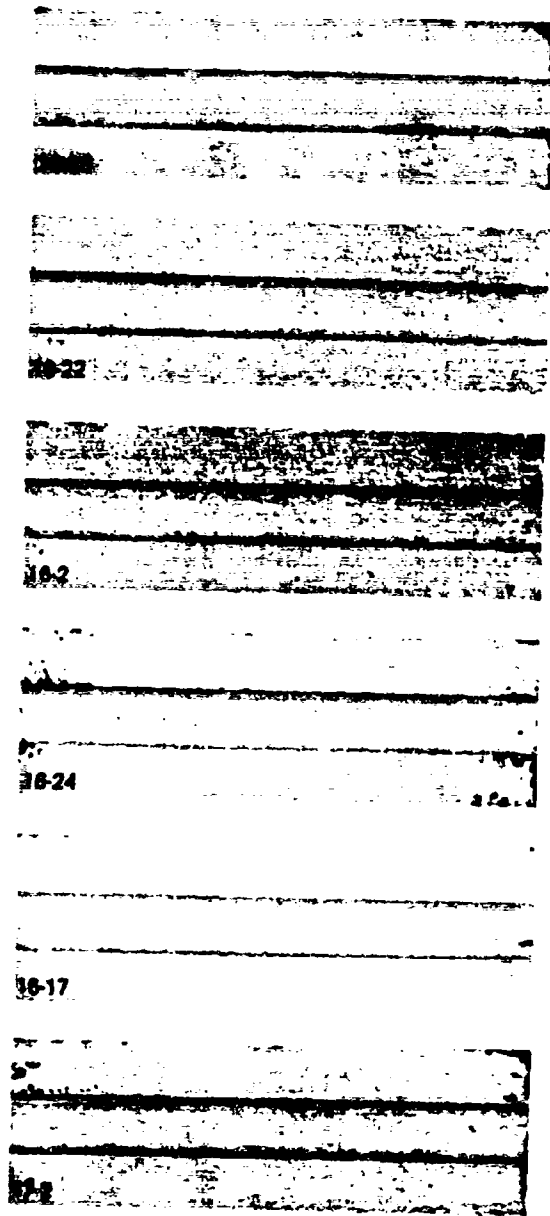
7075-T651-1-1

7075-T651-2-6

(4.1X)

14 KSI  
90 DAYS

(4.1X)



(4.1X)

20 KSI  
90 DAYS

(4.1X)

18-20

19-2

18-22

20-24

18-24

20-22

19-24

20-20

19-20

20-17

19-22

20-2

19-17

7075-T651-1-17

(4.1X)

20 KSI  
90 DAYS

(4.1X)



7075-T651-1-10

AZ74.81-A-5

7075-T651-1-24

7075-T73-B-8

7075-T651-1-22

X7080-T7-D-8  
FAILED 44 DAYS

7075-T651-1-2

7079-T611-A-C-4

7075-T651-2-5

7079-T611-G-F-7

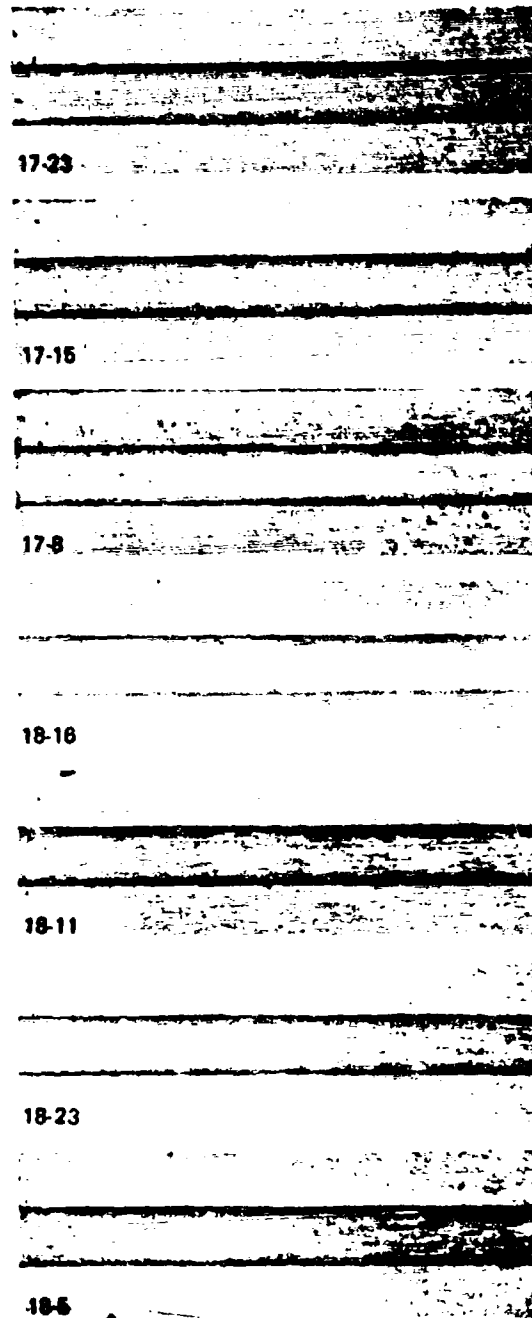
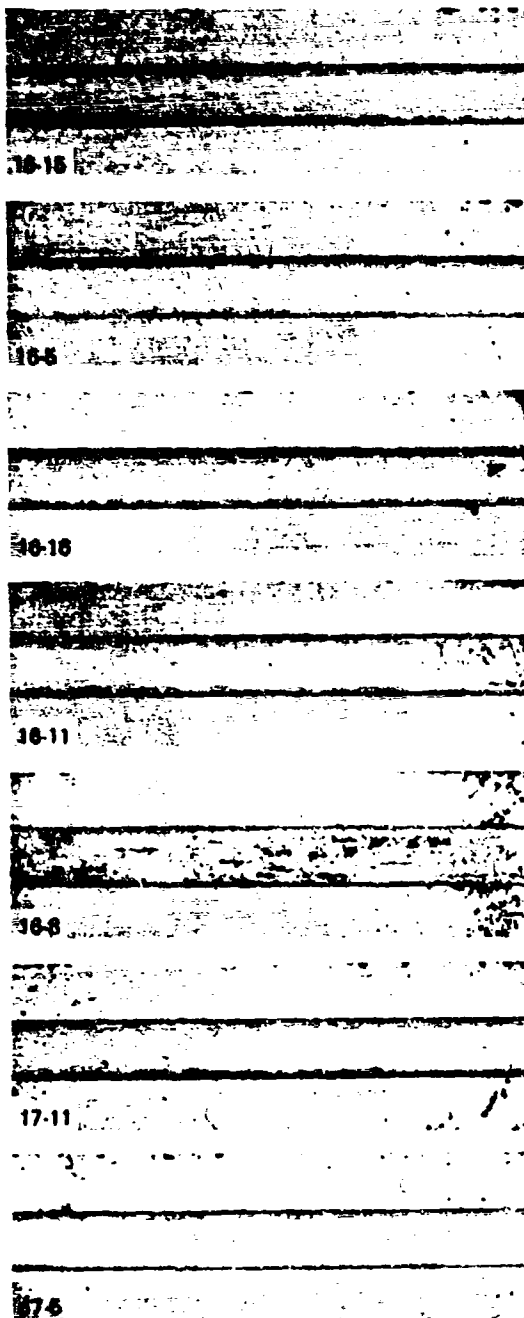
7075-T651-2-10

7079-T6-G-E-7

(4.1X)

20 KSI  
90 DAYS

(4.1X)



(4.1X)

26 KSI  
90 DAYS

(4.1X)

18-15

20-5

19-23

20-23

19-11

20-8

19-16

20-16

19-15

7075-T651-1-15

19-8

7075-T651-1-5

20-15

7075-T651-1-8

(4.1X)

26 KSI  
90 DAYS

(4.1X)

7075-T651-1-11

X7080-T7-D-7

7075-T651-1-16

7079-T611-A-C-5

7075-T651-2-7  
FAILED 47 DAYS

7079-T611-G-F-8

AZ74.61-1-1

7079-T6-G-E-8  
FAILED 4 DAYS

AZ74.61-A-6

7575-1

7075-T73-B-8

7578-1

7178-T7651-8

(4.1X)

26 KSI  
90 DAYS

(4.1X)

16-9

17-9

16-21

17-19

16-14

18-9



16-3  
FAILED 44 DAYS

18-14

17-14

18-21

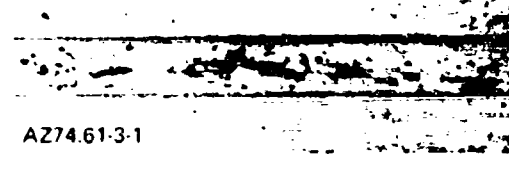
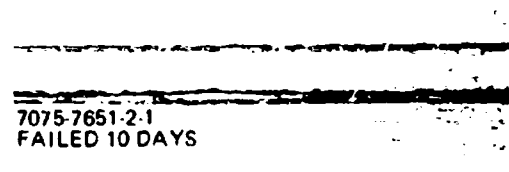
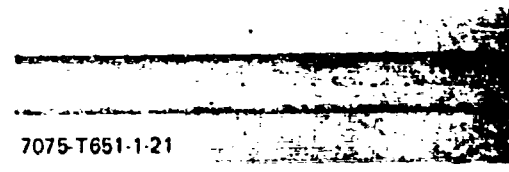
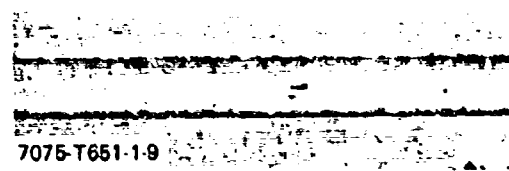
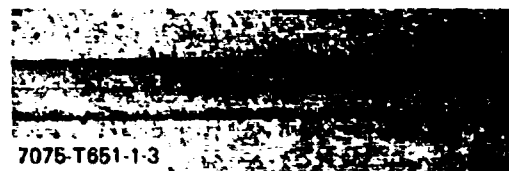
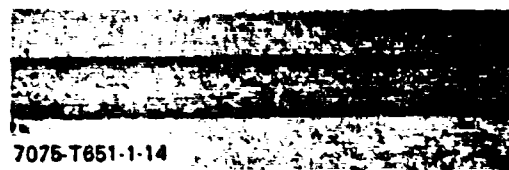
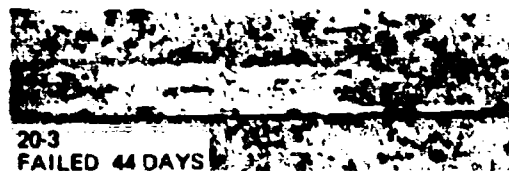
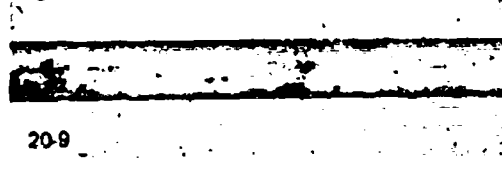
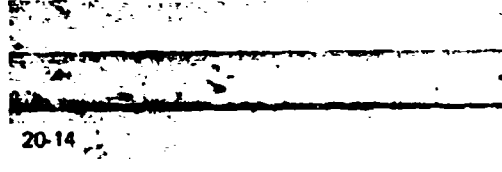
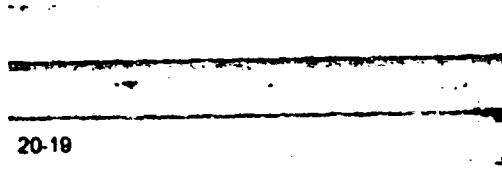
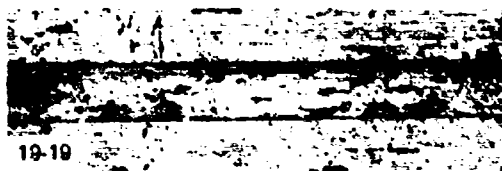
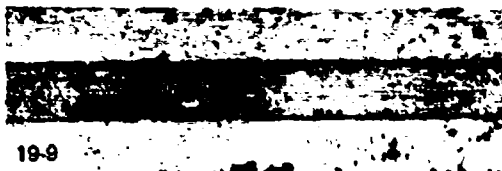
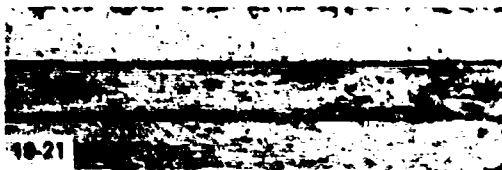
17-3

18-19

(4.1X)

32 KSI  
90 DAYS

(4.1X)



(4.1X)

32 KSI  
90 DAYS

(4.1X)

AZ74.61-1-2

7575-4  
FAILED 90 DAYS

7575-6  
FAILED 37 DAYS

7578-6

7578-4

7178 T7651-4

7178-T7651-6

32 KSI  
90 DAYS

(4.1X)



16-10



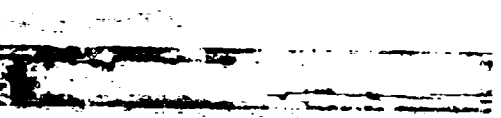
16-13




17-10



17-6



18-10  
FAILED 90 DAYS



18-3  
FAILED 83 DAYS



18-6



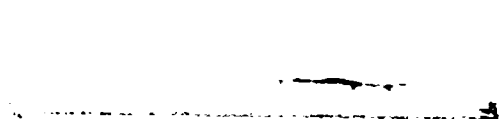
18-13



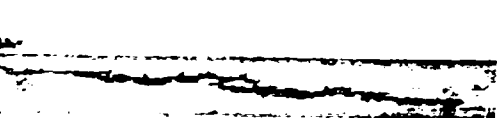
20-8



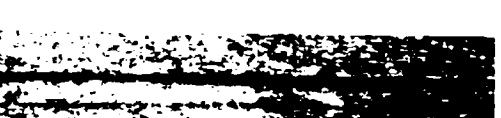
20-10



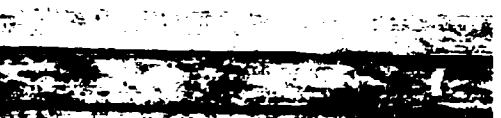
7075-T651-1-10



7075-T651-1-6  
FAILED 90 DAYS



7075-T651-2-12  
FAILED 28 DAYS



AZ74.61-2-1

(4.1X)

44 KSI  
90 DAYS

(4.1X)



AZ74.61-4-1

7079-T611-A-C-8

AZ74.61-A-9

7079-T611-A-C-10

7075-T73-B-10

7079-T611-G-F-11

7075-T73-B-9

7079-T611-G-F-10

X7080-T7-D-9

7079-T6-G-E-10  
FAILED 2 DAYS

X7080-T7-D-11

7079-T6-G-E-11  
FAILED 2 DAYS

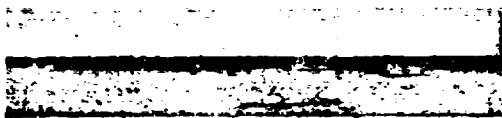
(4.1X)

44 KSI  
90 DAYS

(4.1X)



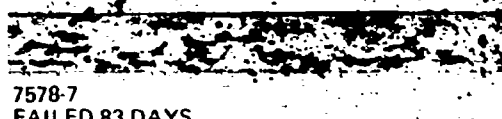
7575-5



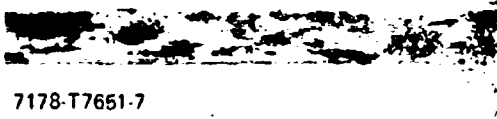
7575-7  
FAILED 42 DAYS



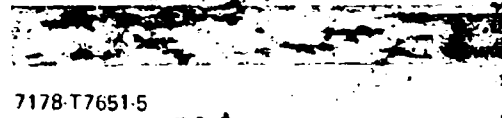
7578-5



7578-7  
FAILED 83 DAYS



7178-T7651-7



7178-T7651-5

44 KSI  
90 DAYS

(4.1X)



16-18



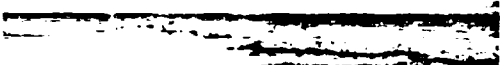
16-12




17-18



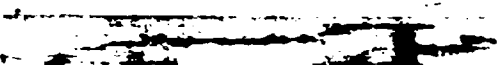
17-12



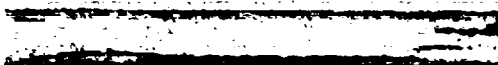
18-18  
FAILED 62 DAYS



18-12  
FAILED 61 DAYS



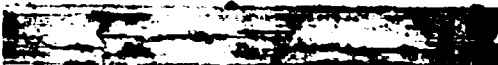
19-12  
FAILED 58 DAYS



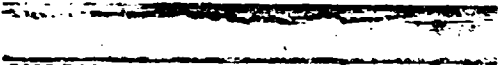
19-18  
FAILED 29 DAYS



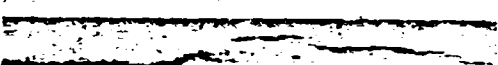
20-18



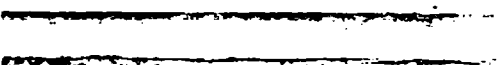
20-12  
FAILED 83 DAYS



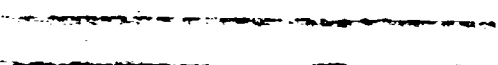
7075-T651-1-18  
FAILED 50 DAYS



7075-T651-1-12  
FAILED 29 DAYS



7075-T651-2-3  
FAILED 6 DAYS



7075-T651-2-4  
FAILED 6 DAYS

(4.1X)

56 KSI  
90 DAYS

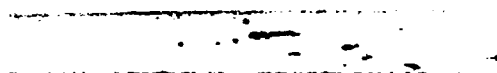
(4.1X)



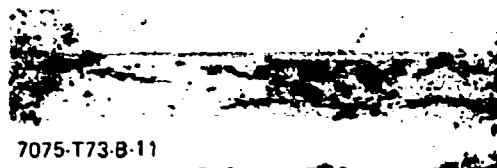
AZ74.61-5-1



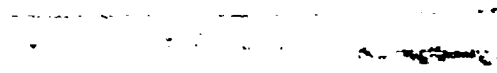
AZ74.61-4-2



AZ74.61-A-10



7075-T73-B-11



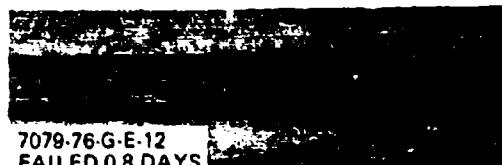
X7080-T7-D-12



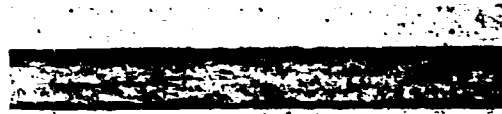
7079-T611-A-C-12  
FAILED 5 DAYS



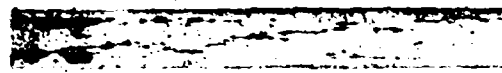
7079-T611-G-F-12



7079-76-G-E-12  
FAILED 0.8 DAYS



7575-2  
FAILED 28 DAYS



7575-3  
FAILED 44 DAYS



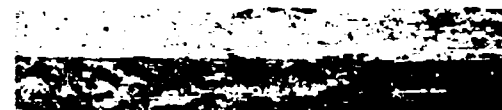
7578-2  
FAILED 83 DAYS



7578-3



7178-T7651-3



7178-T7651-2

(4.1X)

56KSI  
90 DAYS

(4.1X)

Unclassified

Security Classification

DOCUMENT CONTROL DATA - R & D		
(Security classification of title, body of abstract and indexing annotation must be entered when the overall report is classified)		
1. ORIGINATING ACTIVITY (Corporate Author)		2a. REPORT SECURITY CLASSIFICATION
The Boeing Company Commercial Airplane Division Renton, Washington 98055		2b. GROUP
3. REPORT TITLE		
DEVELOPMENT OF HIGH-STRENGTH ALUMINUM ALLOYS WITH IMPROVED STRESS-CORROSION RESISTANCE-PHASE II		
4. DESCRIPTIVE NOTES (Type of report and inclusive dates)		
Technical Report May 1, 1967-March 30, 1968		
5. AUTHOR(S) (First name, middle initial, last name)		
J. Corey McMillan and Michael V. Hyatt		
6. REPORT DATE	7a. TOTAL NO. OF PAGES	7b. NO. OF REFS
June 1968	132	50
8a. CONTRACT OR GRANT NO.	9a. ORIGINATOR'S REPORT NUMBER(S)	
AF 33(615)-3697	D6-60091	
b. PROJECT NO. 7351	9b. OTHER REPORT NO(S) (Any other numbers that may be assigned this report)	
c. Task No. 735105	AFML-TR-68-148	
10. DISTRIBUTION STATEMENT		
This document is subject to special export controls and each transmittal to foreign governments or foreign nationals may be made only with prior approval of the Air Force Materials Laboratory, MAMP, Wright-Patterson Air Force Base, Ohio 45433.		
11. SUPPLEMENTARY NOTES		12. SPONSORING MILITARY ACTIVITY
		Air Force Materials Laboratory (MAMP) Air Force Systems Command Wright-Patterson Air Force Base, Ohio 45433
13. ABSTRACT		
<p>The objective of this program was to develop a stress-corrosion-resistant, high-strength aluminum alloy through addition of minor elements and variations in heat treatment. On the basis of Phase I results, five step-aged special-chemistry alloys were selected for study in Phase II, along with commercial 7075-T651 plate material. The Phase II alloys consisted of a base alloy (6.4% Zn, 2.55% Mg, 1.0% Cu) with the following additions: silver; silver + zirconium (no chromium); silver + higher copper content; and silver + higher zinc and magnesium content. The materials evaluation consisted of metallographic, aging, and quench-sensitivity studies; stress-corrosion testing; and determination of mechanical, fracture, and fatigue properties. The resulting data were compared with data from evaluation of 11 other commercial and experimental aluminum alloys including 7079-T611, 7075-T73, AZ74-61, 7178-T7651, and X7080-T7. All of the five step-aged special-chemistry alloys met the goals of the program in that they had longitudinal 0.2-percent yield strengths above 70 ksi and stress-corrosion resistance superior to that of alloys 7079-T6 and 7075-T6. The use of silver in a production alloy does not appear warranted. Silver did not increase stress-corrosion resistance in the overaged condition. Strength properties were slightly increased by silver (0.25 in. thick), but quench sensitivity also increased, thus negating this slight strength advantage for thicker sections. The allowable chemistry range for the alloy that best meets the goals of this program should be: 5.9-6.9% Zn, 2.2-2.9% Mg, 0.7-1.5% Cu, 0.10-0.25% Zr, 0.05-0.15% Mn, 0.05% max Cr, 0.10% max Ti, 0.20% max Fe, 0.20% max Si. The ease with which the Phase II alloys were cast and fabricated indicates that the recommended alloy is commercially feasible. Additional testing is recommended to complete the development of this alloy.</p>		

DD FORM 1473

Unclassified

Security Classification

Unclassified

Security Classification

14 KEY WORDS	LINK A		LINK B		LINK C	
	ROLE	WT	ROLE	WT	ROLE	WT
7000-Series Aluminum Alloys						
Stress-Corrosion Resistance						
High-Strength Alloys						
Silver Addition						
Chromium Addition						
Zirconium Addition						
Overaging						

Unclassified

Security Classification